Winter 1-31-2021

The Antioxidant and Antimicrobial Activities of Cornsilk Extract Encapsulated in Polysaccharide Nanoparticles

Maryam Mady
mariammadi@aucegypt.edu

THE AMERICAN UNIVERSITY IN CAIRO
الجامعة الأمريكية بالقاهرة

School of Sciences and Engineering

The Antioxidant and Antimicrobial Activities of Cornsilk Extract Encapsulated in Polysaccharide Nanoparticles

A Thesis Submitted to
The Nanotechnology Master's Program
In partial fulfilment of the requirements for
The degree of Master of Science
By:

Maryam Gamaleldin Mady

Under the supervision of:
Dr. Wael Mamdouh
Associate professor, Department of Chemistry,
The American University in Cairo
29th June, 2020

Table of Contents

Acknowledgement I

Absract II

List of abbreviations III

List of figures IV

List of tables VII

List of equations VIII

Chapter 1 Introduction and literature reviews 1

1.1 Bacterial infection 2

1.1.1 Bacterial flora 2

1.1.2 Bacteria 3

1.1.3 Bacteria from Symbiosis to Pathogenesis 4

1.1.4 *Escherichia coli* and *staphylococcus aureus* infections 5

1.1.5 Biofilm formation 7

1.1.6 Treatment with antibiotics 8

1.1.7 Antibacterial resistance 9

1.2 Oxidative stress 11

1.2.1 Antioxidant agents 12

1.3 Fruit and vegetable waste management 14

1.3.1 Fruit and vegetable waste amount 14

1.3.1.1 Corn and its wastes production in Egypt 17

1.3.2 Bioactive compounds from the fruit and vegetable Wastes 20

1.3.3 Phenolic\polyphenols 21

1.3.3.1 Phenols structure and classification 21

1.3.3.2 Polyphenols bioactivities 22

1.3.3.3 Promising utilization of corn silk waste in Egypt and Asian countries 25

1.4 Nanotechnology 27

1.4.1 Nanomedicine 28

1.4.1.1 Drug delivery applications 29

1.4.1.1.1 Polymeric nano-based materials: natural versus synthetic 29

1.4.1.1.2 Chitosan 33

1.4.1.1.2.1 Chitosan nanoparticles 33

1.4.1.1.2.2 Chitosan preparation 34
1.4.1.1.2.3 Chitosan NPs applications 35
1.5 Scope of the study 35
Chapter 2 Materials and methods 37
2.1 Materials 38
2.2 Preparation of corn silk, husk, and cob extract powder 39
2.3 Physiochemical characterization of corn parts' extract 40
2.3.1 2,2-diphenyl-1-picryl-hydrazyl-hydrate (DPPH) assay 40
2.3.2 Total phenolic concentration (TPC) assay 41
2.4 Formulation of corn silk extract encapsulated CS NPs 42
2.5 Physiochemical characterization corn silk Extract CS NPs 45
2.5.1 Particle size, PDI, and zeta potential 45
2.5.2 Entrapment efficiency (EE%) 45
2.6 Morphological, analytical and *in vitro* release characterization of SE x\CS NPs 46
2.6.1 Scanning electron microscope (SEM) 46
2.6.2 Fourier-transform infrared FTIR spectroscopy 46
2.6.3 *In vitro* release study 47
2.7 Chemical and biological activity of SE x\CS NPs 47
2.7.1 Antioxidant activity 47
2.7.2 Antibacterial activity 48
2.8 Statistical study 48
2.9 Theoretical background 49
2.9.1 DPPH and Folin reagents 49
2.9.2 Ionic gelation technique for CS NPs preparation 49
2.9.3 Freeze dryer 50
2.9.4 Dynamic light scattering 51
2.9.5 Fourier transform infrared FTIR spectroscopy 53
2.9.6 Scanning electron microscope (SEM) 54
2.9.7 Probe sonicator 55
2.9.8 UV-visible spectrophotometer 56
Chapter 3 Results and discussion 58

3.1 DPPH and TPC assay for the three corn parts 59
3.2 Preparation and physicochemical characterization of the optimum formula 61
3.3 Morphological, analytical and *in vitro* release characterization of SE x\CS NPs 66
3.3.1 Scanning electron microscope (SEM) 66
3.3.2 Fourier-transform infrared FTIR spectroscopy 68
3.3.3 *In vitro* release study 70
3.4 Chemical and biological activity of SE x\CS NPs 71
3.4.1 Antioxidant activity 71
3.4.2 Antibacterial activity 73
Chapter 4 Conclusion and future works 78
References 81

Acknowledgement

Above all, I owe my deepest gratitude Allah and to, after him, my supervisor Professor **Dr. Wael Mamdouh** whose guidance paved the way to make this thesis work possible. He supported me throughout my academic, and lab work. He provided me with immense knowledge and advised me to keep developing this research work. I really appreciate having the opportunity to work under his supervision, especially under the hard circumstances of COVID 19.

Thanks to all the professors from whom I learned a lot throughout the courses of the nanotechnology program, **Dr. Hassan El-Fawal**, **Dr. Adham Ramadan**, **Dr. Nageh Allam**, **Dr. Hanadi Salem**, **Dr. Mayyada El-Sayed**, and **Dr. Tarek Madkour**.

Also, it was an honor to work with **Amro Shetta**, **Wessam Delann**, **Sara Omar**, **Nouran Sharaf**, **Jailan Essam**, **Omar Zidan, Haidy Yehia, Khadiga Sadek**, **Yasmine El-Kashef**, **Fatma El-Shishiny**, **Hend Amr**, and **Israa Ali,** who helped, encouraged, and supported me. Special thanks to my colleague, **James Kegere,** who helped me in the SEM imaging and antibacterial tests. Thanks to The supportive staff of the chemistry department at AUC; **Mr. Mahmoud Abdel Moez** and **Ali Reda** who helped me with FTIR experiments.

I am indebted to my mother **Dr. Fardous Soliman** and my uncle **Medhat Soliman** without their support and prayers, I would have not been able to get where I am. They encouraged me as they witnessed my hard work through this journey, I would like to dedicate my success to them. Last but not least, all the credits go to my partner during the journey of the master degree, my husband **Dr. Mohamed Samy** who was very patient and understanding to support me through my thesis work and kept pushing me forward until I reached this point. To my sister, **Sarah,** who has never let me down and always had an extraordinary power to cheer me up in the hardest time. I would also like to thank all, unnamed, people who provided me with corn that helped me as the sample of my research.

I cannot neglect the role of The American University in Cairo, which was as a second home to me. I got all the support, needed equipment, and materials in addition to welcoming atmosphere that made me able to academically improve myself.

I would like to thank my committee members, **Dr. Anwar Abd ElNaser** and **Dr. Medhat Al-Ghobashy.** Thank you for giving me your time and patience to evaluate my thesis.

Abstract

Corn silk possess antibacterial and antioxidant activities due to its phenolic compounds but they are of low bioavailability that requires some innovative techniques to develop such active ingredients in a safe and less toxic manner. Accordingly, silk extract SE was encapsulated in chitosan nanoparticles CS NPs, which is a natural and abundant polymer derived from chitin. Among 15 experimental trials via design expert software, the optimum formula of SE x\CS NPs was prepared at 800 rpm, 5hrs. on magnetic stirrer, and by CS: TPP ratio was 2.5:1. Then SEM showed the majority of particles size diameter in the range of 24.72, 36.89, 39, and 55.58 and 76.71 nm were confirmatory for DLS particle size measurements of SE 0.5\CS NPs, SE 1 \CS NPs, SE 1.5\CS NPs, and SE 2\CS NPs. FTIR results were confirmed the successful encapsulation and of SE in CS NPs by the appearance of the aromatic group bands at the wavenumber 1577.9 and 1417.5 cm^{-1}. The cumulative extract release percentage was compared in two pH media showing no difference in their release profile. The release behavior of SE from CS NPs in those pH was indicative for using SE x\CS NPs as a topical preparation. SE x\CS NPs were tested for their antioxidant activities where % inhibition (free radical scavenging activity) of the four preparations SE 0.5\CS NPs, SE 1 \CS NPs, SE 1.5\CS NPs, and SE 2\CS NPs showed 83.7, 84.7, 87.4, and 95.4% respectively higher than their corresponding amounts of free extract 31.5, 61.1, 74, and 87.4%. The TPC assay showed much lesser results for the four preparations of SE x\ CS NPs ranged from 2.6 to 3.7 mg GAE\ gm sample than that of their corresponding amounts of free extract which ranged from 16.5 to 35.7 mg GAE\gm sample. Also, the decreased values of TPC was indicative for the successful encapsulation of SE. The antibacterial test against *S.auerus* showed 100% BGI. In contrary, the antibacterial test against *E.coli* for the four preparations SE 0.5\CS NPs, SE 1\CS NPs, SE 1.5\CS NPs, and SE 2\CS NPs showed 70.44, 76.10, 82.51, and 98.27% BGI which was higher than that of their corresponding amounts of free extract 40.11, 59.30, 73.40, and 84.01% BGI.

List of abbreviations

BGI: Bacteria growth inhibition

CS NPs: Chitosan nanoparticles

SE: Silk extract

SOD: Superoxide dismutase

EPA: Environmental protection agency

FAO: Food and agriculture organization

FLW: Food loss and waste

IBC: Intercellular bacterial communities

MMT: Million metric tons

QIR: Quiescent intercellular reservoirs

RNS: Reactive nitrogen species

ROS: Reactive oxygen species

UTIs: Urinary tract infections

USDA: The United States department of agriculture

WHO: World health organization

List of figures

Figure 1.1 Human body organs colonized by bacterial flora (order of magnitude\ ml). [1,2] 2
Figure 1.2 Illustrative diagram for types of bacterial flora presents in case of hospitalized and non-hospitalized person.[5] 3
Figure 1.3 Atypical structure of gram positive and gram negative bacterial cell. [6] 4
Figure 1.4 Biofilm formation by S. aureus on an implant surface. [28] 6
Figure 1.5 Attachment of bacterial cells to surface followed by sequenced stages for the biofilm formation. [29] 7
Figure 1.6 (A) Hip acetabular implant surrounded by a remnant of biofilm.[31] **(B)** Autopsy of Lung with cystic fibrosis belongs to patient died with chronic P. aeruginosa infection. [32] 8
Figure 1.7 WHO data for antibiotic consumption by human health care as represented by 65 countries.[38] 10
Figure 1.8 According to UK government, the last discovery of the antibiotic agents was 30 years ago. [40] 11
Figure 1.9 Illustrative diagram for the consequences of oxidative stress. 12
Figure 1.10 FAO organization conceptual framework for food loss and waste management.[58] 14
Figure 1.11 Percentage of food loss based on the contributing countries referring to FAO**.** [58] 15
Figure 1.12 Percentage of food loss based on the type of food referring to FAO. [58] 15
Figure 1.13 Chart represents the estimated amounts of internationally produced corn in some countries (million bushels).[60] (adapted from USDA 2019/2020) 17
Figure 1.14 Corn shipments from different countries to Egypt (between 2015-2018).[66] 18
Figure 1.15 Corn kernel\seed worldwide usage, the estimated amounts (in million bushels) of corn kernels to produce these utilities. (USDA, between 1989 and 2019) [67] 18
Figure 1.16 The corn kernels edible and inedible parts (e.g. silk, husk, cob). (taken in the AUC laboratory) 19
Figure 1.17 (A) Simple phenolic compounds and polyphenols widely distributed in plant origins**. (B)** Modified chemical structures of subclasses of flavonoids and the basic chemical structure of anthracyanidines. 22
Figure 1.18 One of the structures of polyphenolic compound where the hydroxyl group is responsible for free radical scavenging activity. [116] 23
Figure 1.19 Four mechanisms explain the mode of action for the hydroxyl groups reacting with the free radicals.[117] 23
Figure 1.20 Global market size of nanomedicine by years and its influence on a wide range of sectors.[180–182] 29
Figure 1.21 Natural sources for formulating polymer based nanocarriers. [186] 30
Figure 1.22 Encapsulation or conjugation of drugs in nano-formulated systems which leads to the listed strengthen features of nanocarriers loading.[189,190] 31
Figure 1.23 Different herbal\plant extracts' biological activities tested after nano-encapsulation. [28] 32
Figure 1.24 Chitosan chemical structure after the deacetylation of chitin. [197] 33
Figure 1.25 (A) Ionic cross-linking \ Ionic interaction. **(B)** Precipitation \ Via a compressed air nozzle. **(C)** Emulsion droplet coalescence \ two separated preparations of emulsions are mixed eventually. [199] 34
Figure 1.26 Shredded corn husks, cobs, and silk were soaked in 85% methanol solvent. (taken in AUC laboratory). 36
Figure 2.1 Residue and filtrate prepared after Buchner apparatus filtration of corn husks, cobs, and silk. 40
Figure 2.2 TPC was determined as assay testing the serial dilution of gallic acid. 42
Figure 2.3 Schematic illustration for preparing corn silk extract followed by loading CS NPs with the extract and the characterization of the produced NPs. 43

Figure 2.4 Design expert software optimization after 15 experimental trials by controlling three variable factors. 44
Figure 2.5 Calibration curve of Corn silk extract in acetic acid solution. 46
Figure 2.6 DPPH mechanism of reaction with phenolic cimpounds.[20] 49
Figure 2.7 Ionic gelation technique for NPs preparation. (modified)[23] 50
Figure 2.8 The triple point of transformation at which solid matter turns into gaseous state. [25] 51
Figure 2.9 An illustration of the difference between scattered light intensity, correlation function and size distribution between the small particles and the large particles. [27] 52
Figure 2.10 The folded capillary cell representing the negative and positive electrodes. [29] 52
Figure 2.11 A Michelson interferometer in FTIR spectroscopy instrument to quantify and qualify the spectral fingerprint of any sample.[33] 54
Figure 2.12 Schematic illustration of sample electron beam interaction.[34] 55
Figure 2.13. SEM 1- electrons released from the gun. 2- the sealed vacuum chamber. 3-positively charged electrode. 4-the electromagnetic coil to force the electron beam into a lens. 5- electromagnetic coil to steer the electron beam. 6- scanning the beam through the tested object. 7-hitting of the object with the electrons. 8-detecting the electrons and transforming into visible picture.[36,37] 55
Figure 2.14 (A) Components of probe sonicator (B) schematic figure of the growth and collapse of bubble in acoustic cavitation process. [39] 56
Figure 2.15 Simplified Schematic diagram for principle of working of UV visible spectrophotometer. [42] 57
Figure 3.1 DPPH assay where the % inhibition plotted versus the serial dilution Ascorbic acid (Ref.), SE, HE, and CE. 59
Figure 3.2 Chart graph for $\%IC_{50}$ was obtained from the previous curve and plotted with SD for Ascorbic acid, SE, HE, and CE. 60
Figure 3.3 Chart graph for the phenolic concentration of SE in comparison to HE and CE, and plotted with SD… 60
Figure 3.4 Perturabtion plots and 3D graphs for the repsonses (A) particle size, (B) PDI, and (C) zeta potential influnced by CS:TPP mass ratio. 63
Figure 3.5 The responses (A) particle size, (B) PDI, (C) Zeta potential, and (D) EE% of the SE 0.5\CS NPs, SE 1\CS NPs, SE 1.5\CS NPs, and SE 2\CS NPs. 64
Figure 3.6 SEM pictures and histograms, at the magnification of 15.48 K (A) and (C) SE 0.5\CS NPs while at the magnification of 25 k; (B) and (D) SE 1\CS NPs. At the magnification of 25 k; (E) and (G) SE 1.5\CS NPs , (F) and (H) SE 2\CS NPs. 67
Figure 3.7 FTIR Chart graph for SE, empty CS NPs, and SE 2\CS NPs. 69
Figure 3.8 Release study patterns of SE 2\CS NPs in $_{P}$H 7.4 and 5.8. 71
Figure 3.9 DPPH assay (scavenging activity) expressed as the inhibition percentage for free SE, empty and encapsulated CS NPs. 72
Figure 3.10 TPC values for free SE, empty and encapsulated CS NPs. 73
Figure 3.11 Agar plates of E.coli colonies for SE corresponding amounts (A1) 0.5 mg\mL. (B1) 1 mg\mL. (C1) 1.5 mg\mL. (D1) 2 mg\mL. 74
Figure 3.12 E.coli colonies counted via imageJ software with their histogram for SE corresponding amounts (A2) 0.5 mg\mL. (B2) 1 mg\mL. (C2) 1.5 mg\mL. (D2) 2 mg\mL. 75

Figure 3.13 Agar plates of E.coli colonies for SE x\CS NPs (E1) SE 0.5 \CS NPs. (F1) SE 1 \CS NPs. (G1) SE 1.5 \CS NPs. (H1) SE2 \CS NPs. (I1) Empty CS NPs. 75
Figure 3.14 E.coli colonies counted via imageJ software with their histogram for SE x\CS NPs (E2) SE 0.5 \CS NPs. (F2) SE 1 \CS NPs. (G2) SE 1.5 \CS NPs. (H2) SE2 \CS NPs. (I2) Empty CS NPs. 76

List of tables

Table 1.1 Examples for gram positive and gram-negative bacterial infections. 5
Table 1.2 Classification of antibacterial agents based on mechanism of action either bacteriostatic or bactericidal action. [35] 9
Table 1.3 Examples for exogenous antioxidants and their mechanism of actions. 13
Table 1.4 Percentage of the wasted parts of some fruits and vegetables. (Adapted table)[59] 16
Table 1.5 Bioactive compounds extracted from various segments of the fruit and vegetable wastes. [59,90,92–100] 20
Table 1.6 The antioxidant phenolic compounds extracted from different natural sources and biological activities other than their antioxidant efficiency……..……..24
Table 1.7 Corn silk extracts biological activities and specifically the antioxidant and antibacterial activities.....25
Table 1.8 Nanomaterials-based applications in multiple fields among of which is the pharmaceutical\nutraceutical industry. 27
Table 1.9 Plant based- chitosan nanoparticles investigated for their antioxidant efficacy……..…32
Table 1.10 Biomedical applications of chitosan loaded nanoparticles.[199]…… 35
Table 1.11 Formulations and their abbreviations. 36
Table 2.1 Testing the influence of increasing silk extract concertation while fixing all the other conditions of preparing encapsulated NPs. 45
Table 3.1 Design expert's proposed factors and the responses which are estimated by DLS for each prepared sample (encapsulated NPs). 62
Table 3.2 SE\CS NPs at different SE concentrations and their responses particle size, PDI, zeta potential, and EE%. 64
Table 3.3 Particle size, zeta potential, and EE% of another encapsulated phenolic compounds in CS NPs. [192,194,241] 65
Table 3.4 Spectral bands that have been shifted, disappeared, and appeared in SE, empty CS NPs, SE x\CS NPs. . 69
Table 3.5 Antibacterial activity expressed as % of bacterial growth inhibition for (corresponding concentrations) SE, empty CS NPs, and SE x\CS NPs. 76
Table 3.6 Various SE concentration antibacterial activity against S.aureus and E.coli. [161 250 251] 77

List of equations

Equation 1 Antioxidant percentage of inhibition 42
Equation 2 Gallic acid caliberation curve equation..... 43
Equation 3 Total phenolic content equation..... 43
Equation 4 Silk extract in acetic acid solution caliberation curve..... 46
Equation 5 Encaspulation effeciecy percentage 47
Equation 6 Bacterial growth inhibition percentage..... 48
Equation 7 Amount of the released extract 49
Equation 8 Folin reagent interaction with phenolic compounds..... 50
Equation 9 Bohr model equation 57
Equation 10 Beer Lambert law 58
Equation 11 Relation between transmitted and incident light..... 58

Chapter 1

Introduction and literature reviews

1.1 Bacterial infection

1.1.1 Bacterial flora

In our bodies, bacterial cells are 10 times human cells. These bacteria are called normal flora and they reside on, and on body surfaces such as skin, gut, and mucous membrane. Most of them are harmless or even have beneficial proposes such as vitamins synthesis, transformation of food into less complex forms, and the stimulation of our immune system. Bacteria, in general, are considered ancient organisms, which existed 3 billion years ago as seen in fossils. They have passed through several evolutionary stages which enabled them to survive in various habitats, adhere to cells, produce poisons and toxins, resist drugs and our endogenous antibodies as well. [3]

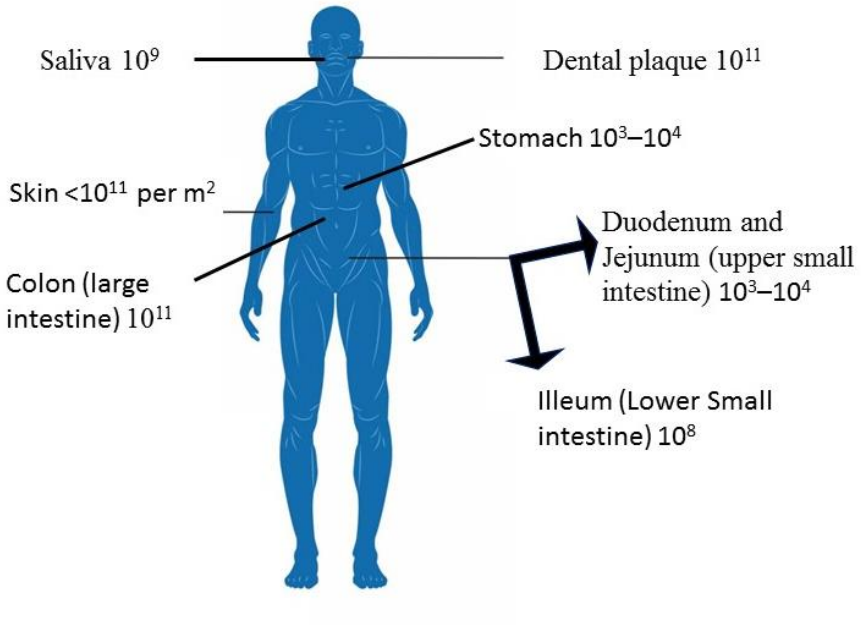

Figure 1.1 Human body organs colonized by bacterial flora (order of magnitude\ ml). [1,2]

As shown in **figure 1.1**, normal flora is resident all over our body. They represent the normal habitat of our bodies since the moment of birth. Normal flora reside within and on our body, roughly, to protect us from the diseases caused by pathogenic bacteria and help in the digestion process[3]. For example, *Staphylococcus aureus* is present in 10 to 40 percent of adults' nose and perineum whereas *Staphylococcus epidermidis* 90 percent of the aerobic inhabitants of the skin as shown in **figure 1.2**. Bacterial florae are also present in urogenital area differs from person to another based on his\her age, pH, and hormonal levels. For example, *E. coli* mainly dominates in the pH 7. [4]

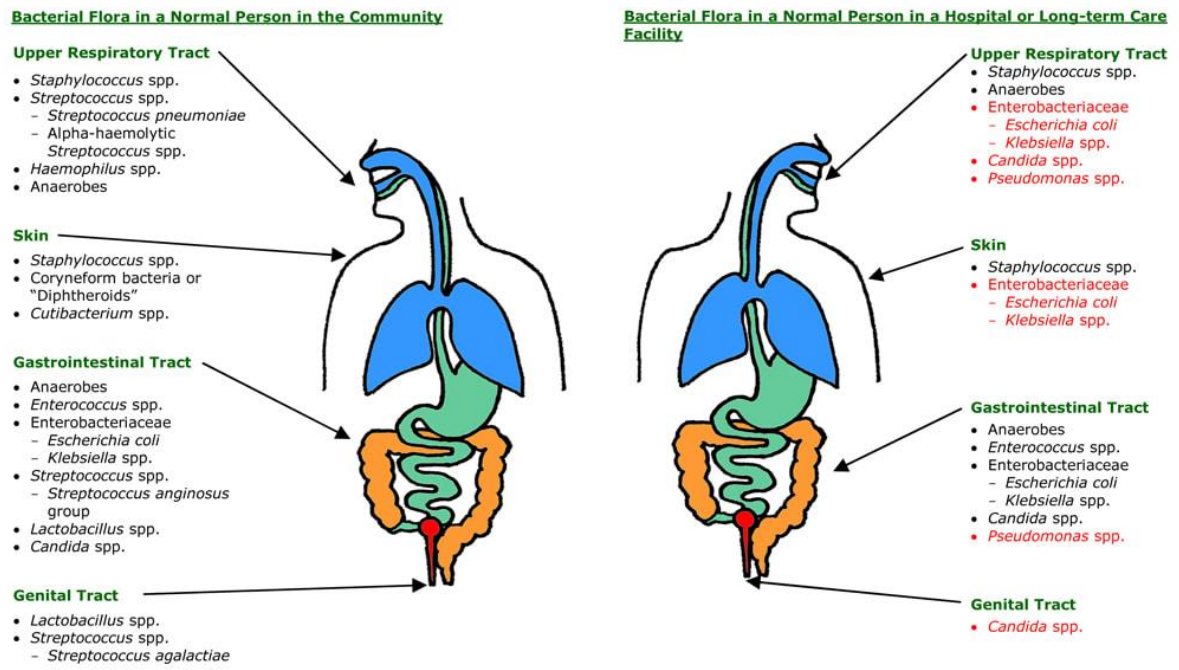

Figure 1.2 Illustrative diagram for types of bacterial flora presents in case of hospitalized and non-hospitalized person.[5]

1.1.2 Bacteria

Antoni van Leeuwenhoek was the first scientist who studied bacteria under the microscope in the late seventeenth century. Bacteria are prokaryotes which are characterized by having nuclear body without membrane-bound cytoplasmic organelles and reproducing by binary fission. Under the microscope, they are classified based on their shapes either cocci, rods, or spirals. Examples for cocci, rods, and spiral shaped bacteria are *Staphylococcus aureus* and *Streptococcus*, *Bacillus* and *Clostridium* species, and *Vibrio cholera* and *Treponema pallidum* respectively. Flagella, as shown in **figure 1.3**, help the bacteria to move and Pili are hair-like surface structures which allow the bacteria to adhere to host surface. Capsules' structure composes either of a viscous polysaccharide gel or a slime like layer. The thickness of capsules plays a significant role in the resistance of the bacteria to phagocytosis[3,6,7]. In 1884, a staining method was developed by and named after Hans Christian Gram. This method enabled scientist to classify the bacteria by gram staining into a gram positive and gram-negative bacterium according to their gram staining susceptibility. Gram-positive bacteria such as *staphylococcus aureus* are characterized by having peptidoglycan cell wall of thickness ranges from 20-80nm, whereas gram negative bacteria such as *Escherichia coli* have thinner cell wall that ranges from 5-10nm thickness. Thus, Gram positive bacteria can retain the crystal violet dye "gram dye" in contrary to the gram negative. [6,7]

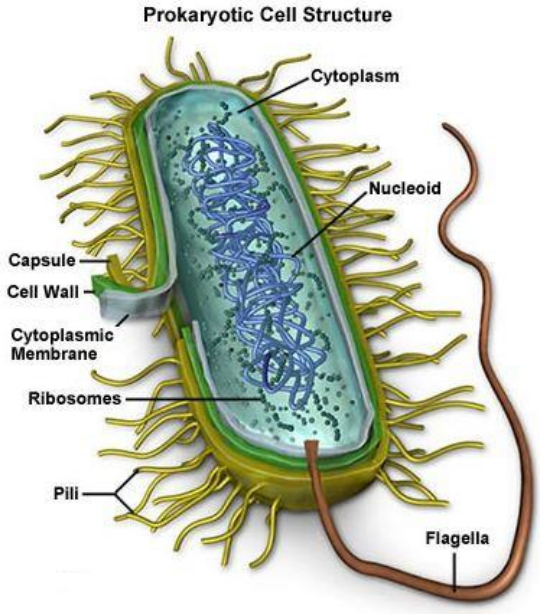

Figure 1.3 Atypical structure of gram positive and gram negative bacterial cell. [6]

1.1.3 Bacteria from Symbiosis to Pathogenesis

Symbiosis is a term referred to a mutual benefit relationship between the bacteria and the human host. As explained in the above paragraphs, generally bacteria are harmless, with no interest to kill the human host, and their survival depends on their multiplying. [8] However, the first two scientists who revealed the role of bacteria in causing diseases were Louis Pasteur and Robert Koch during the nineteenth century.[5] Bacterial infectivity, in general, is as a result of imbalance between the host resistance mechanism (e.g. immune system) and the bacterial virulence factors. In other words, bacterial invasion along with their multiplication in the host tissues, is defined as infection. Genetic and molecular basis in bacterial cells controls their virulence factors which are encoded on their cellular chromosomes, plasmids, or transposon. Virulence factors enable the bacteria to cause the infection which varies from adherence factors, invasion factors, capsules, siderophores, endotoxins, to exotoxins. [9] As shown in **table 1.1**, most of the infection caused by gram positive and gram negative bacteria.

Table 1.1 Examples for gram positive and gram-negative bacterial infections.

Gram positive bacteria	e.g. *Staphylococcus aureus*	Skin infections, pneumonia, endocarditis, septic arthritis, Osteomyelitis, and bacteremia.	[7,10,11]
	e.g. *Streptococcus pneumoniae*	Otitis media, meningitis, pneumonia, and sinusitis.	[7,12,13]
	e.g. *Clostridium difficile*	*C. difficile*-associated diarrhea (CDAD), severe pseudomembranous colitis (PMC)	[14–16]
Gram negative bacteria	e.g. *Klebsiella*	Pneumonia, wound or surgical site infections, and meningitis, intra-abdominal infection, bloodstream infection (BSI), meningitis and pyogenic liver abscess (PLA	[17–19]
	e.g. *Pseudomonas aeruginosa*	Malignant external otitis, meningitis, pneumonia, and septicemia.	[20,21]
	e.g. Escherichia *coli*	Hemorrhagic colitis and UTIs	[22–24]

1.1.4 *Escherichia coli* and *staphylococcus aureus* infections

Bacterial infection happens when the host immune system is evaded by the bacterial invasion. This type of infection can be presented with or without apparent clinical symptoms. Accordingly, bacterial infection is categorized as asymptomatic and symptomatic persistent infection. The significance of the asymptomatic infection is the appearance of malignancy in most cases after a long period of time. For example, at the beginning, *Helicobacter pylori* primary cause gastritis and subsequently it can turn into gastric carcinoma in case of disseminative disease condition. On the contrary, symptoms that are associated with *Escherichia coli (E. coli)* or *Staphylococcus aureus (S. Aureus)* infections can be both acute and chronic. Accordingly, *E. coli* and *S. aureus* are on the top of the examples of pathogens that cause symptomatic persistent infections. Host environment and the type of bacteria are important factors that enable the pathogen to be persistent. On the other hand, excessive intake of antibiotics provokes the host immune response to intensive oxidative stress mechanism. As a consequence, Intensive oxidative stress leads to host cell deterioration.[25]

The WHO has reported that antimicrobial resistance to be the most threatening perspective of bacterial infections, which is becoming an excruciating public health threat. WHO has specifically mentioned *E. coli*, as multi-resistant enteric pathogen, and *S. aureus*, such as methicillin resistant as two of the leading resistant pathogens; *E. coli* is commonly co-existing in the human guts as a normal flora. However, under certain circumstances, *E. coli* can be pathogenic. This can happen

when there're an increased concentration of *E. coli* from being transmitted through contaminated water or food and suppressed host immune system.

E. coli can cause variety of infections such as urinary tract infections (UTIs). UTIs are reported to be more prominent between women than men. Furthermore, the percentage of women who suffer from recurrent UTIs (e.g. six episodes or more) yearly is 1-2%. [24] Accordingly, the recurrence of this infection is a substantial social and fiscal cost as the amount of money spent on UTIs treatment estimated around billions of dollars every year. More importantly, UTIs have a serious impact on the patients' quality of life. [26]

One the other hand, *S. aureus* can cause medical devices related infections such as biofilm formation on the surface of a medical device (e.g. intravascular catheter). *S. aureus* has this tendency owing to its virulence capability on the cell surface and immune evasion ability even though it plays a role as human commensal bacteria. Moreover, 14 % of the surgical site infections are caused by the pathogenic *S. aureus*. Among the serious consequences of medical devices related infections is the *S. aureus bacteremia* where its mortality rate has been reported to be more than 60 %. [27] **Figure 1.4** demonstrates the mechanism of biofilm formation by *S. aureus* strain in which the first stage involves the attachment of the organism to the medical device surface. The second stage includes multi-layered biofilm formation due to organism cellular proliferation. Uncontrolled cases can develop into planktonic state where the pathogenic *S. aureus* will form biofilms in other sites of the host. [28]

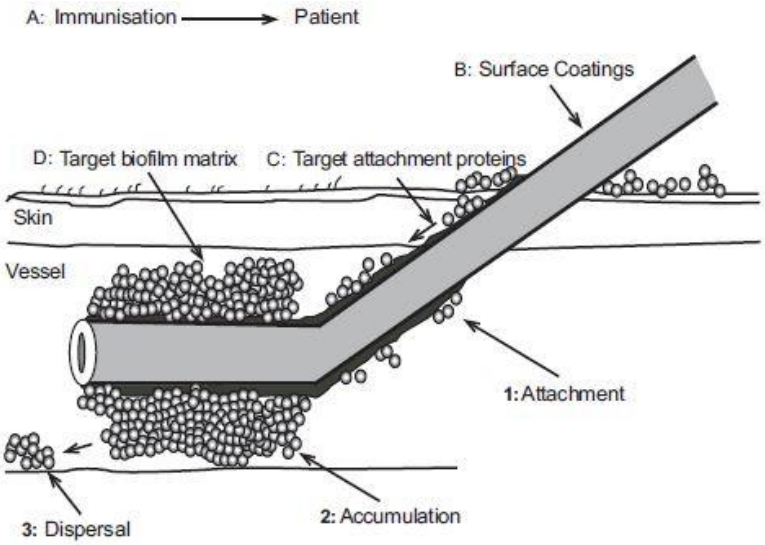

Figure 1.4 Biofilm formation by *S. aureus* on an implant surface. [28]

1.1.5 Biofilm formation

Microbial cells have the tendency to be densely accumulated on various surfaces, either living or inanimate surfaces to form very complex and sedentary communities. The surfaces can start from industrial pipes reaching to biomaterials such as contact lenses and implants. Bacterial biofilm role is to overcome the antibacterial actions as well as the immune defense mechanism of the host. **Figure 1.5** illustrates the first stage of biofilm formation where the planktonic bacteria tend to adhere to the surface reversibly. Then, irreversible attachment takes place in the second and third stages where the bacteria favors to form monolayer of extracellular matrix followed by multi-layer formation as a protection mechanism. Once the biofilm growth reaches maturation stage (fourth stage), portions of the mature biofilm start to detach as planktonic cells for initiating another cycle in other sites.

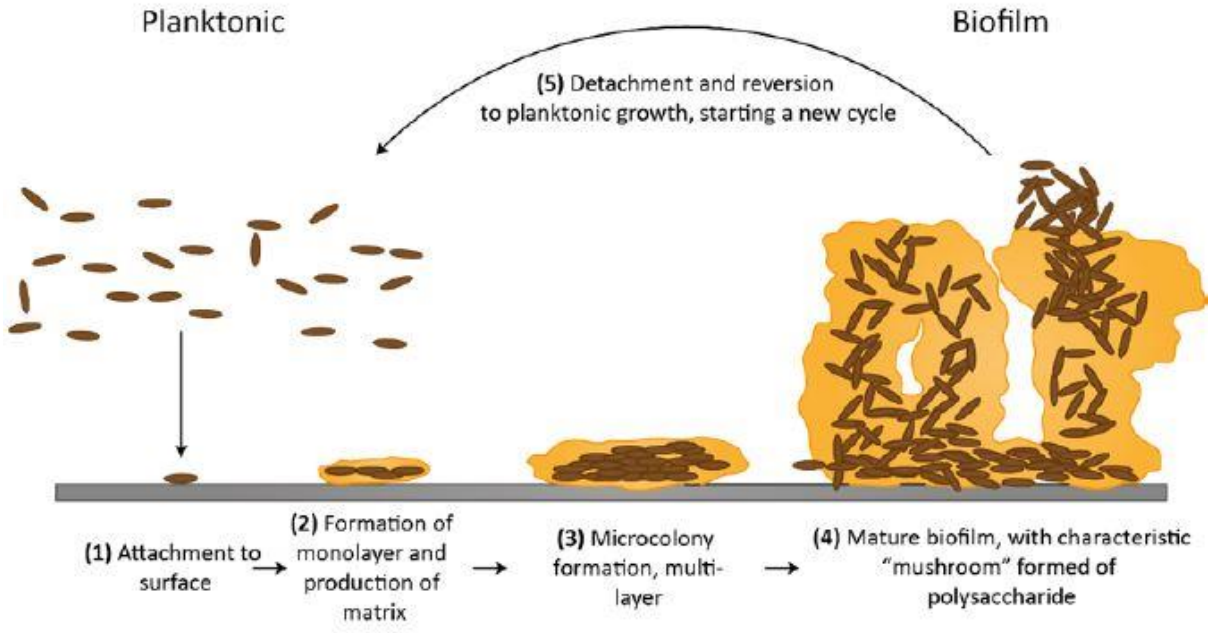

Figure 1.5 Attachment of bacterial cells to surface followed by sequenced stages for the biofilm formation. [29]

Accordingly, it was found that the chronicity of diseases such as cystic fibrosis, diabetic chronic wounds, otitis media, and osteomyelitis is significantly correlated to the biofilm formation.[29,30] **Figure 1.6** shows two examples of biofilm formation consequences.

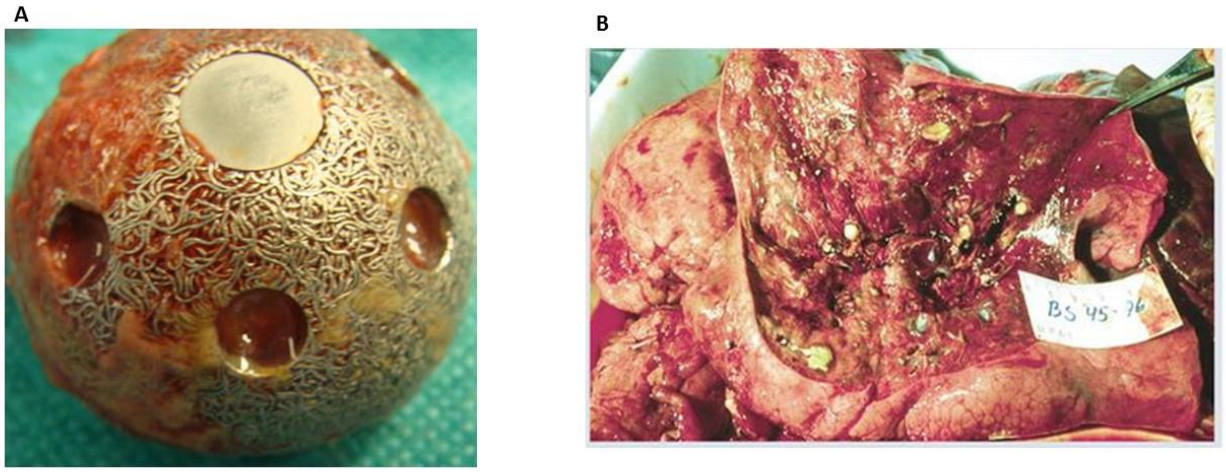

Figure 1.6 (A) Hip acetabular implant surrounded by a remnant of biofilm.[31] **(B)** Autopsy of Lung with cystic fibrosis belongs to patient died with chronic P. aeruginosa infection. [32]

Microbial biofilm formation is one of the serious consequences of bacterial multiplication as 65 percent of all bacterial infections are associated with its formation. Among the serious complications of biofilm formation is the native valve endocarditis in which the bacterial growth leads to inflammation in the cardiac vascular endothelium and the pulmonic valves. Biofilm formation can be associated with either device or non-device related infections. The highest percentage of biofilm formation was recorded for ventricular-assisted devices to be 40% followed by 10% for ventricular shunts, 4% for pacemakers and defibrillator, and 2% for joint prostheses and breast implants. Moreover, biofilm formation on soft and hard contact lenses are mainly caused by *E. coli, P. aeruginosa, Staphylococcus aureus,* and *Staphylococcus epidermidis* while on urinary catheters by *E. coli, Enterococcus faecalis, S. epidermidis,* and *P. aeruginosa*. On the other hand, non-device related infections involve periodontitis which casued by *P. aerobicus* and *Fusobacterium nucleatum* and Osteomyelitis. [33]

1.1.6 Treatment with antibiotics

Throughout the past decades, scientist have done extreme efforts to overcome the bacterial infections. In 1909, Paul Ehrlich discovered a chemical substance named arsphenamine with antibacterial activity against syphilis infection. At that time, he considered this chemical substance as a chemotherapy other than an antibiotic agent. After 20 years later, Alexander Fleming accidently discovered penicillin which was produced by a fungus called *Penicillium notatium* (named in the modern history). Penicillin was nicknamed “the wonder drug” at the end of world war II owing to its role in treating many common diseases at that period. [34] **Table 1.2** summarizes some of the antibacterial agents that kills bacteria by either targeting bacterial cell wall

(bactericidal) or inhibiting the growth of bacteria (bacteriostatic). Some of those antibacterial agents are effective against gram negative and others are against gram positive bacteria with a narrow spectrum. Whereas others possess broad spectrum efficiency over a wide range of bacteria, both gram negative and gram positive. [35] The golden era of discovering new antibiotic classes is between 1950s and 1970s. However, bacterial resistance emerged after years of misusing antibiotics in addition to the lack of any new discovery for antibacterial agents. Researchers focused on making modification for the existed antibacterial agents. [36,37]

Table 1.2 Classification of antibacterial agents based on mechanism of action either bacteriostatic or bactericidal action. [35]

Antibacterial classification	**Bacteriostatic antibacterial**	**Bactericidal antibacterial**
Examples	Sulphonamides	β-lactams e.g. penicillin, cloxacillin, and flucloxacillin. (narrow spectrum)
	Spectinomycin	Carbapenems, β-lactam/β-lactamase inhibitors. Cephalosporin first generation,(narrow spectrum), cephalosporin third, fourth, and fifth generation (broad spectrum).
	Amphenicols, e.g. chloroamphenicol	Aminoglycosides (broad spectrum)
	Tigecycline	Quinolones and flouroquinolones (broad spectrum)
	Erythromycin, clarithromucin and azithromycin (broad spectrum)	Vancomycine (narrow spectrum)
	Linezolid	Polymyxin B and colistin

1.1.7 Antibacterial resistance

"Overuse and misuse of antibiotics are the leading causes of antimicrobial resistance. Without effective antibiotics and other antimicrobials, we will lose our ability to treat common infections like pneumonia," said by Dr Suzanne Hill, WHO. As shown in **figure 1.7**, in the WHO report, the European region supplied a complete data for antibiotic usage. It was found to be 17.9 drug daily doses per 1000 inhabitants. Other regions showed limited access for their data about antibiotic consumption. [38]

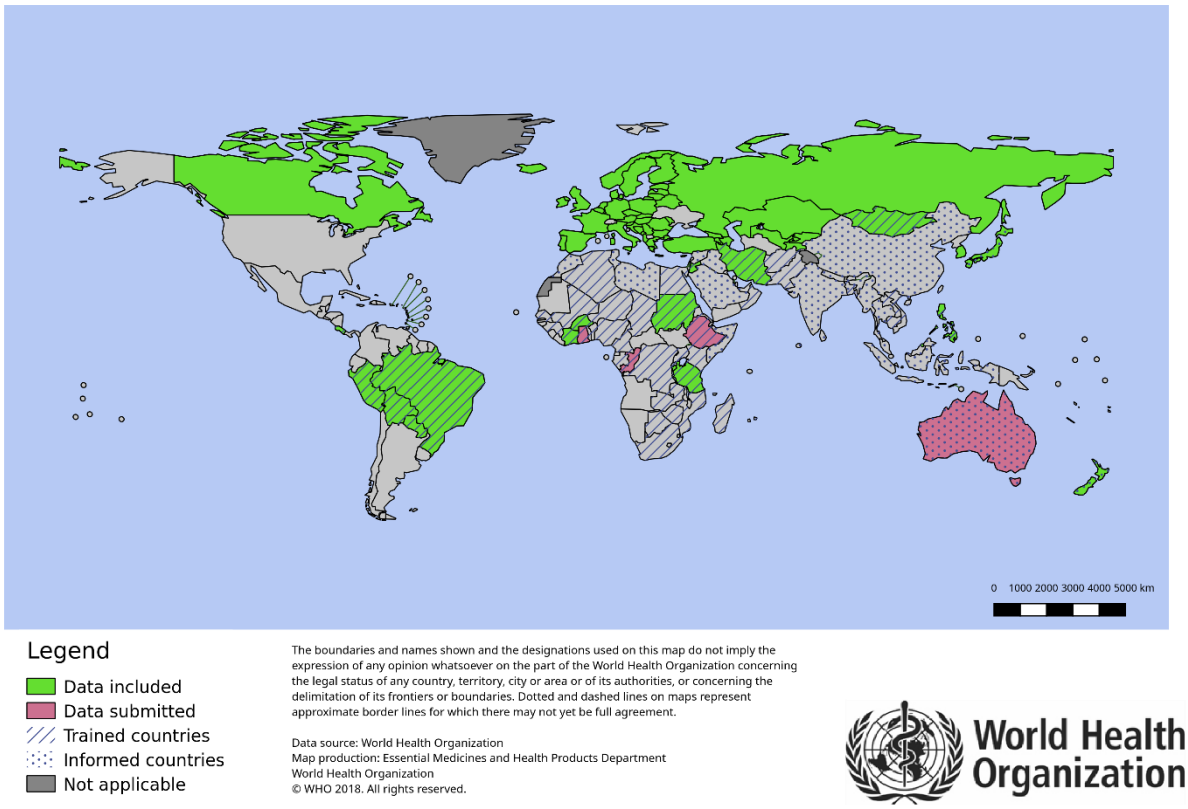

Figure 1.7 WHO data for antibiotic consumption by human health care as represented by 65 countries.[38]

Antimicrobial resistance is an urgent threat for the public health. According to the centers of disease control, in the united states, more than 35,000 people die due to the antibacterial resistance infections annually[39]. The UK government has also referred to the significance of antibiotic resistance. As shown in **figure 1.8**, UK government directed the focus on the absence of discovering any new classes since 30 years ago. They forecasted that if the global action failed to target the current problem, the number of deaths will reach 10 million deaths yearly until 2050. Financially, they expect the loss of 66 trillion pounds as a result of lower productivity worldwide.[40] In addition, food and agriculture organization of the unites nations revealed that the excessive usage of same antibiotics is not limited for humans only, it also includes plants. Thus, the problem of antibacterial resistance was magnified to involve the appearance of plant-origin resistant bacteria. [41]

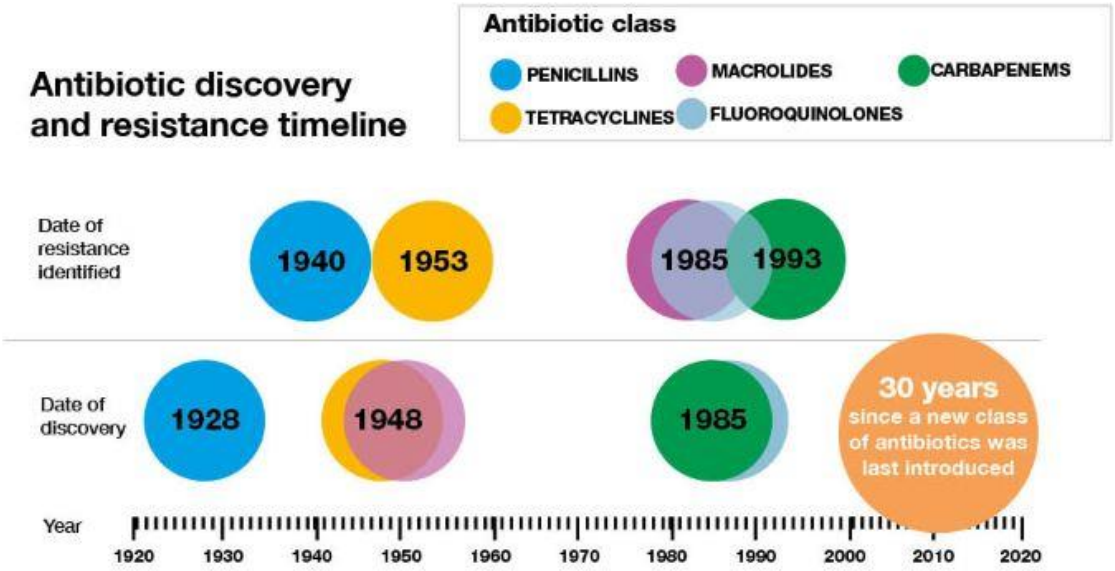

Figure 1.8 According to UK government, the last discovery of the antibiotic agents was 30 years ago. [40]

1.2 Oxidative stress

Recent studies have been focused on the correlation between the chronic diseases and the oxidative stress phenomenon. Human body has auto-oxidative mechanism within the normal cells (e.g. mitochondria) [42,43] by which it is capable to defend itself against any abnormality either a bacterial invasion or biomolecules deterioration. In normal cases, this mechanism is controlled by two balanced systems known as: the reactive oxygen species (ROS) or the reactive nitrogen species (RNS) and the endogenous antioxidant agents. However, the tendency of the imbalance between ROS\RNS and the antioxidant agents in the body is the leading factor of chronic diseases occurrence[44]. ROS are represented by free radicals and non-radicals (eventually converted into radicals). For example, radicals could be superoxide radical anion ($^{\bullet}O_2^-$), hydroprexoyl radical ($HO_2^{\bullet}$), hydroxyl radical ($HO^{\bullet}$), and peroxyl radicals ($ROO^{\bullet}$). The fundamental cause of ROS excess level in our biological system could lead to exposing the humans to multiple harmful conditions. Some of the basic levels of free radicals that affect our lives are the surrounding UV radiations, pollution, and chemicals (e.g. heavy metals) that pose a threat to humankind on daily bases.[45,46] This is in addition to the high level of endogenous sources of ROS which arises from the human biological process and not encountered by enough endogenous antioxidant agents. ROS are known to induce damaging to biomolecules within nucleic acids, lipids, proteins, and carbohydrates in our body**.** [47]Therefore, this leads to increase in the incidence of chronic diseases, among wide range of the population, such as cardiovascular dysfunctions, diabetes millets,

hypertension, aging, and cancer.[48] Moreover, despite the neuronal dysfunction and neurodegenerative diseases that are accompanied with Alzheimer disease, Parkinson disease, and amyotrophic lateral sclerosis (ALS) have been a mystery for centuries, recent investigations have revealed that ferroptosis caused by oxidative stress can be a major factor in these neurodegeneration processes. Ferroptosis involves the production of lipid soluble ROS facilitated by transition metal iron (Fe), and eventually cell apoptosis along with cell death occurs.[49] **Figure 1.9** summarizes the leading factors and the propagation of cellular damage based on oxidative stress consequences.[47]

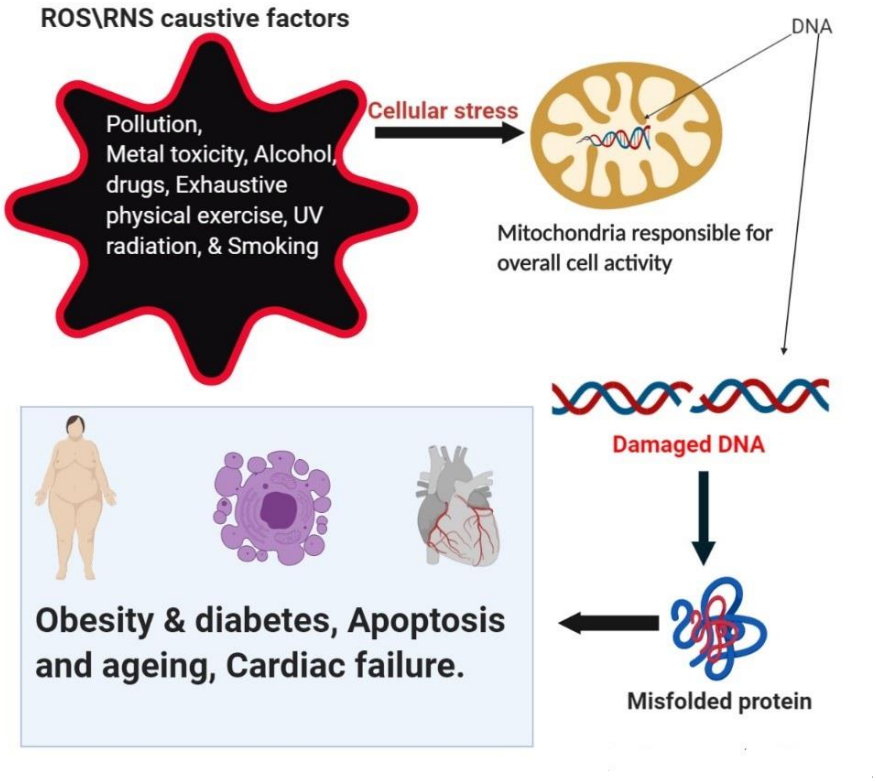

Figure 1.9 Illustrative diagram for the consequences of oxidative stress.

1.2.1 Antioxidant agents

Antioxidants are categorized into direct and indirect antioxidants. The direct antioxidants play significant role in counteracting the adverse effect of ROS\RNS. In this regards, antioxidants can be in the form of either a single oxygen quencher, an electron donor, a hydrogen donor, an enzyme inhibitor, a metal chelating agent, or a radical scavenger.[50] As a general rule, free radicals or named pro-oxidants are stabilized and neutralized to overcome the damage of any normal biomolecule by two possible mechanisms of actions either by: (i) chain breaking mechanism which relies on donating an electron to the free radical, or (ii) ROS\RNS initiators removal mechanism which involves the quenching of the initiator catalyst. The indirect endogenous

antioxidants can be classified as enzymatic based antioxidants. [51] For example, superoxide dismutase (SODs) is an enzyme that catalyzes the transformation of superoxide anion free radical into oxygen and hydrogen peroxide. This enzyme is in the mitochondria, the cytoplasm, and extracellular environment as well.[52] Another enzyme based system is glutathione enzyme system that contains glutathione, glutathione-s-transferase, glutathione reductase, and glutathione peroxidase enzymes. The four selenium co-factors present in the structure of glutathione peroxidase enzyme can catalyze the breakdown of hydrogen peroxides. Whereas glutathione-s-transferase act on the lipid peroxides.[53,54] On the contrary, uric acid, ascorbic acid (vitamin C), α-tocopherols (vitamin E), melatonin are non-enzymatic based antioxidants that interact directly with the free radicals and undergo reduction. [45,51]

There is another type of antioxidants known as exogenous antioxidants which can only be supplied from an external source as our diets. The most known exogenous antioxidants are vitamins E and C. Vitamin C has the capability to recycle vitamin E, and that is why the presence of these two vitamins together is essential in case of a good dietary intake. Also, vitamin C concentration range from 60-70µmol\L in the plasma is a good indication for normal human status. [55] **Table 1.3** shows more examples of exogenous antioxidants that are available in both dietary and plant sources.

Table 1.3 Examples for exogenous antioxidants and their mechanism of actions.

Exogenous antioxidants	Mechanism of work	Source
Vitamin E	Vitamin E is a lipid soluble that prevent lipid peroxidation leading to cell membrane stabilizing. Also, its Antiproliferative activity against vascular smooth muscle cells.	[45,46,48]
Polyunsaturated fats intake e.g. Fish oil (rich in ϙ 3 PUFA)	Inhibits nitrogen free radical generation (increasing the gene expression of glutathione-s-transferase enzyme).	[56]
Minerals e.g. magnesium	Reduces glutathione reductase activity. In turn, it prevents the oxidation of proteins.	[57]
Phytochemicals (plant origin) e.g. Flavonoids, phenols, terpenoids, steroids, and polyphenols.	Blocks the propagation of oxidative reactions.	[46,48,57]

1.3 Fruit and vegetable waste management

1.3.1 Fruit and vegetable waste amount

Figure 1.10 presents most of the possible ways for the food loss and waste (FLW). Generally, Food loss and waste is major issue that has been under investigation for years by various national or international organizations, among of which is the FAO. Referring to the latest FAO report in 2019, it is confirmed that FLW is a globalized problem, and many countries all over the world adversely contributes as demonstrated in **figure 1.11**. Specifically, fruits and vegetables wastes represent more than 20% of the total food loss globally. More than 25 percent of food loss is occupied by root, tubers and oil-bearing crops wastes as illustrated in **figure 1.12.**

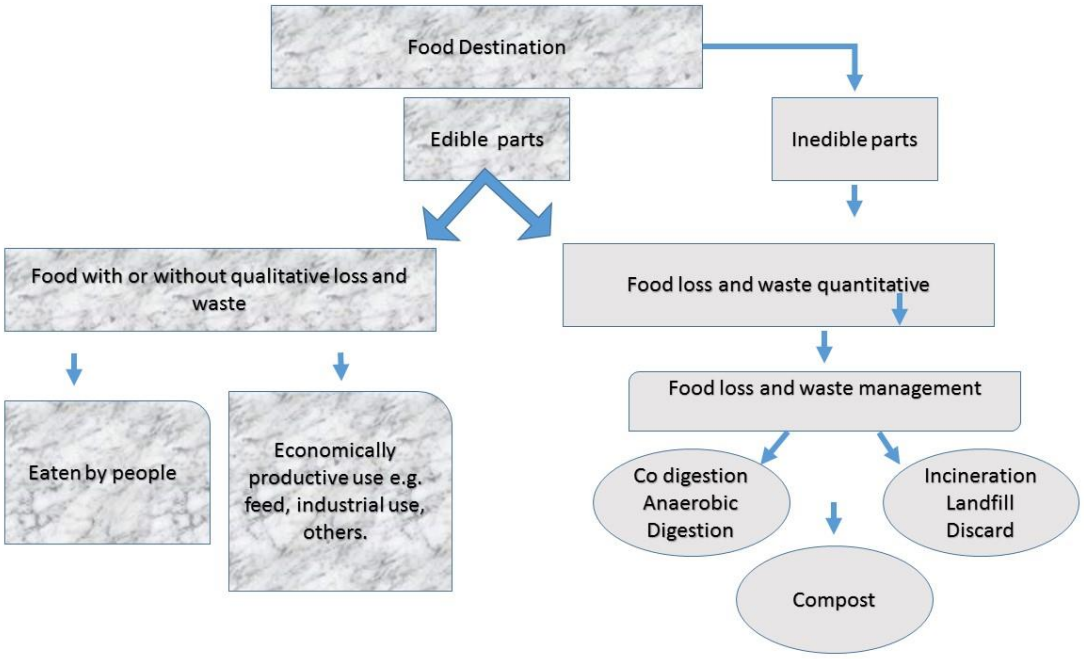

Figure 1.10 FAO organization conceptual framework for food loss and waste management.[58]

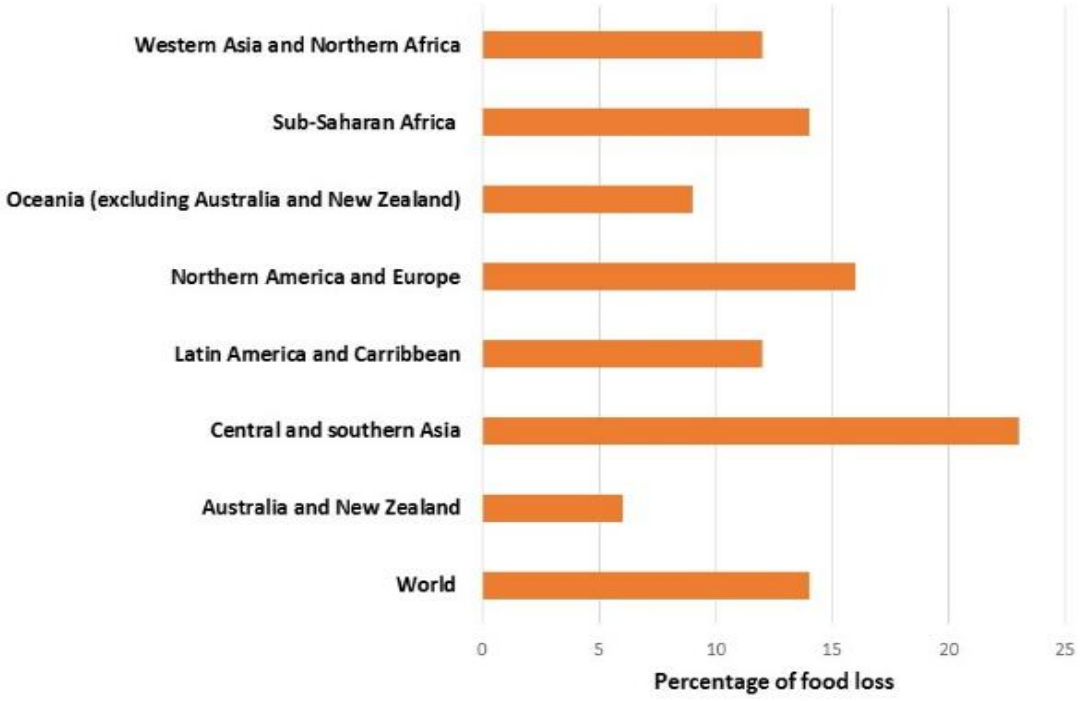

Figure 1.11 Percentage of food loss based on the contributing countries referring to FAO**.** [58]

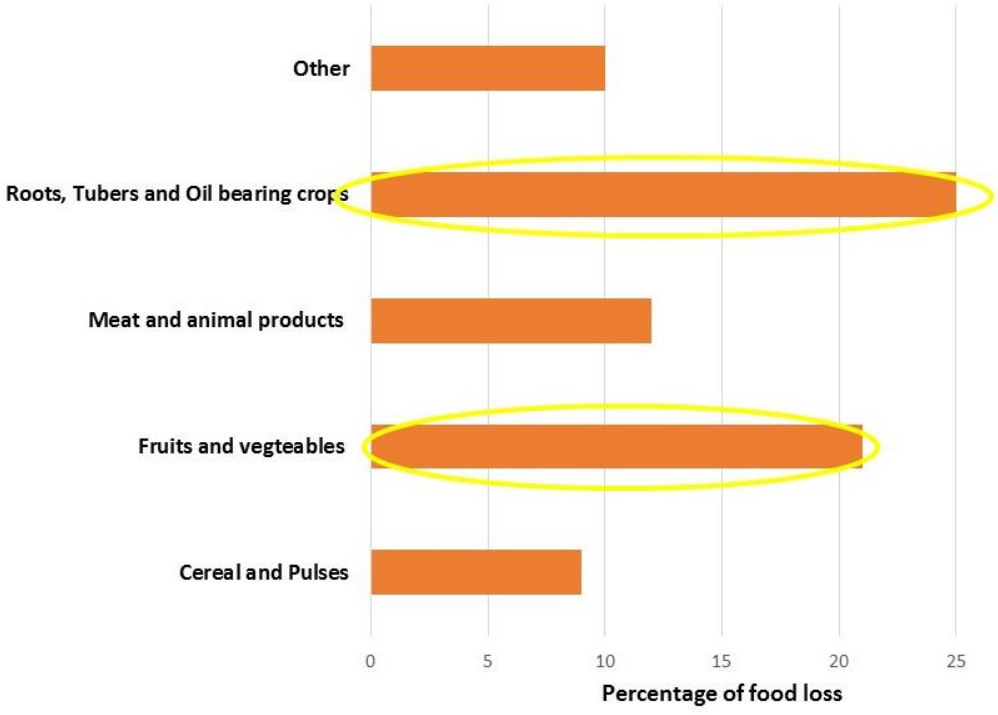

Figure 1.12 Percentage of food loss based on the type of food referring to FAO. [58]

The global production of fruits and vegetables reaches 124.73 million metric tons (MMT) for citrus, 84.63 MMT for apples, 114.08 MMT for bananas, 45.22 MMT for mangoes, guavas, and mangosteens, 3820 MMT for potato, and 171 MMT for tomatoes. In parallel to this high

production amounts there are improper handling methods throughout food handling and supply chain. Improper handling starts from the harvesting stage until it is ready for consumption. During all these stages, food undergo stressful circumstances under which it became a loss or waste which reflects on the environment through emitting greenhouse gases due to their decomposition in the landfill or being burned. As demonstrated in **table 1.4**, Sagar *et al* reported the amount of wasted parts which obtained from processing some fruits and vegetables. [59]

Table 1.4 Percentage of the wasted parts of some fruits and vegetables. (Adapted table)[59]

Commodity	Nature of waste	Typical losses and waste (%)
Apple	Pomace, peel, and seeds	-
Banana	Peel	35
Citrus	Rag, peel, and seeds	50
Dragon fruit	Rind, seeds	30 to 45
Durian	Skin, seeds	60 to 70
Grapes	Skin, stem, and seeds	20
Mango	Pell, stone	45
Passion fruit	Skin, seeds	45 to 50
Peas	shell	40
Pineapple	Core, skin	33
Potato	Peel	15
Rambutan	Skin, seeds	50 to 65
Tomato	Core, skin, seeds	20
Onions	Outer leaves	-
Papaya	Rind and seeds	10 to 20
Jackfruit	Rind and seeds	50 to 60

In addition to the table mentioned fruits and vegetables, corn crops by products are also included among food wastes. According to USDA world corn production is substantial as seen in **figure 1.13.** [60]Consequently, inedible\unwanted parts of corn are left useless in huge amounts after corn processing such as cob, husk, and silk. At that point, studies are conducted on utilizing the unwanted parts of corn. [61–63]

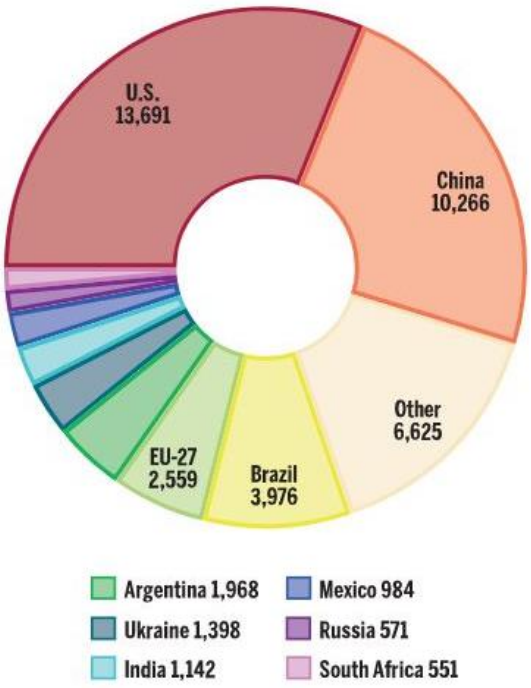

Figure 1.13 Chart represents the estimated amounts of internationally produced corn in some countries (million bushels).[60] (adapted from USDA 2019/2020)

1.3.1.1 Corn and its wastes production in Egypt

In general, corn dominates the third place among the produced crops worldwide after wheat and rice as corn production reaches 780 million metric tons every year. Corn is from kingdom (Plantae), Family (Poaceae), Subfamily (Panicoideae), Genus (Zea), Species (mays), and Synonyms (Maize, corn). The genus Zea is subdivided into four species *Z. diploperennis*, *Z. luxurians*, *Z. nicaraguensis*, and *Z. perennis* which are wild grasses. Expect for the fifth species is *Zea mays L*. (corn) which is cultivated.[64,65]

Egypt's corn production in the marketing year 2018/2019 to 2019/2020 has increased by 6 percent from 6.8 to 7.2 million metric tons (MMT), according to the United States Department of Agriculture (USDA). USDA reported that the harvest area for the white corn is 600,000 hectares that is much higher than that of the yellow corn. Yellow corn production covers only 20 percent of the Egyptians feed demand. Thus, Egypt imports yellow corn from three main suppliers; namely Argentina, Ukraine, and Brazil, and the amounts of shipments (in metric tons) are illustrated in **Figure 1.14** versus the years of importing. [66]

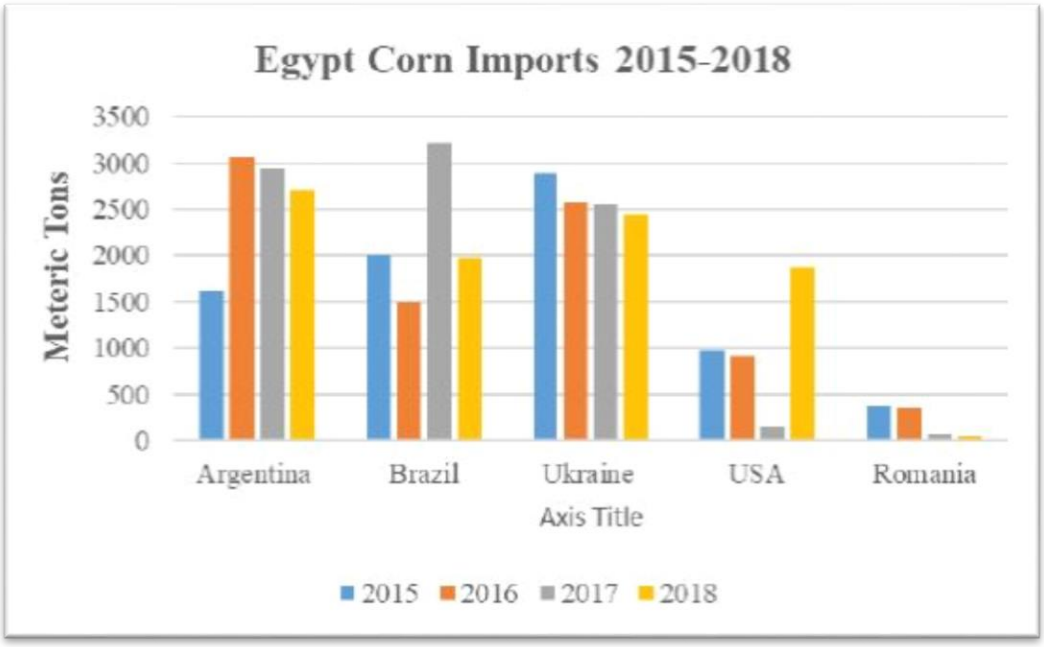

Figure 1.14 Corn shipments from different countries to Egypt (between 2015-2018).[66]

Therefore, there are numerous benefits that can come out of the high production of corn and its wastes. All corn parts are inedible except for the corn seeds or kernels. As estimated by USDA, corn seeds can be utilized in many levels as shown in **figure 1.15.**[67]

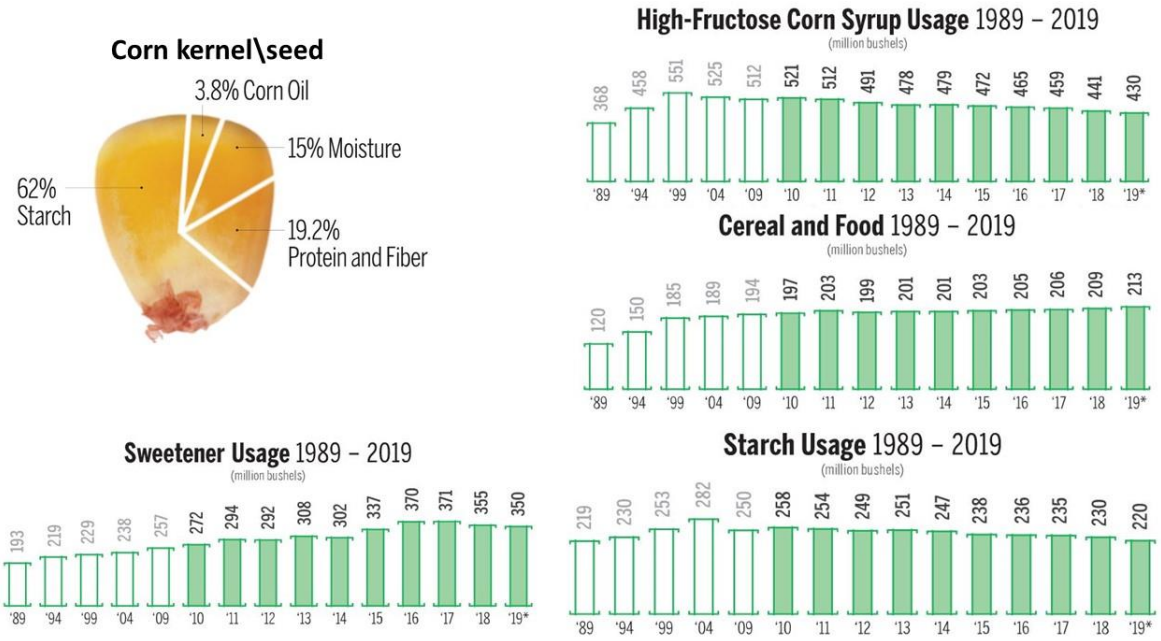

Figure 1.15 Corn kernel\seed worldwide usage, the estimated amounts (in million bushels) of corn kernels to produce these utilities. (USDA, between 1989 and 2019) [67]

In **figure 1.16**, three corn parts and their possible utilization are demonstrated. The inedible parts are considered unwanted waste or byproducts of corn. Corn cob is known for its usage in suitable

animal bedding owing to the role of its compositional parts (e.g. pith, woody ring, and chaff\beeswing parts from the inner to the outside respectively) that absorbs water up to 5 pounds. Also, after their grinding process, their particle size aid in acting as a carrier for pesticides and animal medication. [68,69] Whereas corn husks which are the paper like texture part surround the corn ear, are used for preparing daily products such as baskets, straw hats, and papers. [70] The production of corn increases in an obvious manner; corn wastes rise as well. Henceforth, the scientific community shifted their research focus on the inedible waste corn parts to possible serve variety of scientific purposes such as construction engineering, sustainable development engineering, and pharmaceutical field. Basically, most of the research studies conducted on corn cobs and husks are due to their structural component which mainly composed of lignocellulose as studied by Awosuis *et al*.[71] As reported by Takada *et al*. and Zheng *et al*., hemicellulose and lignin are the main components of corn cob.[72,73] Tsai *et al.* reported the preparation of high surfaced area carbon adsorbent by potassium hydroxide, carbon hydroxide, and carbon dioxide for the purpose of utilizing corn cob wastes in water treatment and toxic gas purification. [62] Another study confirms the transformation of corn cob into beneficial eco-friendly biosorbent that can treat contaminated water with carbofuran.[74] Another studies proves the effectiveness of preparing adsorbents from corn cob wastes.[75,76] Also, Biofuel production has been the focus scope for the studies on corn cob. [77–80] Regarding corn husks, the most abundant component in their structural formula is cellulose, hemicellulose and lignin. [81–84] Their produced fibers are value-added products to reinforce other low density polymers through increasing their mechanical properties via enzymatic treatment. [85–89]

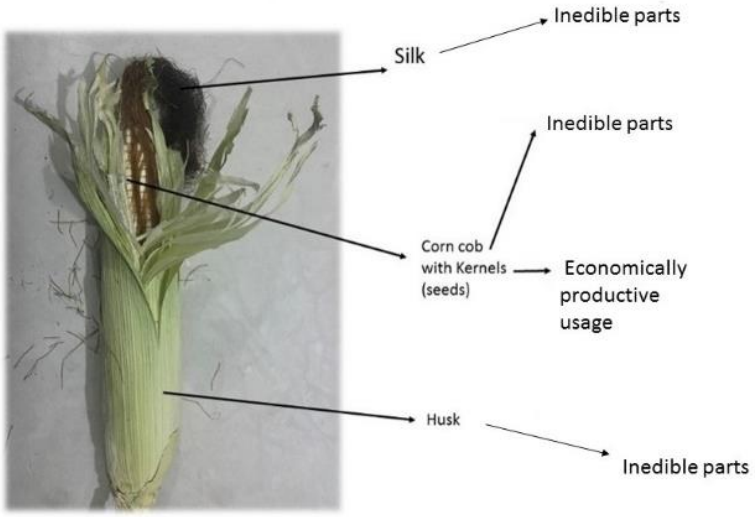

Figure 1.16 The corn kernels edible and inedible parts (e.g. silk, husk, cob). (taken in the AUC laboratory)

1.3.2 Bioactive compounds from the fruit and vegetable Wastes

Table 1.5, Types of bioactive compounds obtained from fruit and vegetable wastes are polyphenolic compounds, proteins, lipids, and cellulose via different extraction methods or fermentation technique. The scientific community has been able to functionalize the bioactive compounds in order to serve several fields such as chemical industries, pharmaceutical\nutraceutical industries, and food sector. [59,90] Phenolic compounds are secondary metabolites which are the most widely distributed in dietary plant (fruits and vegetables) and medicinal herbs. [91] Especially, corn silk has much potent capability as antioxidant because of its enriched phenolic compounds.

Table 1.5 Bioactive compounds extracted from various segments of the fruit and vegetable wastes. [59,90,92–100]

Segments of fruit and vegetables waste	Phenolic compounds	Cellulose	Lipids and\ or proteins
Apple pomace and leaves	✓	✓	
Banana bract and peel	✓	✓	
Citrus peel	✓		
Mango peel and seed kernel	✓		✓
Grapes pomace and skin	✓		
Potato peel	✓		
Onion skin	✓		
Tomato skin	✓	✓	
Garlic husk	✓		
Plum pomace and seeds	✓		✓
Wild and cultivated berries			✓
Pomegranate seeds	✓		
Avocado seeds	✓		✓
Guava seeds and pomace	✓		
Artichoke internal and external bracts	✓		
Corn husk	✓	✓	
Corn cob	✓	✓	
Corn silk	✓		

1.3.3 Phenolic\polyphenols

1.3.3.1 Phenols structure and classification

Around 8000 compounds that are naturally produced belong to the term "phenolic compounds. Phenolic structures chemically have one or more hydroxyl group linked to an aromatic ring which is a common feature among phenolic compounds. The presence of aromatic ring makes phenols weak acids. One phenolic compound is mainly distinguished from another by the number of carbons and phenol subunits, the presence or absence and the location of carboxylic and the hydroxyl groups. The classification methodology varied since the discovery of phenolic compounds. The latest classification was by Ribereau-Gayon in 1972 where the phenolic compounds were divided into three main families e.g. more common, less common and phenols with polymeric composition. **Figure 1.17 (A) and (B)**, the widely distributed phenolic compounds have been under intensive investigations and received the attention of the pharmaceutical, industrial, and food sectors. [101,102]

An organized handling for these massive amounts of wastes is required to protect the environment and achieve sustainability approaches. As mentioned by FAO, food loss and waste management is facilitated by three possible approaches either co digestion\ anaerobic digestion, incineration landfill discard, and\or compost. Also, wastes can be used as feed to livestock[104]. United States Environmental Protection Agency have released a campaign called "Food Recovery Challenge (FRC)" to encourage all different societal sectors to lower down the wasted food. The united states department of agriculture (USDA) along with EPA have launched in 2015 the 2030 FLW reduction goal that target the reduction of discarding food waste in landfills by 50 percent in 2030. The aim behind those trails is to stabilize the climatic changes and guarantee a secure household environment.[105,106]

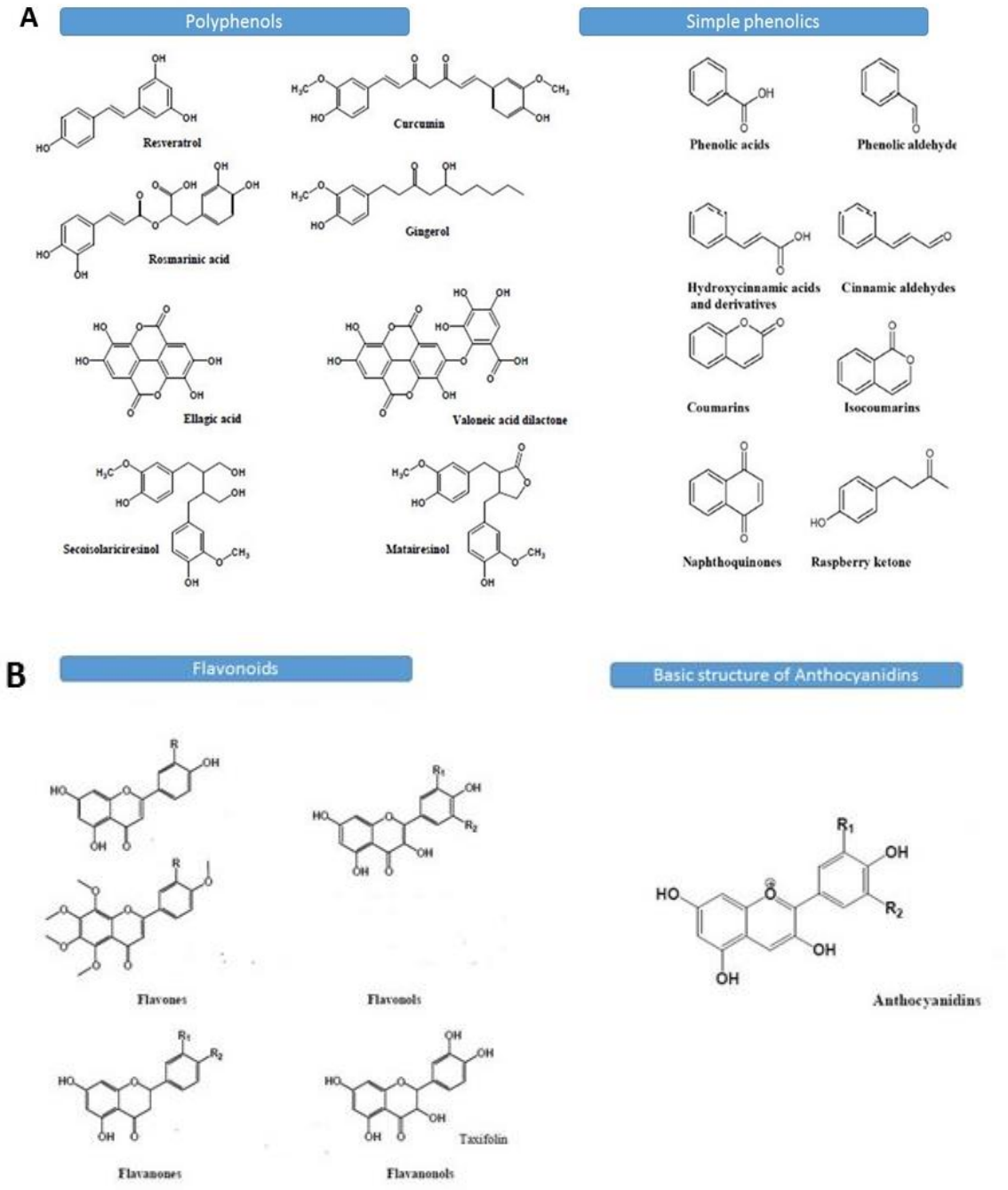

Figure 1.17 (A) Simple phenolic compounds and polyphenols widely distributed in plant origins**. (B)** Modified chemical structures of subclasses of flavonoids and the basic chemical structure of anthracyanidines. [101,103]

1.3.3.2 Polyphenols bioactivities

The beneficial actions of polyphenols have involved both the plant and the humans. For illustration, in plants, flavonoids play a protective role in absorbing sunlight at specific wavelength in order to prevent the accumulation of reactive oxygen species and allow the delay of oxidative stress occurrence.[107] In humans, polyphenols bioactivities involves antioxidant, cardio-protection [108,109], anticancer [110,111], antimicrobial, anti-inflammatory[112], and antiaging activities.[113] The most notable bioactivity is the antioxidant activity of the

phenolic compounds. Thus, they were introduced into the industrial world as a food additive to increase the shelf life of food, and a chemical additive for manufacturing of rubber and plastic without being deteriorated by oxygen. [114,115]As reported by Faga *et al*., polyphenols tend to act as free radical scavengers and metal chelators. In **figure 1.18,** we present the factors that affect the free radical scavenging ability. These factors are double bond in the 2, 3 position, the two hydroxyl groups in the 3', 4' position on the B ring, and 3- and 5- hydroxyl groups with a 4-oxo function. These functional groups and bonds help in the formation of highly stable radical with higher conjugation with other double bonds[116]. Moreover, Papuc *et al*. reported four mechanisms for hydrogen transfer from the phenolic OH groups to the free radical as shown **figure 1.19**.[117,118] Additionally, their action as a metal chelators is a result of the conjugation between the dihydroxy groups of polyphenols and the metals to prevent the formation of metal catalyzed free radicals.[119,120]

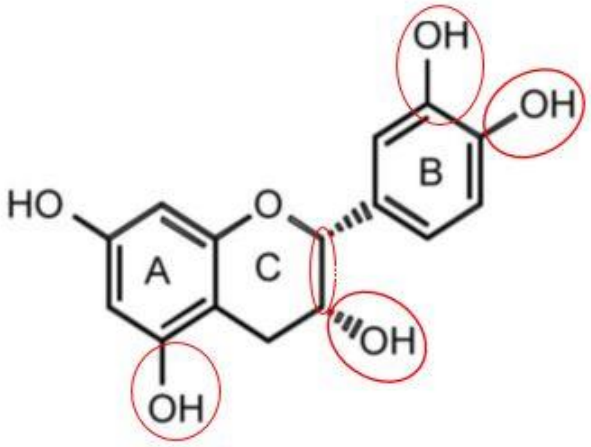

Figure 1.18 One of the structures of polyphenolic compound where the hydroxyl group is responsible for free radical scavenging activity. [116]

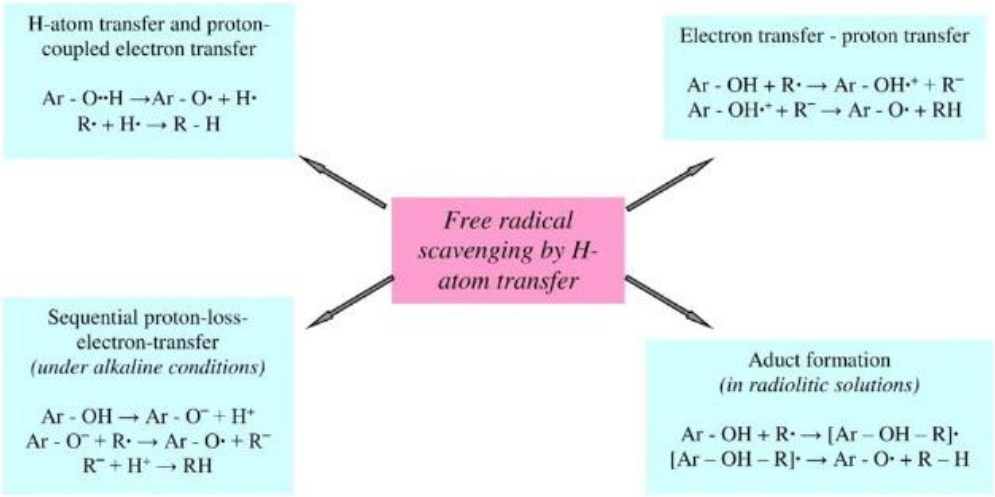

Figure 1.19 Four mechanisms explain the mode of action for the hydroxyl groups reacting with the free radicals. [117]

In the **table 1.6** below, recent in vitro\vivo studies have been conducted on investigating the antioxidant efficiency of plant origin polyphenols associated with other potentials. On the other hand, low bioavailability of polyphenols was found as an obstacle for facilitating the production of such formulas in a large scale.[121,122]

Table 1.6 The antioxidant phenolic compounds extracted from different natural sources and biological activities other than their antioxidant efficiency.

Phenolic compound	Extraction source	Other activities investigated	**References**
Total phenolic content	Chamomile (in vitro study)	Cancer preventive agent	[123]
Gallic acid, flavonoids and tannins	Acalypha godseffiana leaves (in vitro study)	Hypogycemic potentials	[124]
Total phenolic content	Polana raspberry fruit and juice (in vitro study)	Anti-inflammatory and cytotoxic activity.	[125]
Total phenolic content	Jambolan fruit (in vitro study)	Antimicrobial efficiency	[126]
Hydroxytyrosol	Olive oil (in vitro and animal models)	Cardioprotective agent	[127]
Polyphenols	Aged black garlic extract	Cardioprotective	[128]
Total phenolic content	Red sweet pepper seed and pulp extracts	Cytotoxic and antimicrobial properties	[129]
Total phenolic content	Mushroom species *Inonotus sanghuang*	Antiproliferative and antimicrobial activity	[130]
Total phenolic content	*Eucalyptus* spp. leaf extracts	Antibacterial and antifungal activities	
Quercetin and epicatechin	Black chokeberry	Antimicrobial and neutrophil-modulating activities	[131]
Total phenolic content	Syzygium aqueum	Hepatoprotective (in vivo study) and Antiinfalmmatory (in vitro study)	[132]
Procyanidins	Peach kernels	Antihyperglyemic and antiaging	[133]
Total phenolic content	*Amla*, *sapota* and silymarin extracts (comparative study)	Antiaging properties	[134]
Total phenolic content	Corn silk extract (animal study)	Antihypertensive effect	[135–137]
Total phenolic content	Corn silk extract (in vitro study)	Anti-diabetic	[138–141]
Total phenolic content	Corn silk extract (in vitro study)	Cytotoxicity	[142,143]

1.3.3.3 Promising utilization of corn silk waste in Egypt and Asian countries

For centuries, corn silk tea (the yellow to brown color hairy like part) has been the most known homemade preparation due to its multiple purposes related to medicinal values such as herbal remedy, for the treatment of urinary tract infection, and hypercholesterolemia.[144,145] Intensive studies have been conducted on corn silk to discover its phytochemical composition that is responsible for its antibacterial and antioxidant activity.[146] Corn silk's phytochemical composition are polyphenols, phenolic acids, flavonoids, carotenoids, sterols, tannins, volatile compounds, vitamins, sugars, and other miscellaneous compounds. However, in Ren *et al.* and Falcone *et al.* studies, the bioactivity of corn silk takes place mainly because of the antioxidant related polyphenolic compounds.[147,148] Interestingly, some studies revealed that the extraction method and the type of solvent has an effect on the contents and properties of the antioxidant extracts.[65] In Limmatavpirat *et al*. study, two hybrid types of baby corn silk (e.g. pacific 271 and Zeba SG 17) were extracted by 40% v\v ethanol and distilled water. The total phenolic and flavonoids content via ethanol extraction was higher that of the aqueous extraction which was explained as the solvent polarity was influenced by maturity stage and the difference of hybrid of corn silk. The total phenolic content of pacific 271 and zeba SG 17 extracted by ethanol was 44.58 ± 0.75 and 49.95 ± 0.40 mg GAE/g respectively while extracted by distilled water was 33.57 ± 0.49 and 33.06 ± 0.45 mg GAE/g respectively[149]. Another study was conducted by Nurhanan *et al.* on extracting corn silk by methanol, ethanol, water, ethyl actate solvents via soxhelt extraction method. The total phenolic content obtained 101.99 ± 8.05, 93.43 ±2.26, 35.34 ± 2.17, and 6.70 ± 0.51 mg GAE/g for methanol, ethanol, water, and ethyl acetate solvent extractions respectively. [150] Nurraihana *et al*. reported that 40% ethanol was effective in extracting total phenolic content estimated to be 3839.70 mg GAE/100 g sample which is much higher that of 60% ethanol extraction of corn silk (3537.01 mg GAE/100 g sample).[151] **Table 1.7** summarizes the most recent studies on corn silk extracts investigating their biological activities such as stabilizing the abnormal metabolic syndromes (e.g. obesity, diabetes, and hypertension) and their anti-inflammatory efficiency. In regards of fighting bacterial infection and oxidative related diseases, researchers have focused on the antioxidant and antibacterial agents from natural sources one of which is the corn silk.

Table 1.7 Corn silk extracts biological activities and specifically the antioxidant and antibacterial activities.

Biological activity of corn silk extracts	Study description	References
Diuresis effect	George *et al.* reported the potassium-induced natriuresis and diuresis was caused by the high potassium content in of the corn silk extract. Another study by Oyabambi *et al*., it was reported that corn silk extract reduced the plasma superoxide dismutase (SOD), nitric oxide (NO), and glutathione peroxidase (GPx) in slat –induced enthdothelial dysfunction in rat model.	**135,152**
Neuroprotective effect	Xiao-Li Q *et al.* reported ent-kaurane diterpenoids were isolated from corn extract and tested for their neuroprotective activity against hydrogen peroxide induced neurotoxicity in SH-SY5Y cells. Wei-Yu Zhou *et al*. tested five macrocarpene-type sesquiterpenes for their neuroprotective efficiency against H2O2-induced toxicity in human neuroblastoma SH-SY5Y cells .	**153,154**
Metabolic syndromes e.g. antihypertensive, antidiabetic, anti-cholesterol effects, and obesity	Referring to Zhang *et al.* study, the administration of corn silk flavonoids treatment in 300 mg/kg or 500 mg/kg concentrations to diabetic induced mice was reduced the blood glucose (BG) concentration and serum lipid values including total cholesterol (TC), triacylglycerol (TG), low and lipoprotein cholesterol (LDL-C) while the high density lipoprotein cholesterol level (HDL-C) was increased. Chaiittianan *et al.* reported quercetin glucoside derivative and ferulic acid obtained from sweet corn silk while p-coumaric acid and derivatives of gallic acid from waxy corn silk by 50% ethanol extraction. Then, the isolated compounds from sweet corn silk showed anti-pre-adipocyte proliferation, anti-adipogenesis, and lipolysis induction higher than that of waxy corn silk.	**155,156**
Antioxidant and\or antibacterial properties	The antioxidant activity of volatile and non-volatile extract of Egyptian corn silk extract.	157
	Iranian corn silk extract is tested for its antioxidant activity.	158
	Evaluation of antioxidant and free radical scavenging activity of Chinese corn silk extract.	159
	Total phenolic and total flavonoids concentration, and antioxidant evaluation of Indonesian corn silk extract.	160
	Malaysian corn silk extract under investigation for antimicrobial efficiency	161
	Antibacterial activity of the Brazilian corn silk extract.	162

As we mentioned above, Fruit/ vegetables waste, bacterial resistance and oxidative stress related diseases pose a major global issue. The traditional solutions that were adopted to encounter them is not efficient. Therefore, scientific community always seeks for innovative solutions with effective, safe, applicable, available, eco-friendly features. Among these innovative approaches comes the nanotechnology as one of the top go-to approaches.

1.4 Nanotechnology

Nanometer scaled materials significantly differ from the bulk materials in many aspects. One of the important aspects is the morphological features such as size, surface properties and shape. Generally, the morphology of nanomaterials is the leading factor in manipulating and advancing their chemical, physical, catalytic, and confinement properties over the bulk ones. In addition, a wide range of materials can be formulated in a nanometer scale such as in organic metal and nonmetal, carbon based, and polymeric based materials.[166] Nanomaterials are broadly divided into one dimensional (e.g. thin films), two dimensional (e.g. carbon nanotubes), and three dimensional nanoforms (e.g. dendrimers and quantum dots). [167] Thus, heterogeneous applications in some fields can grow out of these diversity in the shape and material nature as represented in **table 1.8**.

Table 1.8 Nanomaterials-based applications in multiple fields among of which is the pharmaceutical\nutraceutical industry.

Field	Application	Material	References
Solar energy	Photovoltaic devices e.g. wearable electronics, electric automobiles, power generated textiles, and space robots	Carbon based nanomaterials	94
Solar energy	Photocatalysis, water splitting, and dye-sensitized solar cells	Core shell structured titanium dioxide	169
Physics	Plasmonic based applications e.g. photodegradation, hydrogen production, photovoltaic cells, and photodetectors.	Hybrid nanostructure of plasmonic metal with 2D materials	170
Biomedicine	e.g. glucose biosensors, acetylcholine and organophosphates biosensors, DNA biosensors, and cancer biomarkers detection.	Carbon nanotubes, gold nanomaterials	171,172
Food science	Active packaging, protection against biological deterioration, sensor, filler and increasing bioavailability	Silver nanoparticles, polymers e.g. polyethylene, gelatin, isotactic polypropylene, and nanocomposites e.g. silver\polyethylene, CuO\polyethylene, ZnO\polyethylen.	173–175
Agriculture	Nanofertilizers, nanoherbicides, nano pesticides, and biosensors	Wide variety of nanomaterials with variable shapes.	176,177
Pharmaceutical\nutraceutical	drug delivery systems and specific targeting	Organic and inorganic nanomaterials	178,179

1.4.1 Nanomedicine

In the past few years, nanomedicine applications and products have dominated the EU market. 92 startups, 67 small and medium enterprises, and 41 large pharmaceutical companies had been established. Nanomedicine is defined as the technology which implement nanotechnology in medicine to improve the healthcare sector. Nanomedicine applications involve drug delivery, *in-vivo* imaging, drug therapy, in-vitro diagnosis, and biomaterials (e.g. hard\soft tissue implants and dental restoratives). As shown in **figure 1.20**, the global market size of nanomedicine was valued $134.4 billion in 2016 then raised to $151.9 billion in 2017, and it is expected to reach $293.1 billion by 2022. [180] Such increment reflects on various sectors; healthcare and industrial sector. Also, the patient compliance is positivity influenced in many ways such as reduced drug side effects, high therapeutic index, low dose frequency, and patients' quality of life improvement. [181]Drug delivery applications have gained the research attention as it is based on designing a novel targeting mechanism to already developed drug. This improves these drugs bioavailability and decrease their systemic toxicity. Drug delivery systems are generally composed of the nanocarriers and the drug to be loaded. The affinity between these two components determines the formation of drug delivery system, which is controlled by their chemical or physical interactions. The drug release from this system takes place through either diffusion, chemical reaction, solvent, or stimuli-controlled release**.**[181] Recently, different materials with significant characteristics (e.g. chemical, physical, and morphological) have been utilized to prepare the nanocarriers.

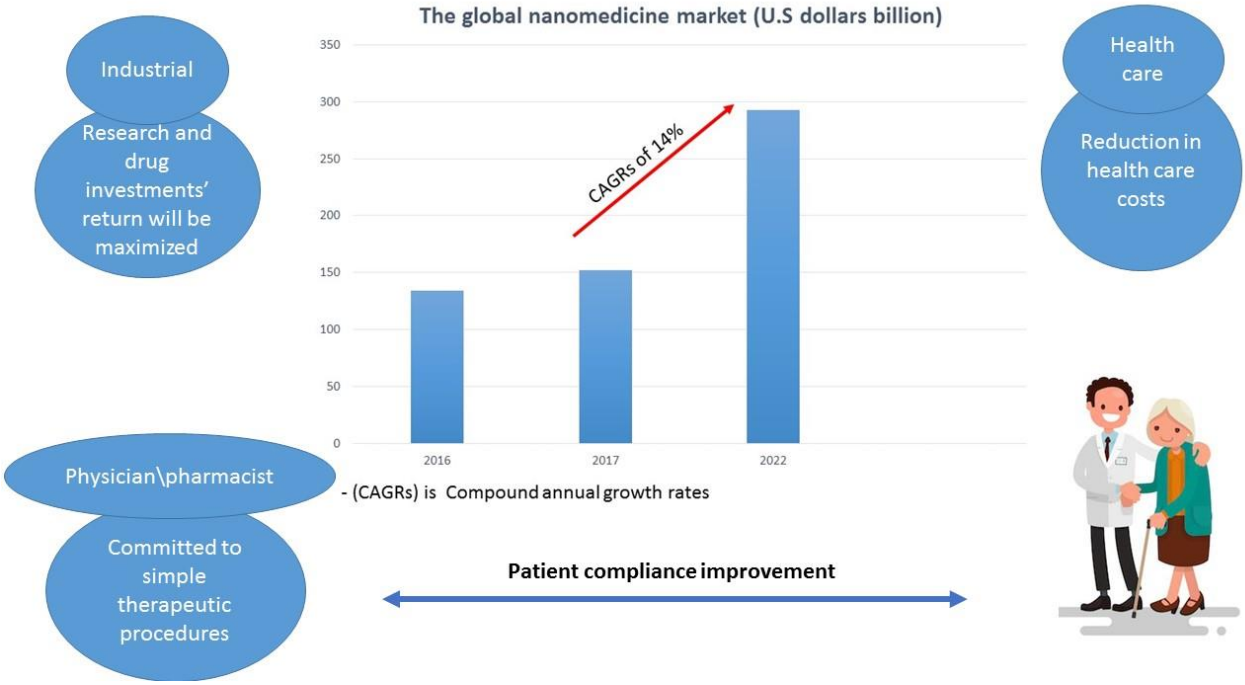

Figure 1.20 Global market size of nanomedicine by years and its influence on a wide range of sectors. [180–182]

1.4.1.1 Drug delivery applications

1.4.1.1.1 Polymeric nano-based materials: natural versus synthetic

Polymeric nanomaterials are characterized by their biodegradability property which enabled them to advance on metals, ceramics, and alloys-based nanomaterials. Biodegradability is a key feature of green and sustainable development in the twenty first century. Biodegradable polymers are of either natural or synthetic source. Synthetic preparation of biodegradable polymers has a crucial advantage over the natural one which is the easily tailored production of a wide range of products with different types via uncounted techniques. Examples for synthetic polymers are poly beta-hydroxybutyrate (PHB), polylactic (PLA), polyurethane, poly (lactic-glycolic acid) (PLGA), and polymethyl methacrylate resin (PMMA). On the other hand, the functional groups of the natural polymers crucially contribute in the biodegradation process with the less toxic effects. Besides, natural polymers have a lower production cost and higher availability than synthetic ones. Natural polymers such as chitosan, hyaluronic acid, alginate, starch, and chondroitin which are naturally abundant, can be isolated from either plant, animal or microorganism source. Natural polymers can be easily isolated from their sources and under certain chemical modifications, it can meet the technological demands. They have high safety index which is represented in their degradation into water, carbon dioxide and inorganic small molecules via enzymatic or hydrolytic reactions in the body. Thus, they are considered eco-friendly.[167,183] Polymeric nanocomposites are polymeric materials in the nanometer scale or polymeric composites that contain nanomaterials. One major

advantage of these nanomaterials is that it combines the properties of both natural and synthetic nano-based polymers for the sake of synergistic potentials. Therefore, it is notable in the latest researches related to biomedical applications that the focus of the research is on the polymeric nanocomposites. [184,185]

The first component of the nanomedicinal composite is the nanocarriers. Polymeric based nanocarriers have been investigated for their controlled release mechanism of the loaded drugs, stability, non-inflammatory, and non-immunogenicity. **Figure 1.21** illustrates multiple natural sources for polymeric nanocarriers in order to guarantee the biocompatibility, biodegradability, and low toxicity over the synthetic materials such as metallic nanoparticles (e.g. zinc oxide and titanium oxide), inorganic nanoparticles (e.g. gold and silver), and quantum dots**.** [186]

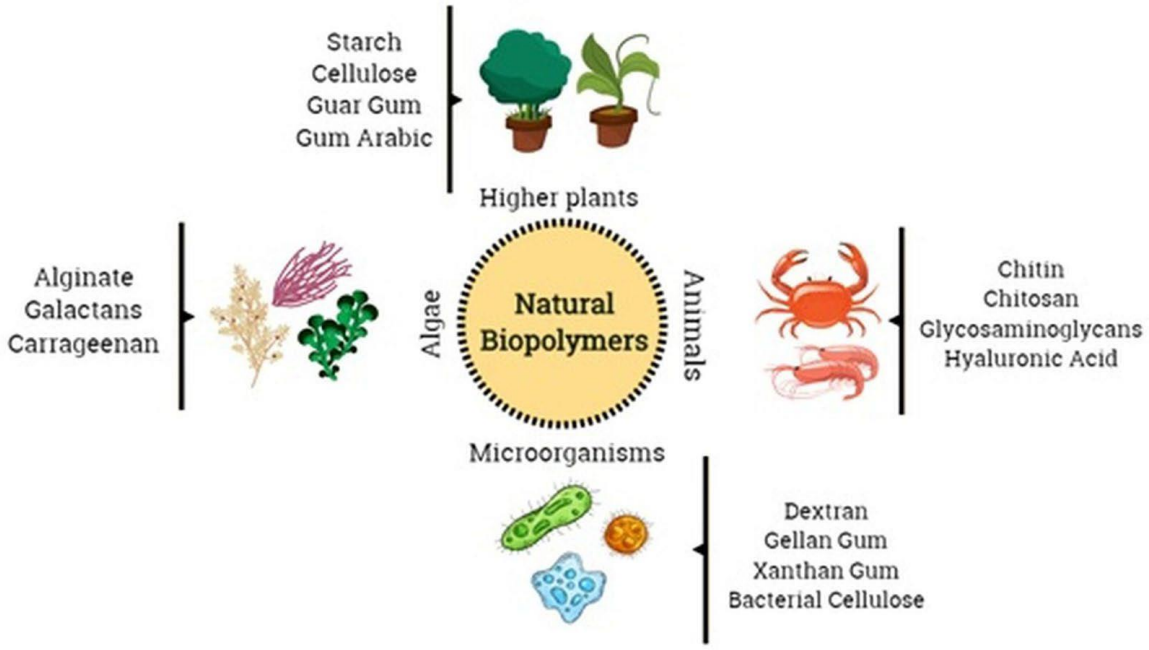

Figure 1.21 Natural sources for formulating polymer based nanocarriers. [186]

The second component of nano medicinal composite is the loaded drug that can be either of synthetic or natural source. In both cases, their bioavailability and efficiency increase by their transformation into nano-form. However, herbal\ plant-based drugs have drawn the attention lately because of three crucial reasons. Firstly, herbal\ plant medicine is widely used since the ancient time throughout many populations to treat and prevent various diseases. Secondly, herbal\ plant-based drugs are less expensive in comparison to the synthetic drugs. Thirdly, economic, political, and social changes worldwide have directed the scientific efforts toward focusing on this research field. Also, their poor bioavailability was reported in several studies due to their improper

molecular size and low lipid solubility.[187] In addition, WHO reported that around 80% of the population in the developing countries relies on the herbal\plant medicine in order to meet with their basic requirements of health care. Moreover, natural based drugs involve biological components of enormous diversity. Therefore, the herbal\plant extracts possess specific chemical complexity that guided researchers to investigate the know-how of manipulating these natural based drugs efficiently.[188] Fortunately, nanotechnology has enabled researchers to succeed in enhancing the basic features of extracts through nano-encapsulation or conjugation as illustrated in **Figure 1.22**. Extracts can be loaded by either encapsulation (e.g. liposomes, nanocapsules, micelles, nanospheres) or conjugation (e.g. dendrimers, micelles, linear polymers).

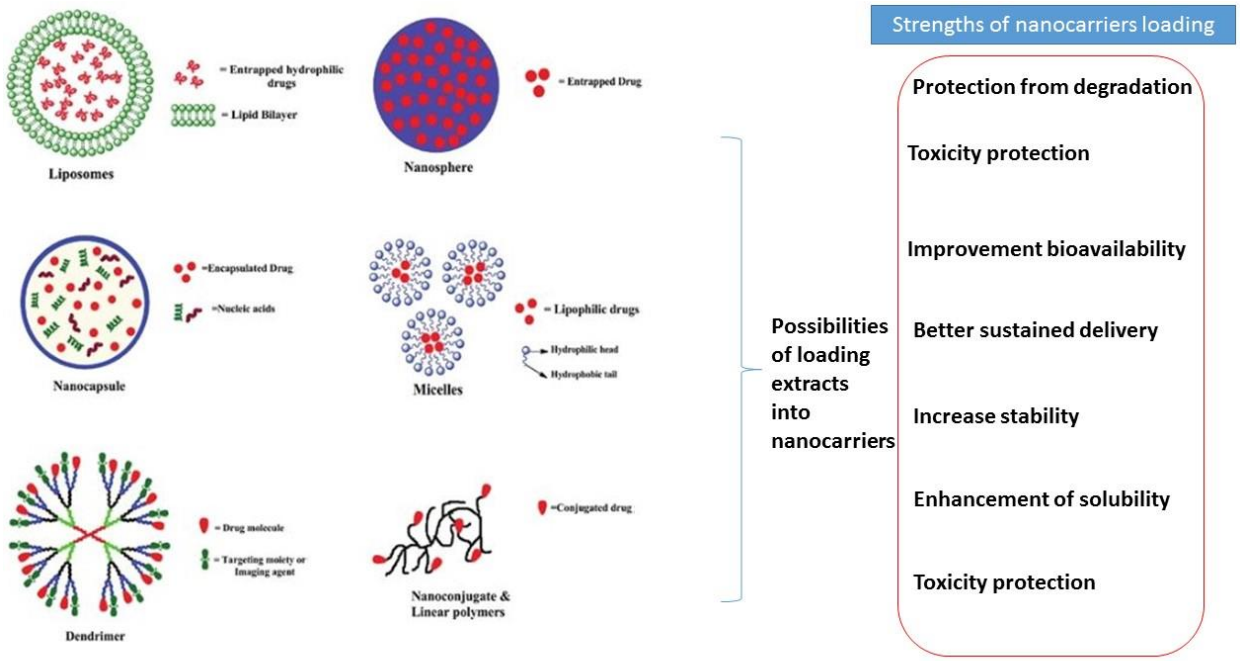

Figure 1.22 Encapsulation or conjugation of drugs in nano-formulated systems which leads to the listed strengthen features of nanocarriers loading. [189,190]

In **figure 1.23** a summary of most of the conducted studies on herbal\plant sources investigating their biological activity after nano-transformation. Specifically, Corn silk, strawberry, *Physalis alkekengi-L*, rose hips and other extracts as shown in **table 1.9**, are examples of loaded plant extracts into chitosan which is on the top of the best nanocarriers candidates.

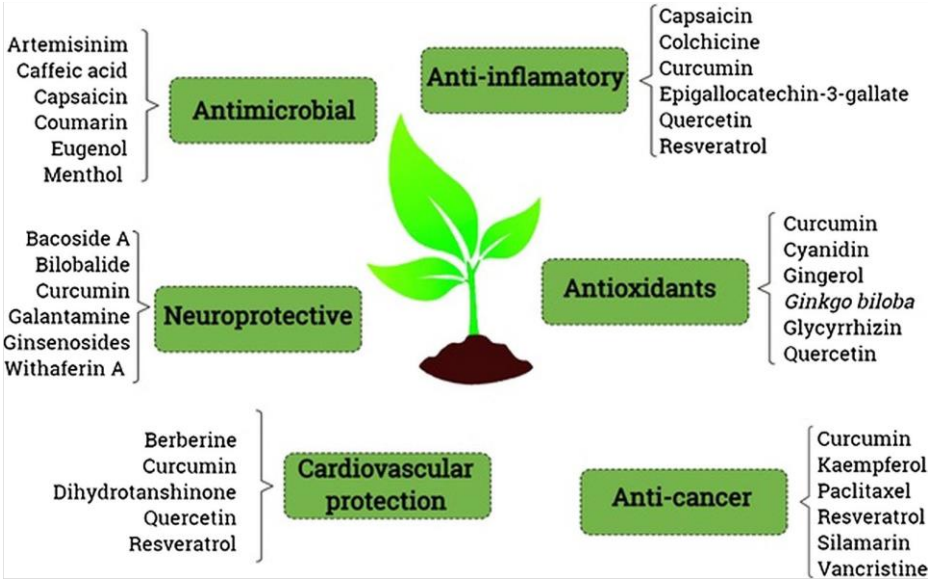

Figure 1.23 Different herbal\plant extracts' biological activities tested after nano-encapsulation. [28]

Table 1.9 Plant based- chitosan nanoparticles investigated for their antioxidant efficacy.

Plant	Corn silk	Strawberry	*Physalis alkekengi-L*	Rose hips	*Thymus serpyllum* L.	Jabuticaba peel
Polymer nanocarriers	Shrimp shell waste protein (SSWP)	High molecular weight chitosan	Low molecular weight chitosan	Medium molecular weight chitosan	High molecular weight chitosan	Medium molecular weight chitosan
Antioxidant efficacy	Antioxidant assay for SSWP-based film modified with oolong tea, corn silk, and black soybean seed coat extracts. Among of which 5%w\w oolong tea extract incorporated in chitosan film showed high antioxidant activity.	Antioxidant assay for the of strawberry polyphenols showed higher antioxidant efficiency for encapsulated strawberry extracts than the pure ones.	Antioxidant capacity improved after encapsulation.	Antioxidant activity of rose hips polyphenols	Film formation by chitosan, starch and polyphenols thyme extracts. The antioxidant activity of the film loaded with thyme extract was higher than that pure thyme extract.	chitosan micro encapsulation of polyphenols jabuticaba peel extracts maintained the antioxidant activity of the extracts although the storage in different temperature.
References	191	192	193	194	195	196

1.4.1.1.2 Chitosan

Chitosan is derived from chitin which is a marine shell waste that undergoes sequential chemical methods involving deproteinization by an alkaline solution, demineralization by an acidic solution, and finally discoloration by an alkaline solution. Although Chitin exists in three various polymorphs (α-, β-, γ- chitin), α- chitin type is the most used structure. Owing to chitin poor solubility, chitin requires further chemical treatment. Thus, by certain chemical conversion, chitin is chemically deacetylated into chitosan. Deacetylation mechanism involves chitosan exposure to hydroxides at 80 °C or above. As these conditions get harsher, the deacetylation degree of chitin structure increases. In turn, chitosan molecular weight decreases. Accordingly, the properties of the final product of chitosan is controlled by the degree of deacetylation[197]. As shown in **figure 1.24**, the chemical structure of chitin is composed of two main units D-glucosamine and N-acetyl-D-glucosamine which are linked by β-1,4 glycosidic linkages. Degree of deacetylation is controlled by D-glucosamine to N-acetyl-D-glucosamine units' ratio. Moreover, when 50% of deacetylation process is achieved, chitosan becomes more soluble in aqueous acidic medium. Therefore, the tendency of protonation of the amino groups (NH_2) in the copolymer backbone increases turning into cationic groups. This explains the scenario of antimicrobial feature of chitosan where the cationic groups allow chitosan polysaccharide to interact with the negative charges present on any microorganisms' cell membrane. In addition, the solubility characteristic of chitosan has enabled researchers to develop multiple forms of chitosan such as nanoparticles, films, pastes, nanofibers, and hydrogels as well. [198]

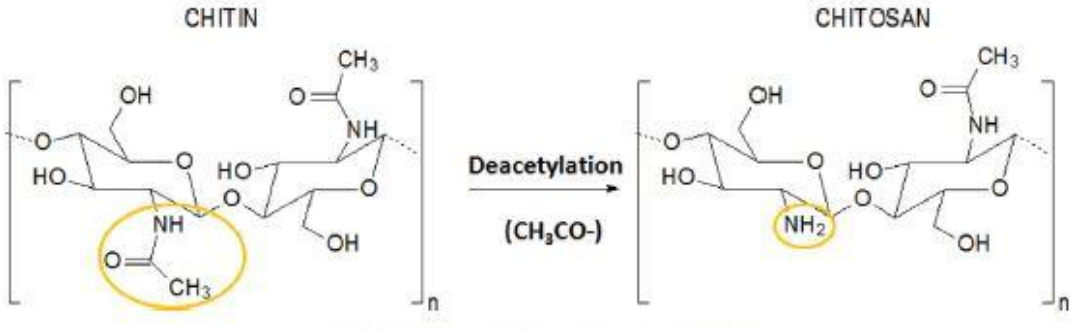

Figure 1.24 Chitosan chemical structure after the deacetylation of chitin. [197]

1.4.1.1.2.1 Chitosan nanoparticles

Generally, nanoparticles act as a drug carrier system because they are in the size of nanometer to micrometer solid particles with a very high surface to volume ratio. Therefore, this system can deliver drug in a sustained and controlled manner at specific target sites. On the level of patient

compliance, improvement can be observed through the lower dose and frequency of the administrative drug. Specifically, GRAS (generally recognized as safe by the United States Food and Drug Administration) approved that chitosan polymer is safe biodegradable and biocompatible natural polymer. Through years of investigations, studies proved chitosan nanoparticles are easily prepared, non-toxic, biocompatible, biodegradable, and of moderate stability. Besides, during the preparation of chitosan nanoparticles, there is no need to use hazardous solvent because they can dissolve in aqueous acidic solutions. [199]

1.4.1.1.2.2 Chitosan preparation

The biological, pharmaceutical, or even medical purpose of the produced chitosan NPs determines the required technique of preparation. Multiple methods have been utilized for the preparation of chitosan NPs such as Ionic cross-linking, reverse micelle, precipitation, and emulsion droplet coalescence mechanism. For example, inverse micelle method has been used to obtain an anticancer (Doxorubicin®) drug encapsulated in chitosan NPs where an organic solvent contains the drug with a surfactant to which chitosan aqueous solution is added.[200] Upon agitation, water is added to this mixture resulting in producing NPs. The rest of the techniques are illustrated briefly in **figure 1.25**. Because ionic gelation (Ionic cross linking) method is simple and not time consuming, it is commonly used for a small scale nanoparticles production**.**[199]

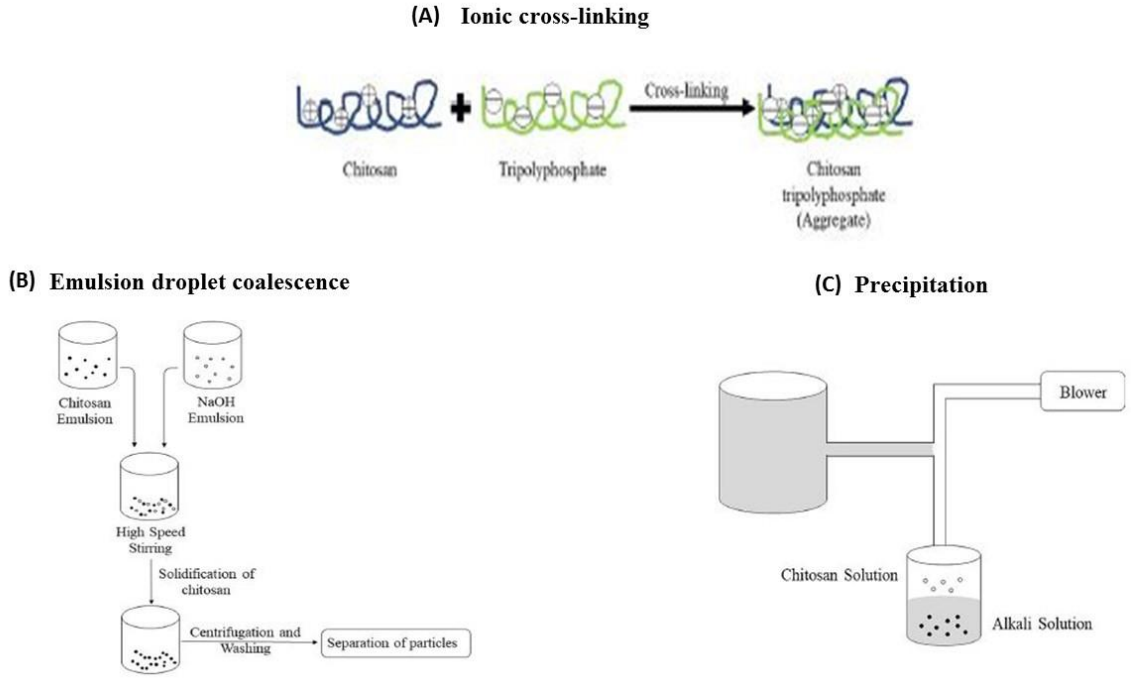

Figure 1.25 (A) Ionic cross-linking \ Ionic interaction. **(B)** Precipitation \ Via a compressed air nozzle. **(C)** Emulsion droplet coalescence \ two separated preparations of emulsions are mixed eventually. [199]

1.4.1.1.2.3 Chitosan NPs applications

Chitosan NPs are applicable in a wide range of applications such as biomedical (e.g. wound healing, tissue regeneration, controlled drug delivery, cosmetics), wastewater treatment, food industry, agriculture, and papermaking. Nevertheless, controlled drug delivery application attracts the attention of the recent studies to deliver various forms of drug efficiently through either non-parenteral (e.g. nasal, oral, ocular) or parenteral routes. In **table 1.10,** we summarize some of loaded chitosan NPs' contribution in drug delivery applications that are under study.

Table 1.10 Biomedical applications of chitosan loaded nanoparticles.[199]

Biomedical purposes	**Examples**	
	Under study	**Purpose of the formulation**
Ocular drug delivery	Sulfobutylether-β-cyclodextrin/ chitosan NPs contains naringenin.	To increase the bioavailability of naringenin in the aqueous humor
Nasal drug delivery	Carbamazepine (anti-epileptic drug)-Carboxymethyl chitosan NPs	To increase the therapeutic efficiency.
Pulmonary drug delivery	Itraconazole (anti-fungal drug) – chitosan NPs	To overcome drug low solubility if administrated orally.
Buccal drug delivery	Curcumin-loaded chitosan-coated polycaprolactone NPs	For periodontal diseases.

Based on what we explained, corn silk extract loaded chitosan extracts is a rich platform for obtaining highly featured drug delivery system with highly efficacious antioxidant, and antimicrobial activities. Consequently, the current experiment's aim is exploring the basic antibacterial and antioxidant activities of corn silk extracts before and after chitosan nano-encapsulation. The aimed application would be topically applying formulas of SE encapsulated CS NPs as an effective antibacterial agent.

1.5 Scope of the study

Corn silk plant waste was selected as the best candidate to encapsulate its extract in CS NPs and investigate their antibacterial and antioxidant potentials. As shown in **figure 1.26**, the Egyptian white corn main parts are divided into: i) the corn cob, which is composed of the white kernels (seeds); ii) the corn silk (yellowish brown hairy part), and iii) the corn husk which is the outer green colored paper-like part that protects the whole plant. These pictures were taken in our research group Laboratory at the Department of chemistry at AUC. In the current study, three different parts of the white corn were initially compared in terms of their antioxidant activities

from which the corn silk extract showed the highest antioxidant activity in comparison to husk and cob.

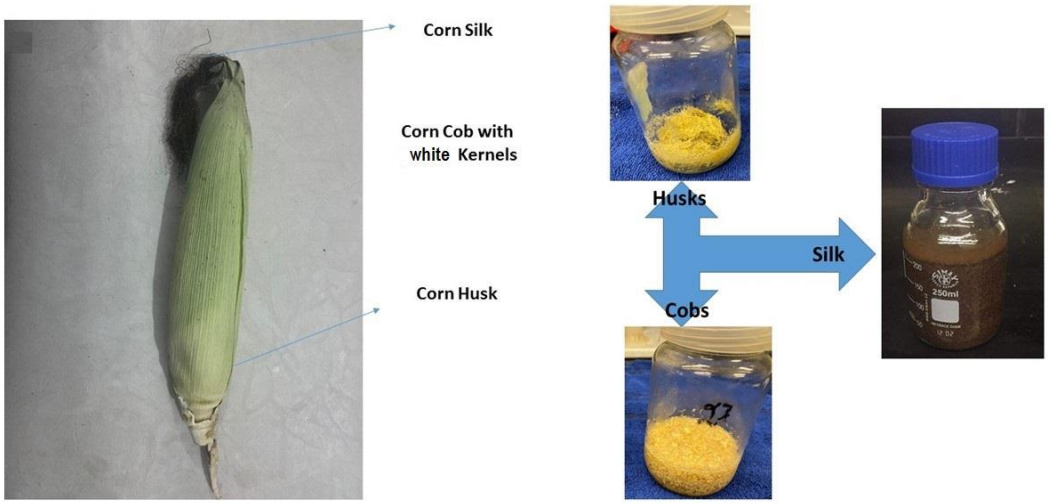

Figure 1.26 Shredded corn husks, cobs, and silk were soaked in 85% methanol solvent. (taken in AUC laboratory).

Initially, the optimum formula of the encapsulated CS NPs was selected among multiple trials conducted through design expert software and based on the optimum responses PDI, particle size, and zeta potential which were suggested by the same software. Then, a separate experiment was done to investigate the influence of increasing the concentration of the encapsulated silk extract on the PDI, zeta potential, particle size and EE%. As a result, 0.5, 1.0, 1.5, and 2.0 mg\mL of corn silk extract was encapsulated in CS NPs preparations. The antibacterial and antioxidant activities of the four preparations were tested. Then, FTIR spectroscopic analysis and *in-vitro* release studies were examined for the best encapsulated CS NPs formula with the highest antibacterial efficiency and the scavenging activity. Accordingly, the focus of this work is to encapsulate corn silk within CS NPs aiming at having unique antioxidant and antibacterial activities of these novel nano-encapsulated systems versus the bulk extract. **Table 1.11** shows the different formulations and their abbreviations:

Table 1.11 Formulations and their abbreviations.

Formulation	Abbreviation
Chitosan nanoparticles	CS NPs
Silk extract	SE
X mg\mL concentration of silk extract encapsulated in chitosan nanoparticles	SE x\CS NPs
0.5 mg\mL concentration of silk extract encapsulated in chitosan nanoparticles	SE 0.5\CS NPs
1 mg\mL concentration of silk extract encapsulated in chitosan nanoparticles	SE 1\CS NPs
1.5 mg\mL concentration of silk extract encapsulated in chitosan nanoparticles	SE 1.5\CS NPs
2 mg\mL concentration of silk extract encapsulated in chitosan nanoparticles	SE 2\CS NPs

Chapter 2

Materials and methods

2.1 Materials

Egyptian white corn (Zea mays L.) species was purchased from the Egyptian local market in the period between August\2019-March\2020. Medium molecular weight chitosan (84.8% degree of dealkylation) was purchased from (Primex ehf, Chitoclear, Iceland). Methanol 99.9%, Sodium tripolyphosphate (TPP), sodium hydroxide and 2,2-diphenyl -1-picryl hydrazyl (DPPH) were purchased from (Sigma Aldrich Co, USA. L (+)-Ascorbic acid was purchased from (Scharlab S.L., Spain) while Folin-Ciocalteu reagent (Fisher chemical) and Gallic acid were purchased from (Merch chemicals Co., Germany). Glacial acetic acid and sodium carbonate were purchased from Adwek Co, Egypt. Two strains of bacteria were investigated which are *Escherichia coli* (*E. coli*, ATCC 8739) and *Staphylococcus aureus* (*S.aureus*, ATCC 6538). Distilled water was used throughout all experiments carried out in the work described in this thesis.

- Equipements and software

The utilized devices were Biobase freeze dryer (model no. BK-FD10S, China), Jenway UV-Visible spectrophotometer (model no.7415, UK), Malvern DLS (zetasizer Nano S, UK), probe sonicator (Thermo Fisher Polytron, USA), SEM (Gemini Sigma, USA) and FTIR (Thermo Fisher Nicolet 380 ,USA). Design expert version 10, Graphpad prism version 8.0.1, and imageJ softwares were used.

2.2 Preparation of corn silk, husk, and cob extract powder

Grinding and drying corn parts were essential pre-extraction steps to ensure the preservation of the phytochemicals in the extracts. Dried corn parts allowed to extend the time required for the experiments. Emmanuel *et al*. confirmed the antimicrobial activity of the dried corn silk which was higher than that of the fresh one in comparison to ciprofloxacin as a reference antibacterial agent.[1] The three corn parts were dried in air at room temperature where the heat labile compounds were preserved. Also, lowering particle size (e.g. grinding) was fundamental step to increase the particles surface area exposed to the solvent. Solvent penetration occurred by the sufficient contact between the target analytes and the solvent. Maceration was the simple and efficient method for extraction of the complex mixture metabolites from the three corn parts. This method aimed to soften the texture composition of the soaked corn part as it relied on leaving the corn parts for days in the solvent at ambient temperature as shown in **figure 2.1** Thus, solvent to shredded sample ratio and extraction time parameters were important in the maceration method. Moreover, the type of the compounds extracted by maceration was dependent on the choice of suitable solvent.[2,3] Methanol was the best choice for extracting the antioxidant agents e.g. polyphenols.[4] Vijayalaxmi *et al.* studied the extraction of polyphenols from corn husk using aqueous and aqueous/organic solvents. The aqueous/methanol showed higher TPC values than those of water and aqueous ethanol where 70% methanol showed TPC value of 45.45 ± 0.12 and 50% methanol and the $\%IC_{50}$ was determined to be 24.25 μg/mL.[5] The antioxidant efficiency of the three parts were compared in order to confirm what is mentioned in the previous literature that corn silk has sufficient antioxidant activity.

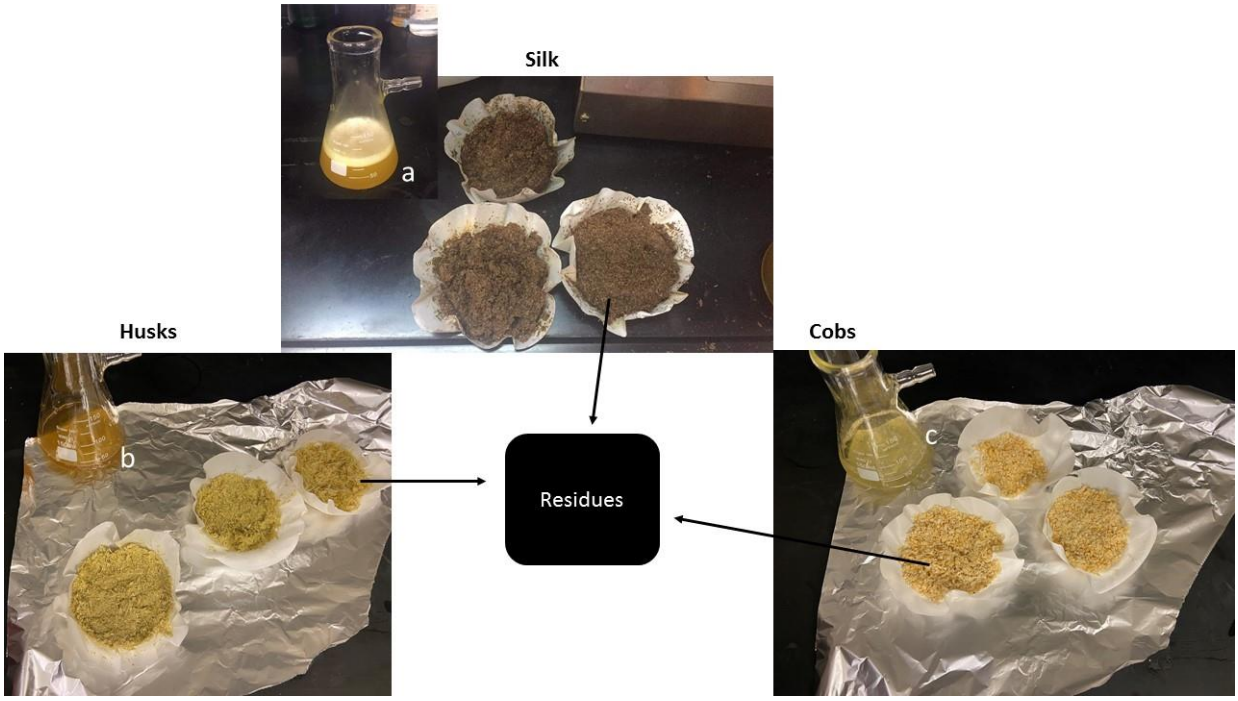

Figure 2.1 Residue and filtrate prepared after Buchner apparatus filtration of corn husks, cobs, and silk.

Freshly collected Corn parts were separated from the whole plant. They were then left for four days at room temperature away from sunlight, to be dried. The dried corn parts were first cut into small pieces to be transformed into powder form by a grinder machine.[6,7] The freshly prepared corn parts' powder were kept in refrigerator in a tight closed zipper bag.

50 gm of corn parts' powder was weighed and placed in a 200 mL bottle. A 200 mL of the co-solvent was added to the powder (volume ratio powder: co-solvent was 1:4) where the co-solvent was (methanol 99.9%: distilled water). After four days of maceration, primary filtration was done by a vacuum filtration using a Buchner funnel connected to a thick-walled tubing, and a suction source placed inside a hood. A secondary filtration process was carried out using standard gravity filtration to ensure having a clear filtrate of the corn parts' extract.[1,8]

Lyophilization process was carried out on the corn parts' extract to convert it to powder form. The corn parts' extract filtrate was diluted by a volume ratio of 1:5 (filtrate: D.W) and was left for 24 hrs. in the freezer. On the following day, the dilutions were placed in the freeze dryer for two hours at a temperature of -55 °C to ensure the solidification of the samples. After 72 hours of lyophilization, corn parts' extract powder was obtained and finally kept at -2 °C for further tests.

2.3 Physiochemical characterization of corn parts' extract

2.3.1 2,2-diphenyl-1-picryl-hydrazyl-hydrate (DPPH) assay

This test involves the transformation of the purple color of the tested samples into a yellow color in response to the presence of antioxidants. This test was carried out as follows; 0.2mM DPPH

solution was prepared by dissolving 0.00394 gm DPPH reagent in 50 mL of 99.9% methanol. A serial dilution of (0, 0.25, 0.5, 0.75, 1, 1.5, 2 mg\mL) of corn parts' extract and ascorbic acid, as a reference, were tested. The test was performed by adding 2 mL of each extract\ascorbic acid to 1 mL of 0.2mM DPPH solution. A Shaker swivel motion type at ambient dark room was used for 1 hr. to homogenously mix the mixture together. After 1 hr., the absorbance of each sample was measured at the wavelength of 517 nm. Methanol was used as the blank whereas DPPH solution was used as the negative control.[8,9] The test was triplicated, and the percent of inhibition was calculated by the following **equation 1**:

Equation 1[10]

$$\%\text{Inhibition} = (1 - \text{As}/\text{Ac}) \times 100$$

Where "As" represents the absorbance of each extract\ascorbic acid concentration reacted with the DPPH solution. "Ac" represents the absorbance of the negative control which is the DPPH solution (Zero conc. of extract\ascorbic acid concentration).

Graphs for the calculated percent of inhibition (Y-axis) of the different extract and ascorbic acid concentrations versus their concentrations (X-axis) were plotted via "Graphpad prism version8.0.1" software. The $\%IC_{50}$ value was obtained from the plotted graph using (XY analyses: Fit spline\ Lowess). The $\%IC_{50}$ value is a specific concentration (extract\ascorbic acid) that scavenges the DPPH free radical by 50%. Accordingly, the lower the $\%IC_{50}$ was, the higher the antioxidant activity would be.

2.3.2 Total phenolic concentration (TPC) assay

The Folin solution (10% v\v) was prepared by adding 10 mL of Folin reagent in 100 mL volumetric flask, then was filled up to 100 mL with DW. Sodium carbonate $NaCO_3$ solution (7.5% w/v) was prepared in 100 mL volumetric flask by adding 7.5 gm of $NaCO_3$powder and dissolved in 100 mL DW. Secondly, a stock solution (0.1mg\mL concentration) of gallic acid in 99.9% methanol was prepared, and a serial dilution out of this stock was prepared of the concentrations (0.003, 0.005, 0.007, 0.009, 0.01, and 0.03 mg\mL). Then, in 10mL test tubes, 2mL of $NaCO_3$ (7.5%) was added to 1 mL of each of the stock solution's serial dilutions. 5 minutes later, 2.5 mL of Folin solution (10% v/v) was added to each test tube. The blank was 2 mL of $NaCO_3$ with 2.5 mL of Folin solution mixed in a test tube. The extract, with a concentration of 2mg/mL, was prepared using the same procedure mentioned above. The shaker swivel motion type was used to mix the test tubes' components of Gallic acid serial dilutions\the blank\corn silk extract in an ambient dark room for 1.5 hrs. UV-visible spectrophotometer was used to measure the absorbance

of each sample at the wavelength of 765nm.[10] **figure 2.2** illustrates the blue color intensity increases as the concentration of the total phenolic increases.

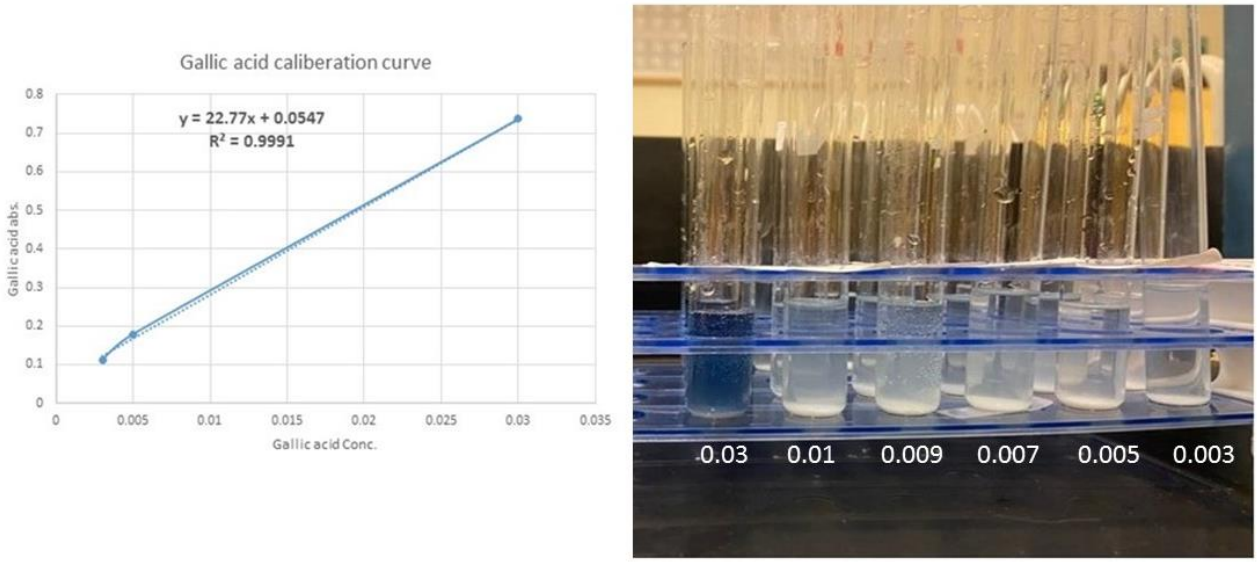

Figure 2.2 TPC was determined as assay testing the serial dilution of gallic acid.

TPC or gallic acid equivalence (GAE) of corn parts' extract was obtained using the absorbance of the 2mg\mL of extract, and substitution on the regression line **equation 2** of Gallic acid calibration curve:

Equation 2

$$y = 22.7x + 0.0547$$

R^2 = 0.9991 where TPC was determined as per **equation 3**;

Equation 3[10]

$$A = (c * v)\backslash m$$

Where A= TPC or GAE.

C= x [conc. of Gallic acid in mg\mL].

V= volume of extract.

m= mass of extract in gm.

2.4 Formulation of corn silk extract encapsulated CS NPs

Nanoparticles using CS polymer along with the TPP cross-linker was prepared. **Figure 2.3** is a schematic illustration for preparing chitosan nanoparticles encapsulated with the corn silk extract, and the produced NPs were characterized by DLS, UV-Visible spectrophotometer, and compared in their antibacterial and antioxidant activities to the pure corn silk extract.

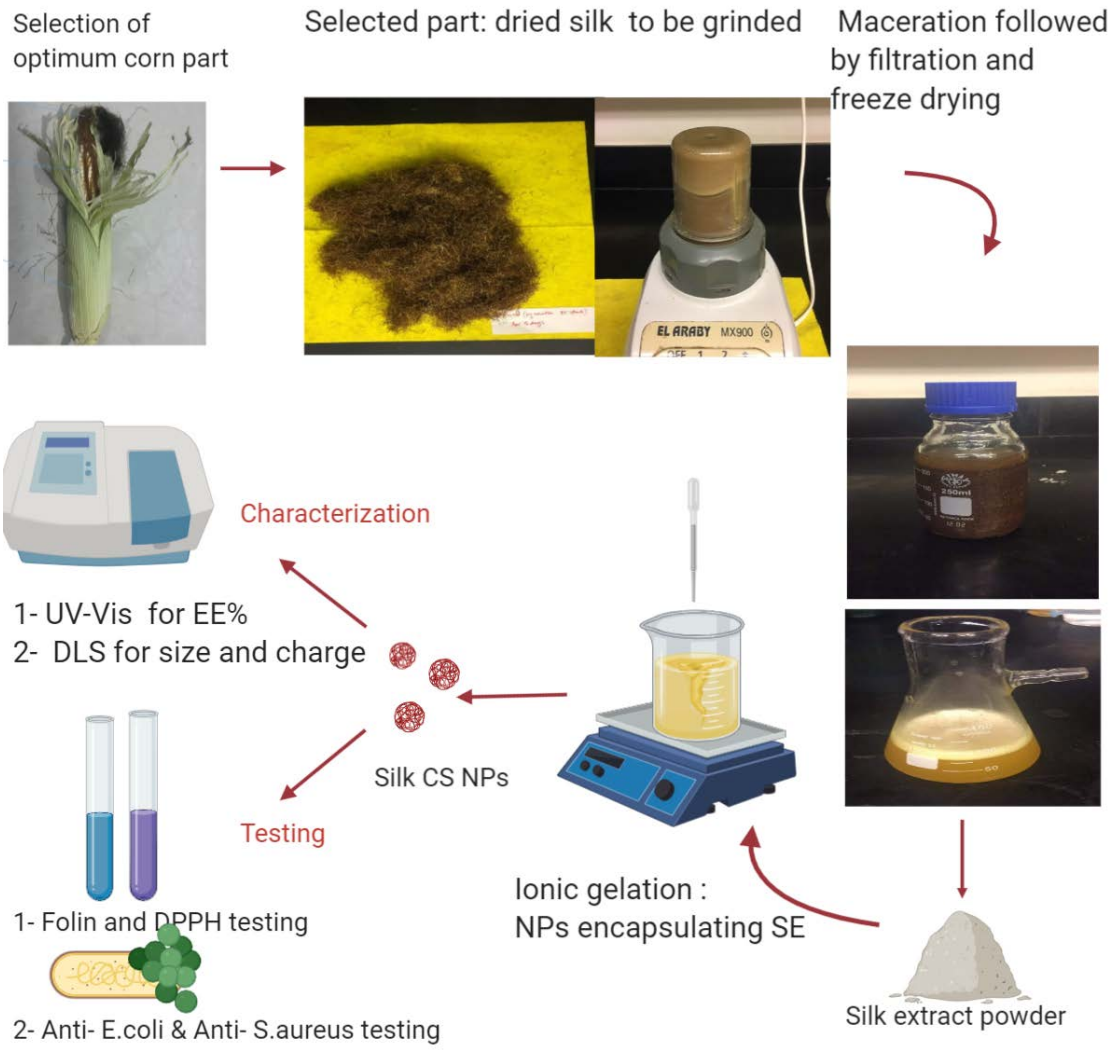

Figure 2.3 Schematic illustration for preparing corn silk extract followed by loading CS NPs with the extract and the characterization of the produced NPs.

Corn silk extract was then encapsulated in the prepared CS NPs by ionic gelation method. This method is simple where all the conditions of the experiment were fixed except for the three factors; time (hrs.) of the reaction, speed (rpm) of stirring on the magnetic stirrer and the CS to TPP mass ratio. Design expert software was the fundamental tool for determining the optimum factors needed for preparing NPs loaded with corn silk extract. As shown in **figure 2.4**, 15 trails were proposed by design expert software where in each trail there was different time, speed, and CS: TPP mass ratio.[11]

Run	Factor 1 A:CS:TPP ratio	Factor 2 B:Speed rpm	Factor 3 C:Time hr.
1	1	800	3
2	5	400	3
3	3	600	3
4	3	800	5
5	5	800	3
6	3	600	3
7	3	600	3
8	5	600	5
9	1	600	1
10	1	400	3
11	5	600	1
12	3	400	5
13	3	400	1
14	3	800	1
15	1	600	5

Figure 2.4 Design expert software optimization after 15 experimental trials by controlling three variable factors.

The output of each trial of design expert software was tested by ZetaSizer to obtain the corresponding zeta potential, particle size, and Polydespersity index (PDI). This process involved the preparation of one stock CS solution of 0.2% concentration by weighing 0.2 gm of CS powder to be dissolved in 100 mL of 0.5% acetic acid solution, with pH adjusted to 5 by adding 1N NaOH. The TPP solution, on the other hand, was prepared in three different concentrations (0.200%, 0.066%, and 0.040%) to achieve the targeted CS to TPP mass ratios (1:1, 3:1, and 5:1).[12] Furthermore, the concentration of silk extract was kept constant at 0.5mg\mL throughout the experiment. During the experiment, 10 mL of CS solution (0.2%) was placed in a 25mL beaker. Upon stirring at 300 rpm, 1 mL of silk extract solution was dropped gradually by a dropper. After 5 minutes of mixing CS with the extract, 10 mL of TPP solution (0.200%, 0.066%, 0.040%) was gradually added by a dropper on this mixture followed by adjusting speed and time according to Design expert software suggested output. Thereafter, all the samples were centrifuged for 1 hr., at 20000rpm and at 4°C then washed twice by DW and centrifuged again at the same conditions to get the pellet of the extract-NPs. The pellets were re-dissolved in DW and by the Probe sonicator for 3 seconds at 50% amplitude to disintegrate the pellet giving a cloudy solution. The particle size (nm), the zeta potential, and the PDI of each test sample were then measured using Zetasizer. Based on the analysis of Design expert software; 0.5mg\mL silk encapsulated NPs with the optimum conditions of CS: TPP mass ratio, time, and speed were 2.5:1, and 5 hrs., and 800rpm respectively were prepared.

Then, three other silk extract concentrations were prepared and loaded to the NPs (optimum formulation of the lowest PDI, Particle size, and the highest zeta potential) to test the influence of increasing the extract concentration loaded in NPs. The encapsulation entrapment for the four different silk extract concentration NPs was compared. **Table 2.1** shows the condition upon which the test was done.[12,13]

Table 2.1 Testing the influence of increasing silk extract concertation while fixing all the other conditions of preparing encapsulated NPs.

Corn silk conc. (mg\mL)	CS conc.	TPP conc.	Volume of CS solution (mL)	Volume of TPP solution (mL)	Volume of extract (mL)	Ratio of CS: extract
0.5	0.2%	0.08%	40	40	4	1.000:0.025
1.0						1.000:0.050
1.5						1.000:0.075
2.0						1.000:0.100

2.5 Physiochemical characterization corn silk Extract CS NPs

2.5.1 Particle size, PDI, and zeta potential

Diluted solution of the extract-NPs of 1mg\mL was prepared, before measuring the three responses via DLS. Then, 1 mL of the diluted solution was placed in the semi-micro disposable cuvette to measure the particle size and the PDI. On the other hand, the folded capillary cell for measuring the zeta potential was used. Three considerations were taken for measuring zeta potential. First, the cuvette was filled up with the sample using a dropper. Second, the cuvette was free from any air bubbles. Third, the cuvette was wiped with a soft wipe to ensure being dry [9,10,12,14].

2.5.2 Entrapment efficiency (EE%)

First, a calibration curve (**figure 2.5**) for corn silk extract in acetic acid solution was plotted with the objective to calculate the EE%. The absorbance of the tested sample was substituted in the regression line as per **equation 4**;

Equation 4

$$y = 2.2441x + 0.0359$$

R^2= 0.999 where y is the absorbance and x is the concentration (mg\mL) of the corn silk extract released in supernatant after the centrifugation of the sample at specific conditions.

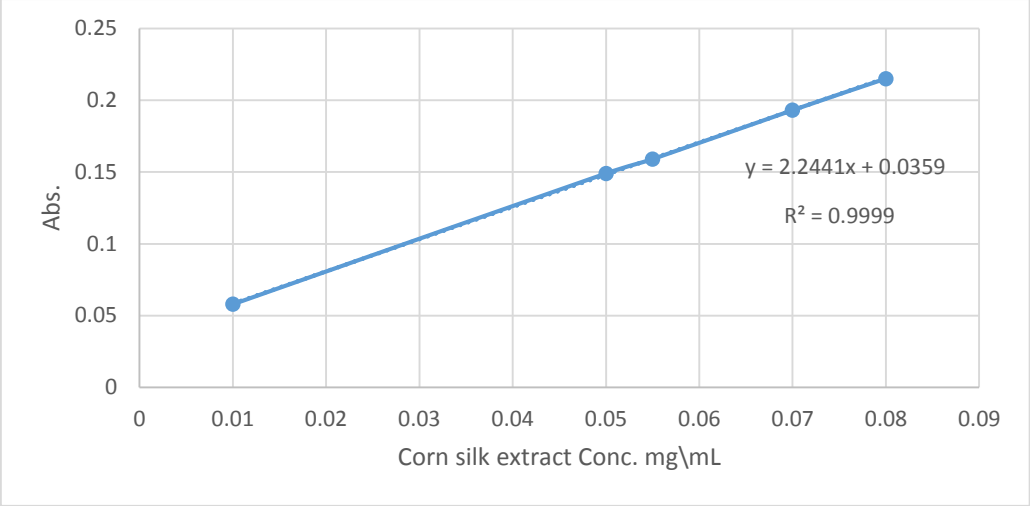

Figure 2.5 Calibration curve of Corn silk extract in acetic acid solution.

Second, the prepared silk extract CS NPs were centrifuged by speed 20000 rpm at 4°C for 1 hr. The absorbance of the supernatant of each preparation was measured at 340 nm wavelength. The resulted absorbance was substituted in the linear regression equation of the acetic acid calibration curve to get the concentration of unloaded extract. [12,15,16]

Then, **equation 5** is substituted with the concentration of the released extract in addition to the original concentration of the extract added at the beginning of the assay.

Equation 5 [12]

$$EE\% = [(total\ amount\ of\ extract\ added - free\ amount\ of\ extract) / total\ extract\ added] \times 100$$

2.6 Morphological, analytical and *in vitro* release characterization of SE x\CS NPs

2.6.1 Scanning electron microscope (SEM)

Morphological characteristics of the encapsulated NPs were assessed using SEM. NPs were first lyophilized to get them in a powder form, then few milligrams of the powder were placed on a one layered aluminum foil of 2 squared centimeter size. Samples were gold sputtered before SEM imaging where the working distance in the SEM was 2µm-200nm, with the excitation voltage (EHT) of 6 Kv, WD=3.1mm, signal A=Inlens, and magnifications of 5000, 10000, 15000, and 25000 x. [14]

2.6.2 Fourier-transform infrared FTIR spectroscopy

FTIR spectroscopic analysis were done using the powder form of the free extract, empty CS NPs, and encapsulated CS NPs. Each sample was mixed with KBr of ratio 1:0.2 (KBr: each sample). Each mixture was compressed into a very thin disc to be analyzed by FTIR spectroscopy. The

resultant data for every sample was compared to each other on the same graph plotted by the Omnic lite software where % transmittance (Y-axis) vs wavenumbers(X-axis). The wave number was ranged from 4000-500 cm^{-1} with a resolution of 4 cm^{-1}. [12]

2.6.3 *In vitro* release study

Calibration curve of corn silk extract in PBS and potassium dihydrogen phosphate media was plotted. In this experiment, a dialysis membrane 16 mm diameter, 5 mm length, 12000-14000 molecular weight and pore diameter of ca 25 A was used. A 40 mg of encapsulated NPs were added to 20 mL of each PBS of pH =7.4 and KH_2PO_4 of pH=5.8. The test tubes were left with the two different media in a water bath at 37 °C and speed 120 rpm. At specific time intervals (0.25,0.50, 1.00, 2.00, 3.00, 4.00, 6.00, 24.00 hrs.), 2 mL from each media was collected and replaced by a fresh media of the same amount. The amount of drug released in the withdrawal 2 mL was estimated by measuring the absorbance at 268 and 214nm respectively and using the following **equation 6**;

Equation 6[12]

$$\%\ \text{Silk extract} - \text{NPs release} = Ct / C0 \times 100$$

C_0 is the total amount of silk extract encapsulated.

C_t is the amount of drug released at a time t.

2.7 Chemical and biological activity of SE x\CS NPs

2.7.1 Antioxidant activity

The four preparations were compared to the corresponding amounts of the encapsulated silk extract. The weighted amounts of extract CS NPs were estimated from their EE%. 1 mL of 0.2mM DPPH solution was added to 2 mL of each sample. After 1 hr. in dark using the shaker, the absorbance of the samples was measured at 517 nm. The IC50 value of the optimum formula, the pure silk extract and the reference ascorbic acid were compared to each other.[8,9]

On the other hand, 1 mL of the extract CS NPs or free extract was added to 2 mL of $NaCO_3$(7.5%w\v) solution. 5 minutes after, 2.5mL of Folin reagent (10%v\v) was added, then the reaction was left for 1.5 hrs. on a shaker away from light. The absorbance of this sample was measured at 765nm to detect the concentration in mg\mL. Accordingly, the GAE of the optimum formula was calculated from the Gallic acid calibration curve.[10]

2.7.2 Antibacterial activity

The antimicrobial assessment was carried out based on Shetta *et al*. study with minor modification.[10] Two strains of bacteria; Gram-positive *Staphylococcus aureus* (*S. aureus*, ATCC 6538). and Gram-negative *Escherichia coli* (*E. coli*, ATCC 8739) were investigated. Agar dilution and colony counting methods were used throughout this process. Initially, the samples (SE, CS NPs, and SE\CS NPs) were kept for 2 hrs to be sterilized under UV light. The two strains of bacteria were cultivated in Luria broth (LB) medium for 24 hrs. at 37°C in the incubator. LB medium was prepared from 10 g L^{-1} sodium chloride, 5 g L^{-1} yeast extract, and 10 g L^{-1} peptone. After allowing the bacterial growth overnight, 2 mL from the bacterial culture was placed in falcon tubes where each tube contained 10 mg of (SE 0.5\ CS, SE 1\CS NPs, SE 1.5\CS NPs, SE 2\CS NPs.), 10 mg empty CS NPs, and corresponding amounts from SE 25 µL contains (0.25, 0.5, 0.75, 0.1 mg\mL). The samples along with the bacterial culture were left overnight at 37°C in the incubator while shaking at 250 rpm. The following day, the sterile LB agar was added to each falcon tube in order to prepare serial dilutions. The 7^{th} fold dilutions were added and distributed evenly on the nutrient agar then cultured at 37°C in the incubator overnight. The resultant colonies were counted to estimate the percentage of bacterial growth of inhibitions. Moreover, the negative control was LB broth only which was used to check the sterility of the agar used in the experiment, while the positive control was LB broth cultivated with bacteria.[10,17] The resulted colonies quantified by image J analysis software then the percentage of bacterial growth inhibition was calculated by the following **equation 7**;

. **Equation 7**[18]

$$\text{The percentage (\%)of the bacterial growth inhibition} = [(Ac - At)/Ac] \times 100$$

Ac is the average bacterial count in the negative control agar (agar of the untreated bacteria). At is the average bacterial count of the sample.

2.8 Statistical study

The statistical analysis was performed by Graphpad prism version 8.0.1 and the results were expressed as mean ±SD. $P<0.05$ which was considered as a significant difference between results. The ANOVA method of analysis was conducted by Design expert version 10.

2.9 Theoretical background

2.9.1 DPPH and Folin reagents

Prior *et al.* reported that DPPH is a compound that consists of a nitrogen free radical which is easily quenched by proton radical scavenger of hydrogen donating antioxidant and subsequently transformed into a nonradical form (DPPH-H). [19] As represented in **Figure 2.6,** the antioxidant (involve aromatic ring (Ar)) donates hydrogen atom to obtain stable non radical molecules (DPPH and ArO-Oar) that stops the chain reaction.

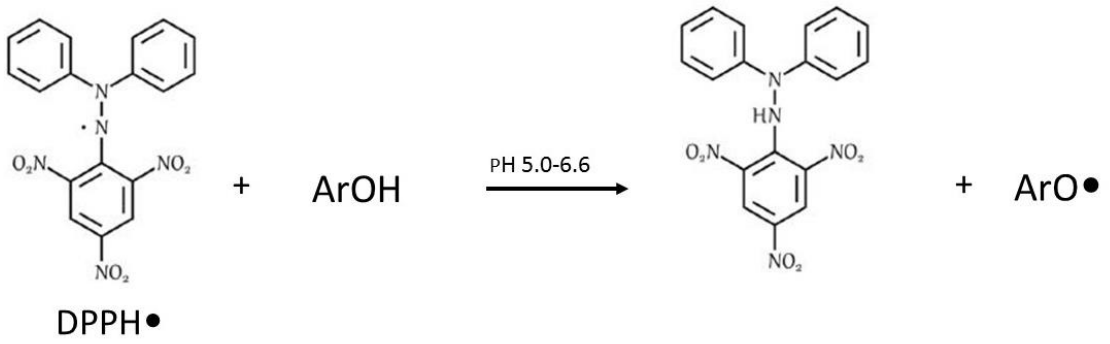

Figure 2.6 DPPH mechanism of reaction with phenolic cimpounds.[20]

On the other hand, **equation 8** demonstrate the reaction between phenolic compounds and Folin reagent which is composed of a mixture of phosphomolybdate and phosphotungstate in highly basic medium.

Equation 8[21]

$$Mo^{6+}\ (\text{yellow}) + ArOH \rightarrow Mo^{5+}\ (\text{blue at } 750\ nm) + [ArOH]^{\bullet}$$

2.9.2 Ionic gelation technique for CS NPs preparation

This technique is very reliable in preparing NPs because of its simplicity. It depends on the ionic formation between the positive charge on the CS NPs and the negative charge of the cross-linking agent (Tripolyphosphate) (TPP). As shown in **figure 2.7**, this reaction is an electrostatic interaction between cationic (NH_3) group of CS and the anionic (phosphoric ions) group of TPP. First, CS solution was prepared by dissolving CS powder in aqueous acetic acid solution and left overnight for complete dissolution. Separately, TPP solution was obtained by dissolving TPP powder in deionized water. TPP solution was added dropwise to CS on magnetic stirrer promoting CS cross-linkage. The cross-linking process was induced as water was expelled from the produced particles and the drug would be replaced inside the NPs. The key phenomenon of NPs formation

was the observation of opalescent suspension. It is worth mentioning that multiple factors affect this process such as the stirring speed, time of the reaction, and the ratio of CS to TPP[22] .

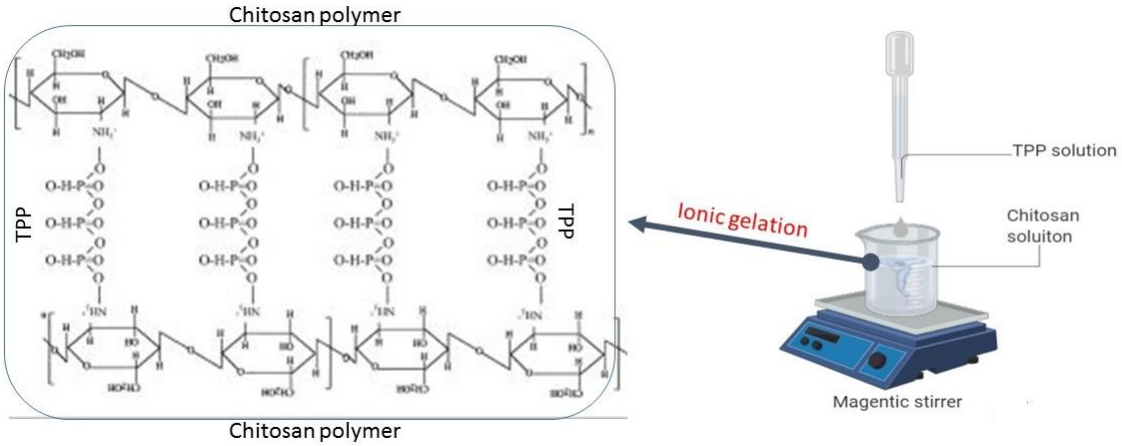

Figure 2.7 Ionic gelation technique for NPs preparation. (modified)[23]

2.9.3 Freeze dryer

Freeze drying or lyophilization includes the freezing of any material contains water at -55°C, followed by the transition of solid phase into gas phase of the moisture leaving the tested material in the form of powder**.** This device is preferable for materials that are thermolabile. Also, it is very beneficial for the purpose of storing materials for a long period of time. The first step in its mechanism of working is the sublimation process where any water content transforms into ice solid form. The second step involves the iced particles evaporates into gas state under vacuum condition and certain temperature above the triple point of water (at 4.579 mm of Hg and 0.0099°C) as shown in **figure 2.8.** Under sever cooling conditions, multiple drying steps take place allowing the ice pieces to separate from the solute and preserving the thermolabile material in its solid structure without being collapsed. Thus, this technique is to keep the samples unchanged biologically and chemically. This technique is applicable to multiple fields such as food industry, chemistry, and biological field.[24]

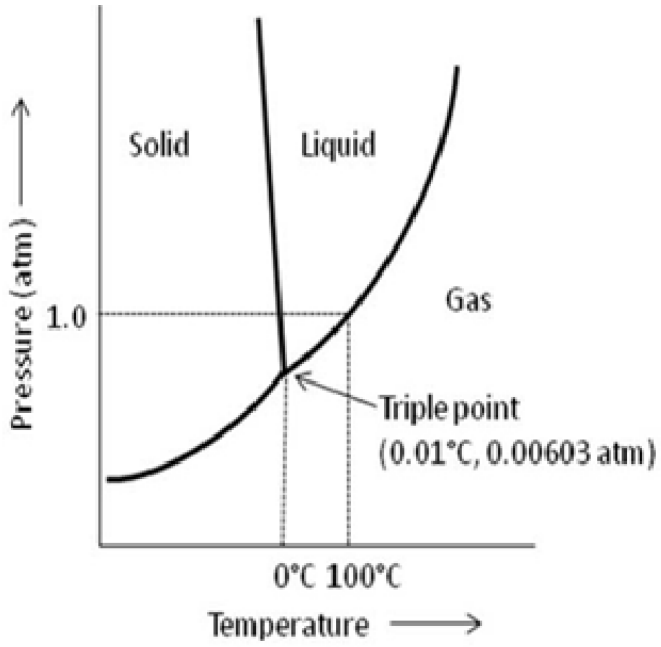

Figure 2.8 The triple point of transformation at which solid matter turns into gaseous state. [25]

2.9.4 Dynamic light scattering

The theoretical explanation behind the dynamic light scattering is simply that a monochromatic beam of light passes through the solution sample of specific concentration. The light incidence leads to light scattering in all directions that depends on the size and the shape of the macromolecules of the solution sample.[26]

Three measurements are determined by zetasizer; size, PDI, and zeta potential for particles ranging from nanometer into micrometer in size. Size measurement is accomplished by a process called dynamic light scattering (DLS). This process relies on Brownian motion of the particles which are illuminated with a laser beam resulting in certain fluctuations with specific intensities in the scattered light. The scattered light is received by a detector in the device in order to calculate the size of the particles. Correlator then correlates between two signals similar to each other during certain period of time. Since, the large particles will have slower motion than the small particles, the correlation function of the large particles will be totally detected different from that of the smaller ones. Accordingly, size distribution (PDI) as well as particle sizes will be analyzed from the correlation function as shown in **figure 2.9**.[27]

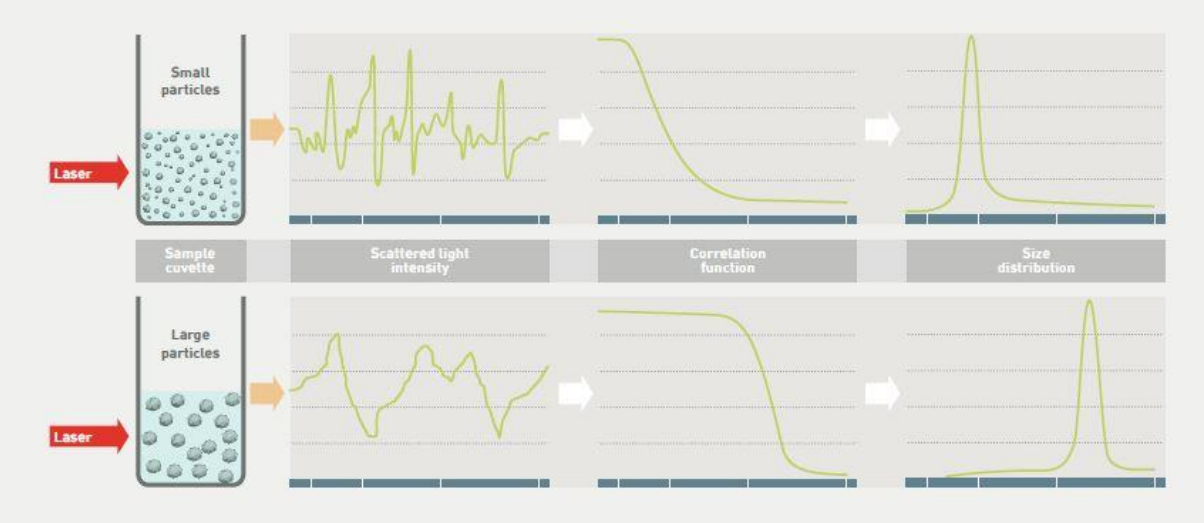

Figure 2.9 An illustration of the difference between scattered light intensity, correlation function and size distribution between the small particles and the large particles. [27]

The concept of measuring zeta potential relies on the electrophoretic mobility and applying Henry equation.[28] Simply, an electrical double layer (zeta potential) is developed in the liquid layer surrounding each particle, and this layer is composed of two layers where an inner part known as "stern layer" where ions are close to each other while in the outer layer, the ions are loosely attached to each other. When the negative or positive charges of zeta potential of the particles is large, the chance of the particles flocculation will be decreased. A specific cell is required for measuring the sample suspension zeta potential that is designed with electrodes to which a potential is applied as shown in **figure 2.10**. Particles prefer the electrodes which is opposite to their charge. The velocity of those particles is measured and expressed by Laser Doppler velocimetry (LDV) technique.[28]

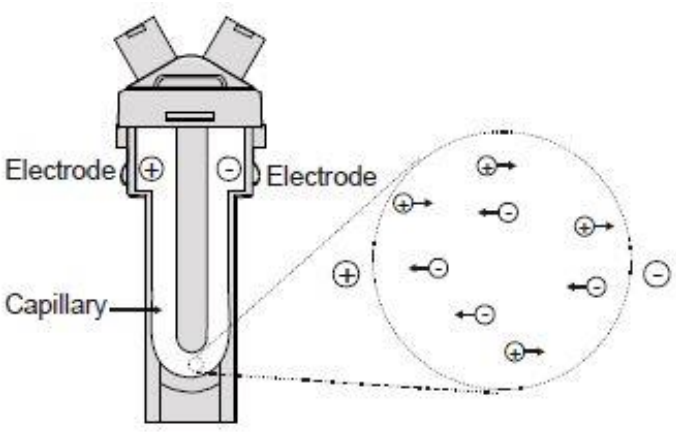

Figure 2.10 The folded capillary cell representing the negative and positive electrodes. [29]

2.9.5 Fourier transform infrared FTIR spectroscopy

The analytical technique of mid-IR spectroscopy has been known for decades where it relies on the identification of any chemical compounds by the means of detecting the functional groups through the appearance of peaks in the IR spectrum. Those peaks are representative for the excitation of electrons to a higher vibrational modes causing molecular bonds to bend or stretch. Mid-IR spectroscopy are detectable for samples with characteristic stretching vibrations occurring between 4000 and 1500 cm^{-1}. The IR spectroscopy showed some limited performance in detecting vibrational stretching below 1500 cm^{-1} which caused the development of FTIR spectrocopy. FTIR spectroscopy instruments works by the interference of two IR beams and this is called interferogram. Interferogram is a function of the change in path between the two beams. [30,31]

FTIR spectroscopy is widely used for the chemical characteristic analysis of polymers and organic compounds. The principle of FTIR spectroscopy is to determine the molecular or the fingerprint of any sample that is displayed on a screen in the form of a signal coming from a detector. The detector role is to receive the absorbed part of the beam by the sample. Basically, the spectrometer works by subjecting the samples into infrared (IR) beam, then it measures the amount and the frequency of that beam absorbed by the sample. Accordingly, **figure 2.11** illustrates using Michelson interferometer where a signal is generated from the Michelson interferometer then transform into frequencies detected as a signal via Fourier Transform algorithms. The Michelson interferometer composed of a light source (e.g. a mercury arc or tungsten), beamsplitter, and two perpendicular mirrors (fixed and moving one). The generated beam split at equal intensity by the beamsplitter which are reflected by the two perpendicular mirrors to recombine again. The recombined beams can be of either constructive or destructive interference. FTIR spectroscopy instrument converts the interferograms which are intensity versus time into intensity versus frequency.[31] Therefore, FTIR spectroscopy instruments are increasingly used because of their advanced computational power of increased resolution output. The FTIR spectral analysis which mainly depends on measuring the wavelength in the range of IR region with a longer wavelength and a lower frequency in comparison to visible light. The sample will be measured on the condition of being a thin slice of 10 microns so as to allow the transmittance of the beam through it. [32]

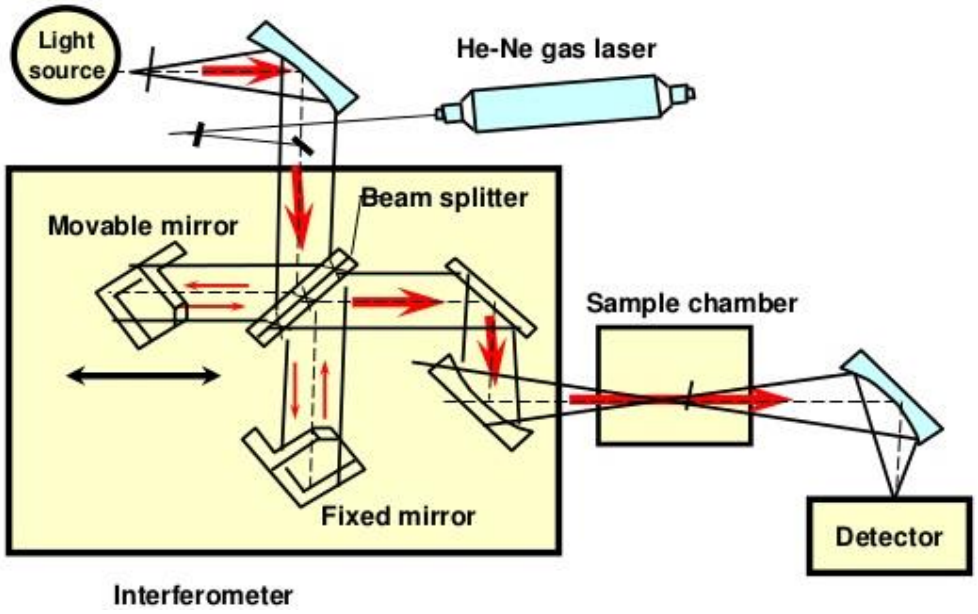

Figure 2.11 A Michelson interferometer in FTIR spectroscopy instrument to quantify and qualify the spectral fingerprint of any sample.[33]

2.9.6 Scanning electron microscope (SEM)

As shown in **figure 2.12**, in SEM, a high-energy electrons beam is directed towards a solid specimen where Auger electrons, secondary electrons, backscattered, and characteristic X-rays are produced. The utilization of Auger electrons, secondary electrons, and backscattered is to give compositional information, average atomic number, and topographical information about the specimen. The depth of the electron beam penetration through the sample surface depends on the density of the sample and the applied accelerating voltage.[34,35] The output of this incidence is the production of signals that illustrate the morphology, and the chemical composition of the sample. Moreover, a 2-dimensional image is displayed on a monitor. The magnification properties of this device can range from a 20 up to 30,000 X and spatial resolution of 50 to 100 nm. In **figure 2.13**, the main device components are Electron source (Gun), Detectors for the signals, and display devices.[36]

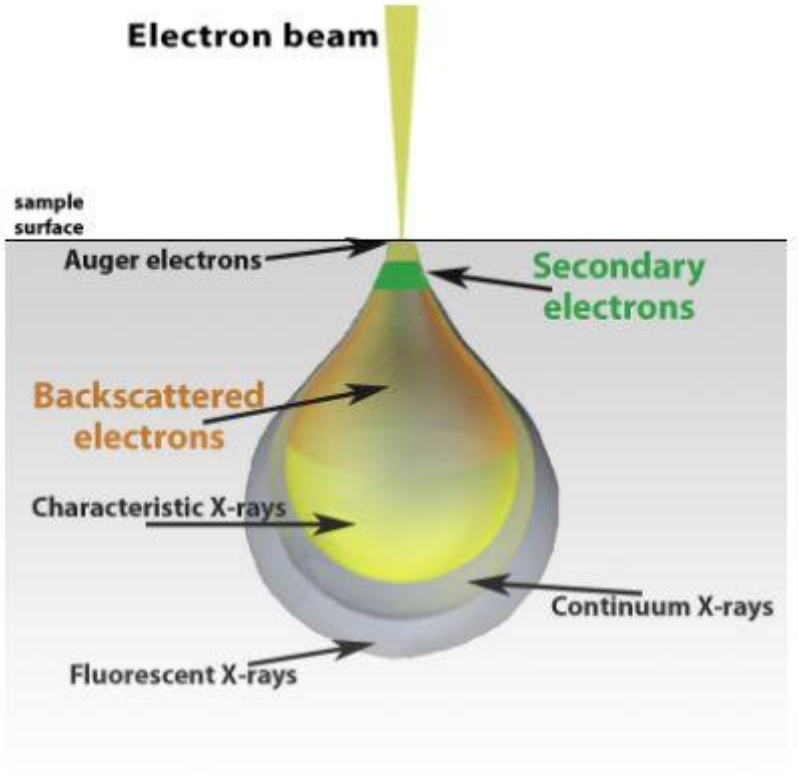

Figure 2.12 Schematic illustration of sample electron beam interaction.[34]

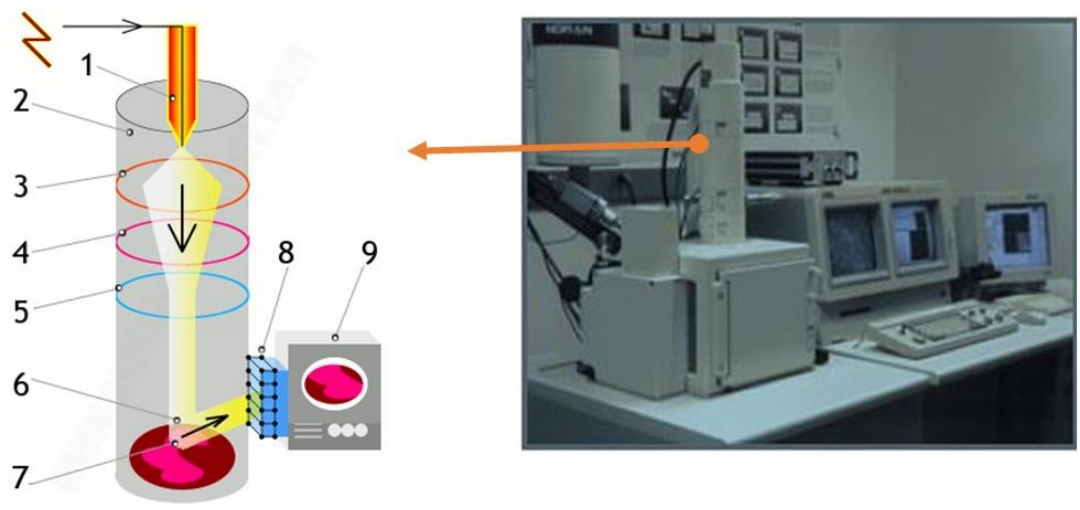

Figure 2.13. SEM 1- electrons released from the gun. 2- the sealed vacuum chamber. 3-positively charged electrode. 4-the electromagnetic coil to force the electron beam into a lens. 5- electromagnetic coil to steer the electron beam. 6- scanning the beam through the tested object. 7-hitting of the object with the electrons. 8-detecting the electrons and transforming into visible picture.[36,37]

2.9.7 Probe sonicator

The basic principle of this device is the electrical signal that is driven by ultrasonic electronic generator then transformed by piezoelectric transducer into mechanical vibration. This vibration increases then transfers through the probe (the tip) which is immersed in the liquid sample. Increasing the amplitude (by controlling from the touch screen) results in increasing the sonication

intensity. Therefore, cavitation and aggressive collapse of microscopic bubbles in the liquid takes place. Followed by the release of significant energy in the cavitation spaces that can disintegrate any particle agglomerates in the liquid. As shown in **2.14 (A),** the vibration amplitude is greatly influenced by the sonication intensity that controlled by the selection of generator, probe, and the tip. **Figure 2.14 (B)** illustrates a series of compression and rarefaction cycles take place when the ultrasound waves induce molecular motion in the liquid sample. As a result, the gas bubbles increase in size and diffuses through the expansion and rarefaction half cycle till the collapse phenomenon occurs. Thus, acoustic cavitation defined as growth and collapse of micro-bubbles under an ultrasonic field. [38,39]

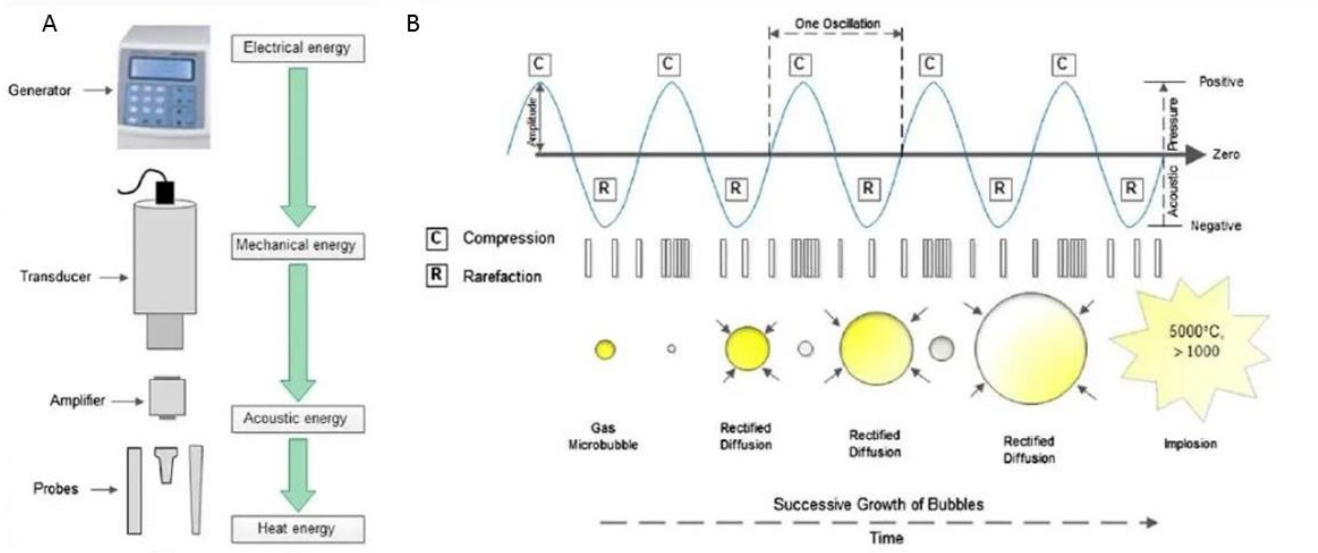

Figure 2.14 (A) Components of probe sonicator (B) schematic figure of the growth and collapse of bubble in acoustic cavitation process. [39]

2.9.8 UV-visible spectrophotometer

In Uv-visible spectroscopy, the incident monochrome radiation which gets absorbed by the sample, has corresponding frequency to the difference of energy between two energy levels allowing the excitation and transition of electrons. These changes cause an excitation of resonance resulting in changing in the electronic density distribution in the molecular orbitals. Boher model expressed such effect by **equation 9**:

Equation 9[40]

$$\Delta E = E2 - E1 = h\nu \rightarrow h\nu = hc\,\bar{\nu} = hc/\lambda$$

Where E1 and E2 are the initial and final energies respectively, h= Planck's constant ($6.62*10^{-34}$), c= light velocity in vacuum ($2.99*10^{8}$ m/s), ν= frequency, λ= wavelength, $\bar{\nu}$= wavenumber.

As shown **figure 2.15**, light source for the monochromatic radiation reaches the transparent cell as the absorption spectrum that will detected by the detector. The absorbed spectrum represents the corresponding frequency that are able to cause the variation in the electronic density and after the relaxation in the molecular orbitals they are released. [40]

The concentration of a sample can be identified by measuring the absorbance of the incident light at specific wavelength ranges from 198 to 1000 nm (UV-visible range). UV-visible spectroscopy measurement relies on Beer-Lambert Law which is represented in **equation 10**:

Equation 10 [41]

$$A = \varepsilon l c$$

where

A is the absorbance

Ɛ is the molar absorption coefficient

l is the path length

c is the concentration

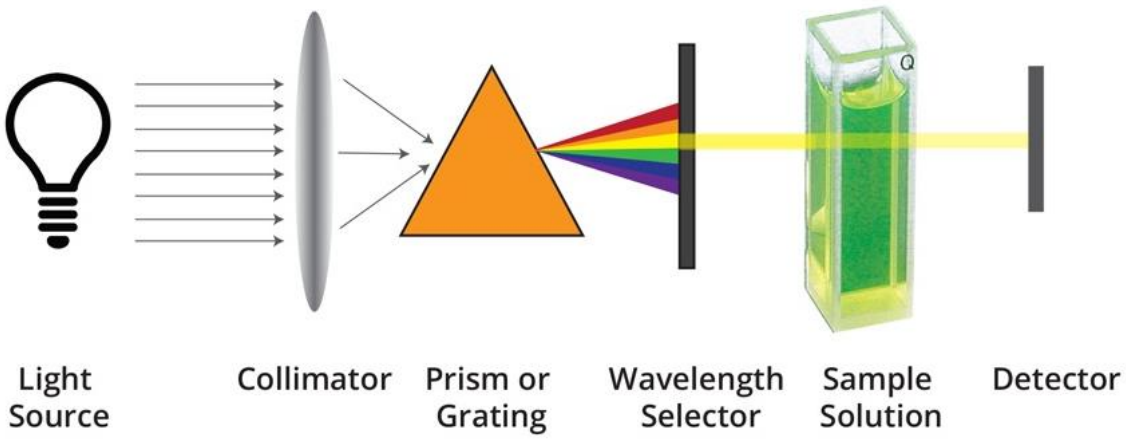

Figure 2.15 Simplified Schematic diagram for principle of working of UV visible spectrophotometer. [42]

Beer lambert law explains the reduction in light intensity after the transmission of the incident light through a transparent cell. Besides, transmittance (T) is the relation between the transmitted and the incident light while the absorbance is the inverse relation to (T) as per **equation 11**:

Equation 11[41]

$$\mathrm{A} = \mathrm{Log}\, 1/\mathrm{T}$$

Chapter 3

Results and discussion

3.1 DPPH and TPC assay for the three corn parts

As represented in **figure 3.1**, ascorbic acid was used as a reference sample where its highest percent of inhibition curve was compared to corn silk, husk, and cob. Percent of inhibition curve of SE dominated over husk and cob. SE showed the highest free radical scavenging activity due to the lowest value $\%IC_{50}$ in comparison to ascorbic acid. As justified by **figure 3.2,** ascorbic acid had the lowest $\%IC_{50}$ which was equal to 0.164 mg\mL while the $\%IC_{50}$ of SE, husk (HE) and cob (CE) were found to be 0.280, 1.080, and 1.837 mg\mL respectively. Moreover, **figure 3.3** shows TPC for SE which was higher than that of husk (HE) and cob (CE). The GAE or TPC were calculated from the gallic acid calibration curve. Silk showed the highest TPC to be 23.444 mg GAE\gm extract powder. On the other hand, husk and cob TPC were determined to be 14.683 and 8.915 mg GAE\gm extract powder, respectively. Subsequently, the antioxidant efficacy and TPC of SE showed the highest values in comparison to the corn cob and husk.

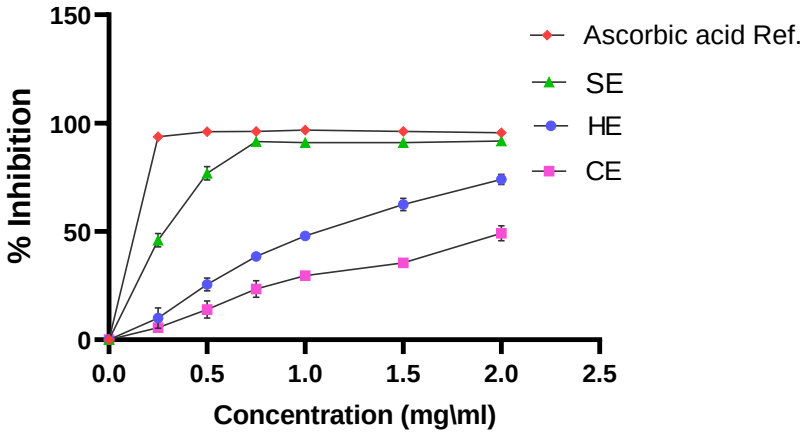

Figure 3.1 DPPH assay where the % inhibition plotted versus the serial dilution Ascorbic acid (Ref.), SE, HE, and CE.

Ascorbic acid Ref= 0.164 ± 0.001 mg\ml
Silk = 0.280 ± 0.013 mg\ml
Husk= 1.080 ± 0.013 mg\ml
Cob= 1.837 ± 0.226 mg\ml

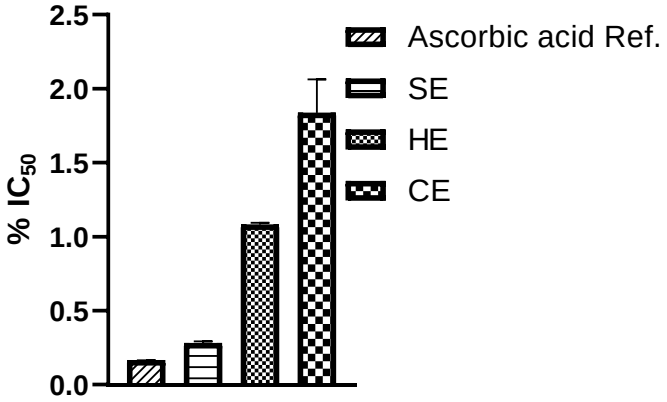

Figure 3.2 Chart graph for $\%IC_{50}$ was obtained from the previous curve and plotted with SD for Ascorbic acid, SE, HE, and CE.

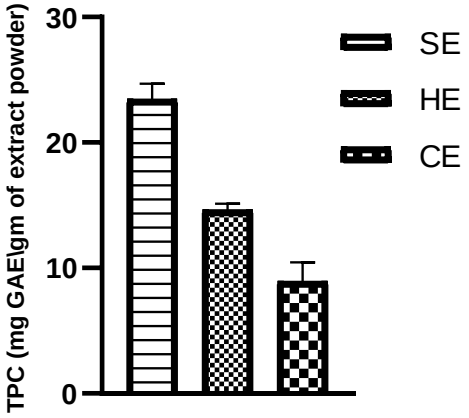

Figure 3.3 Chart graph for the phenolic concentration of SE in comparison to HE and CE, and plotted with SD.

In contrary to Dong *et al*. study, cob and SE were higher in their DPPH scavenging activity than that of husk. While the TPC results for the three parts were almost equivalent to 2.5 mg GAE\g dry weight sample.[238] The current study results for corn parts antioxidant activity were different from Dong *et al.* study because they relied on the ultrasonic cleaner with applied temperature at 40°C which may be a fundamental influencer in the extraction technique. Specifically, SE showed high DPPH and TPC values in several studies. Nurhanan *et al.* who recorded the lowest $\%IC_{50}$ (0.148 mg/mL) for SE associated with the highest free radical scavenging activity in comparison to butylated hydroxytoluene (BHT) (reference) with the highest scavenging activity $\%IC_{50}$ value was 0.059 mg/mL.[150] In addition, Nawaz *et al.* study proved the efficiency of methanol solvent with polarity 5.1 D in extracting phenolic compounds from corn silk where the DPPH % of

inhibition value was 93.5 % ±5.02.[206] Furthermore, Emmanuel *et al.* investigated the scavenging activity of SE in comparison to vitamin C used as a reference antioxidant agent both at the concentration of 5mg\mL. The % inhibition in their study was turned to be 73.54% and 85% for SE and vitamin C respectively.[201] TPC value of SE in Nurhanan *et al.* study illustrated the highest TPC of methanol extract corn silk was 101.99 ± 8.05 mg GAE\g crude plant powder.[150] It is worth mentioning that Soxhlet extraction method was utilized in Nurhanan *et al.* study which might be the reason behind the higher TPC obtained value. However, Solihah *et al.* reported the TPC of methanol extract of corn silk to be 0.048 ± 1.10 mg/g of GAE.[239] Moreover, Nawaz *et a*l. study showed that TPC of individual extraction of corn silk with methanol solvent of 5.1 D polarity was 14.6±0.18 mg GAE\ g dry weight of corn silk sample.[206] Obviously, There is a variation in TPC as well as the scavenging activity values among the conducted studies on corn silk due to the variability in the polarity of the used solvent, the method of extraction (in the presence of apparatus or not), and the utilization of temperature. Consequently, the current study relied on extracting SE with the conservation to protect the active component from destruction by the high temperature during preparation, and target the phenolic compounds by using solvents with the highest polarity. Based on this comparison, SE showed higher values for DPPH and TPC assay than of husk and cob as a result it was encapsulated in CS NPs for further experimental analysis.

3.2 Preparation and physicochemical characterization of the optimum formula

Optimizing the formula of the SE\CS NPs required preforming preliminary experiments via response surface model of design expert software. Response surface study was based on their level three factorial Box-Behnken design. The experimental results were fitted into quadratic model design and analyzed by applying the analysis of variance (ANOVA), response plots, and model graphs. As summarized in **table 3.1**, the effect of the three variable factors (F1) CS: TPP mass ratio, (F2) speed, and (F3) time were estimated on their corresponding responses (R1) particle size, (R2) PDI, and (R3) zeta potential for 15 required experiments in duplicate runs. The predicted responses were estimated by DLS. The model graphs and response plots showed the time and speed had no significant effect on the particle size, PDI, and zeta potential. In contrary, all the responses were mainly influenced by the variable factor CS: TPP mass ratio.

Table 3.1 Design expert's proposed factors and the responses which are estimated by DLS for each prepared sample (encapsulated NPs).

Factors			Responses		
A: CS:TPP ratio	B: Speed (rpm)	C: Time (hrs.)	Particle size (nm)	PDI	Zeta potential (mV)
1:1	800	3	290.8	0.171	14.9
1:1	600	1	277	0.187	15.7
1:1	400	3	284	0.201	15.7
1:1	600	5	319.2	0.19	14.6
3:1	600	3	330	0.393	30.5
3:1	800	5	285.7	0.451	39.2
3:1	600	3	360.4	0.383	33.8
3:1	600	3	349.4	0.285	34.4
3:1	400	5	269.5	0.303	37.9
3:1	400	1	250.7	0.415	34.3
3:1	800	1	318.7	0.302	34.2
5:1	400	3	588.4	0.474	43.1
5:1	800	3	590	1	33.1
5:1	600	5	730	0.867	28.5
5:1	600	1	780	1	37.8

As shown in **figure 3.4**, The perturbation plots illustrated that the change of A: CS:TPP over its range, had dramatically reflected on each response followed by the influence of the B: Speed while C: Time produced non-observed effect as it changes from the reference point. Thus, 3D response surface graphs had been plotted for the two factors A and B to demonstrate their synergistic effect**.** **Figure 3.4(A)** 3D graph displays their effect on the particles size where the concentration of the encapsulated SE kept the same in all preparations. The increase of CS: TPP mass ratio associated with the small particles size at the ratio of 1:1 then it started to increase at the ratio of 3:1 reaching the maximum particles size at the ratio of 5:1. **Figure 3.4(B)** 3D graph reveals the spike rise in the PDI values along with higher CS: TPP mass ratio. **Figure 3.4(C)** 3D graph represents the 1:1 ratio of low zeta potential values then those values kept rising during the 3:1 ratio preparation but they fall again with minor changes in the values. Although the speed had a relative small change on the responses, their effect was insignificant.[240]

These results were similar to Pulicharla *et al.* study where they explained the theory that lower TPP concentration leads to less chances for crosslinking occurrence with CS molecules resulting in smaller particle size formation. Therefore, 1:1 CS:TPP mass ratio preparations showed smaller particle size in relative to that of 3:1 ratio. On the other hand, excess amount of TPP in the preparation causes the formation of larger NPs due to the superfluous of TPP and get linked to already formed CS NPs as showed in the 5:1 ratio preparations. The rise in the positive values of zeta potential throughout the increasing CS:TPP ratio was a significant indicator for the stability of the formulations. [241] PDI values were expected to increase with the increase of CS:TPP ratio. [192]

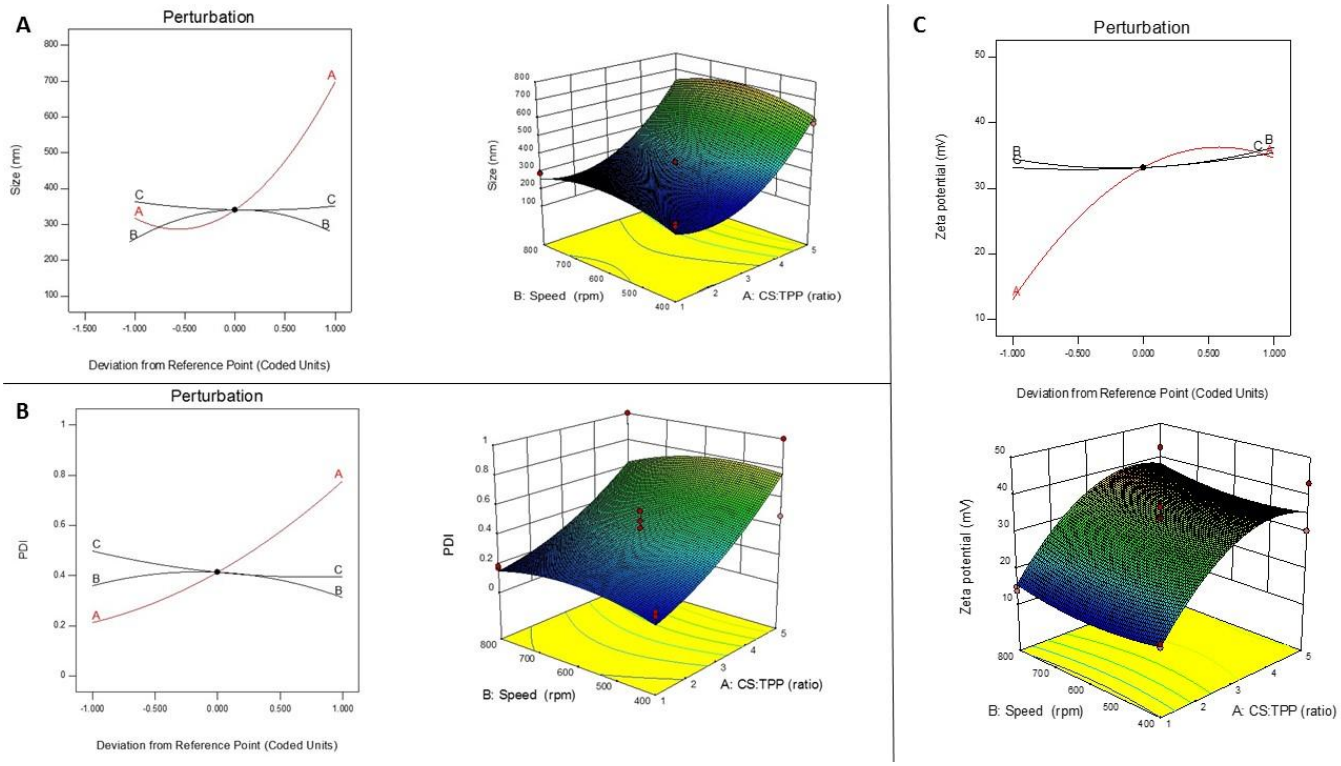

Figure 3.4 Perturabtion plots and 3D graphs for the repsonses (A) particle size, (B) PDI, and (C) zeta potential influnced by CS:TPP mass ratio.

There was more than one proposed solution for obtaining optimized SE\CS NPs formula with the desirable values of smallest particle size, lowest PDI, and highest zeta potential. Eventually, the optimized SE\CS NPs were prepared by 2.5:1 CS: TPP mass ratio during stirring at the speed of 800 rpm for 5hrs. Based on the above stated results, the influence of changing CS:TPP mass ratio was obvious on the prepared SE\CS NPs at a fixed SE concentration. So, the next step of the experiment is to examine the effect of changing SE concentration while keeping the CS:TPP mass ratio constant for the optimized SE\CS NPs.

In comparison to the empty CS NPs, **Table 3.2** and **figure 3.5** demonstrate that The particle size and zeta potential values were in gradual increase along with changing the concentration of the encapsulated SE. Also, the increase in EE% values showed a direct relation to the increase of particle size and zeta potential where the EE % of SE 0.5\CS NPs raised from 6.66%\±3.959 up to 32.91%\±0.947 of SE 2\CS NPs. The values of PDI responses of all the preparations were relatively close to each other. Moreover, **figure 3.5** shows the average values of the estimated responses for each SE\CS NPs preparation plotted against each other.

Table 3.2 SE\CS NPs at different SE concentrations and their responses particle size, PDI, zeta potential, and EE%.

SE\CS NPs	Ratio of CS : SE	Particle size (nm) Mean\±SD	PDI Mean\±SD	Zeta potential (mv) Mean\±SD	EE% Mean\±SD
SE 0.5\CS NPs	1:0.025	217\±2.433	0.19\±0.014	36.9\±0.264	6.66%\±3.959
SE 1\CS NPs	1:0.05	232\±7.081	0.25\±0.033	37.4\±2.569	26.04%\±1.555
SE 1.5\CS NPs	1:0.075	236\±8.540	0.20\±0.022	38.9\±1.816	26.06%\±7.933
SE 2\CS NPs	1:0.1	237\±4.788	0.21\±0.008	39.5\±2.734	32.91%\±0.947
Empty CS NPs	1:0	226\ ±7.505	0.29\±0.096	41.6\±1.154	-

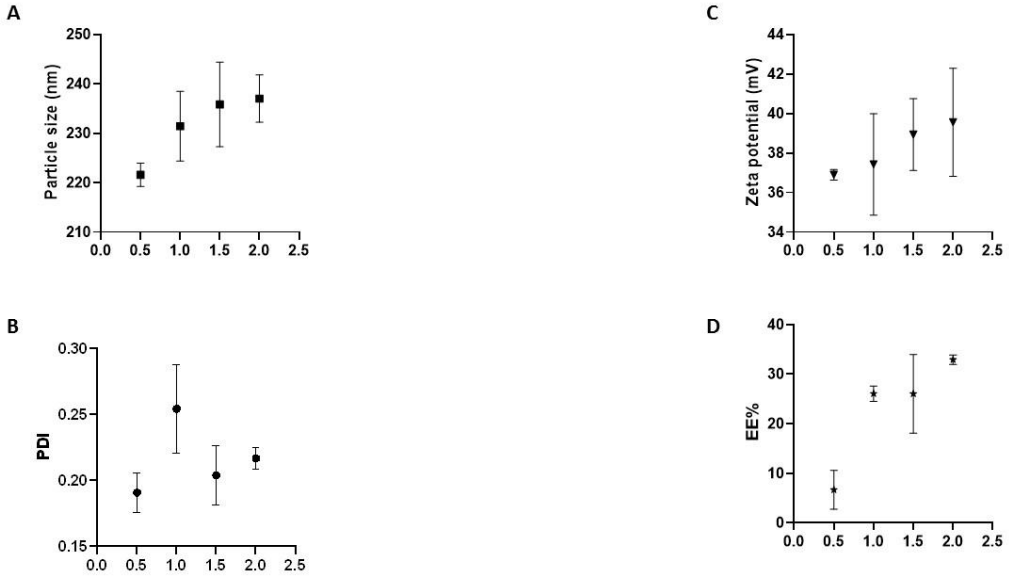

Figure 3.5 The responses (A) particle size, (B) PDI, (C) Zeta potential, and (D) EE% of the SE 0.5\CS NPs, SE 1\CS NPs, SE 1.5\CS NPs, and SE 2\CS NPs.

Table 3.3 summarizes similar studies conducted on estimating the influence of encapsulating increased concentration of extract or phenolic compound on particle size, zeta potential and EE%. Pulicharla *et al.*, Liu *et al.*, and Stoica *et al.* showed the same response of increasing particle size with different concentrations of the phenolic compounds. They explained that the polyphenolic structure penetrated the chitosan network due to the electrostatic interaction between the phosphate groups of TPP and the OH groups that belongs to the phenolic compounds and CS. Pulicharla *et al.* clarified the reason of increased zeta potential values was the interaction between the negative groups of the strawberry polyphenols and the positive amino groups of CS. On the other hand, Liu *et al.* illustrated zeta potential values decreased due to either the entrapping of the

phenolic compounds into the nanoparticles or its absorption onto the surface of the nanoparticles. Entrapment can lessen the crosslinking mechanism while absorption can decrease the positive amino groups exposed on the surface of the chitosan. EE% results of the current study were supported by Liu *et al.* study as they explained that the NPs had a certain capacity of encapsulating the phenolic compounds. In other words, the EE% increases by increasing the concentration of the encapsulated drug until it reaches certain limit beyond which it decreases. Whereas, Pulicharla *et al.* explained that the hydrophilic nature of strawberry extract was considered as a factor that allowed the escaping of extract from chitosan structure without being entangled. Another explanation was mentioned that the hydroxyl groups of both the phenolic compounds and CS could show repletion behaviour in the presence of PH 4.5. [192,194,241]

Table 3.3 Particle size, zeta potential, and EE% of another encapsulated phenolic compounds in CS NPs. [192,194,241]

Study	Encapsulated extract concentrations	Particle size	Zeta potential	EE%	Possible influencing factors
Pulicharla *et al.* study	Polyphenols Strawberry extract 0.25, 0.5, 1, 1.5 mg\mL	298.8nm ± 8.2 to 512.3nm ± 5.9	3.07mV ± 0.9 to 5.37mV ± 0.8	Decreased from 60.07 ± 3.6 to 41.68 ± 2.7	PH less than 5. The optimum formula CS: TPP mass ratio was 3:1
Stoica *et al.* study	Rose hips extract 0.5-10 %v\v	Initially the particles size decreased then it started to increase at 4% v\v	-	-	CS: TPP mass ratio equals 6:1
Liu *et al.* study	Scutellarin (phenolic compound) 1, 2, 3, 4 mg\mL	Increase from 290.3 to 489.7 nm	Decreased from 27.3 to 12.9	Increased from 42.49 ± 0.37 to 77.59 ± 0.05	PH 4.5 CS:TPP mass ratio 5:1

Based on the results of the current and previous studies, it would be confirmed that increasing the concentration of the encapsulated SE influenced remarkably the gradual increase in the particle size, zeta potential, and EE% of the prepared encapsulated CS NPs. So the next step was to examine the SE before and after being encapsulated in CS NPs at those four concentrations. It was significantly important to investigate if there would be any biological activities (e.g. antioxidant and antibacterial) after encapsulating the SE in CS NPs. In other words, the encapsulated CS NPs was expected to be either with provoked or inhibited antibacterial and antioxidant activity. Moreover, morphological and analytical characterization was conducted to ensure that CS NPs was encapsulated and interacted with SE successfully. Besides, there were no studies reported for encapsulating SE in CS NPs however the results for the upcoming experiments were compared to

studies conducted on the encapsulation of phenolic compounds (extracted from other plants) in CS NPs.

3.3 Morphological, analytical and *in vitro* release characterization of SE x\CS NPs

3.3.1 Scanning electron microscope (SEM)

The morphology of the four different concentrations of SE encapsulated in CS NPs was measured by SEM in their powder\ lyophilized form. As illustrated in **figure 3.6 (A) and (C)**, the preparation of SE 0.5\CS NPs at the magnification of 15.48 k is in the range of the sizes between 24.72, 35.15 and 57.11 nm. While at the magnification of 25 K, SE 1\CS NPs are of the particle size range between 26.36 to 46.16 nm as shown in **figure 3.6 (B) and (D).** Then in **figure 3.6 (E and (G)**, the preparation of SE 1.5\CS NPs is of particle size range of 39 to 55.3 nm. Whereas the SE 2\CS NPs preparation has the largest particle size that started from 55.38 up to 84.49 nm as represented in **figure 3.6 (F) and (H).**

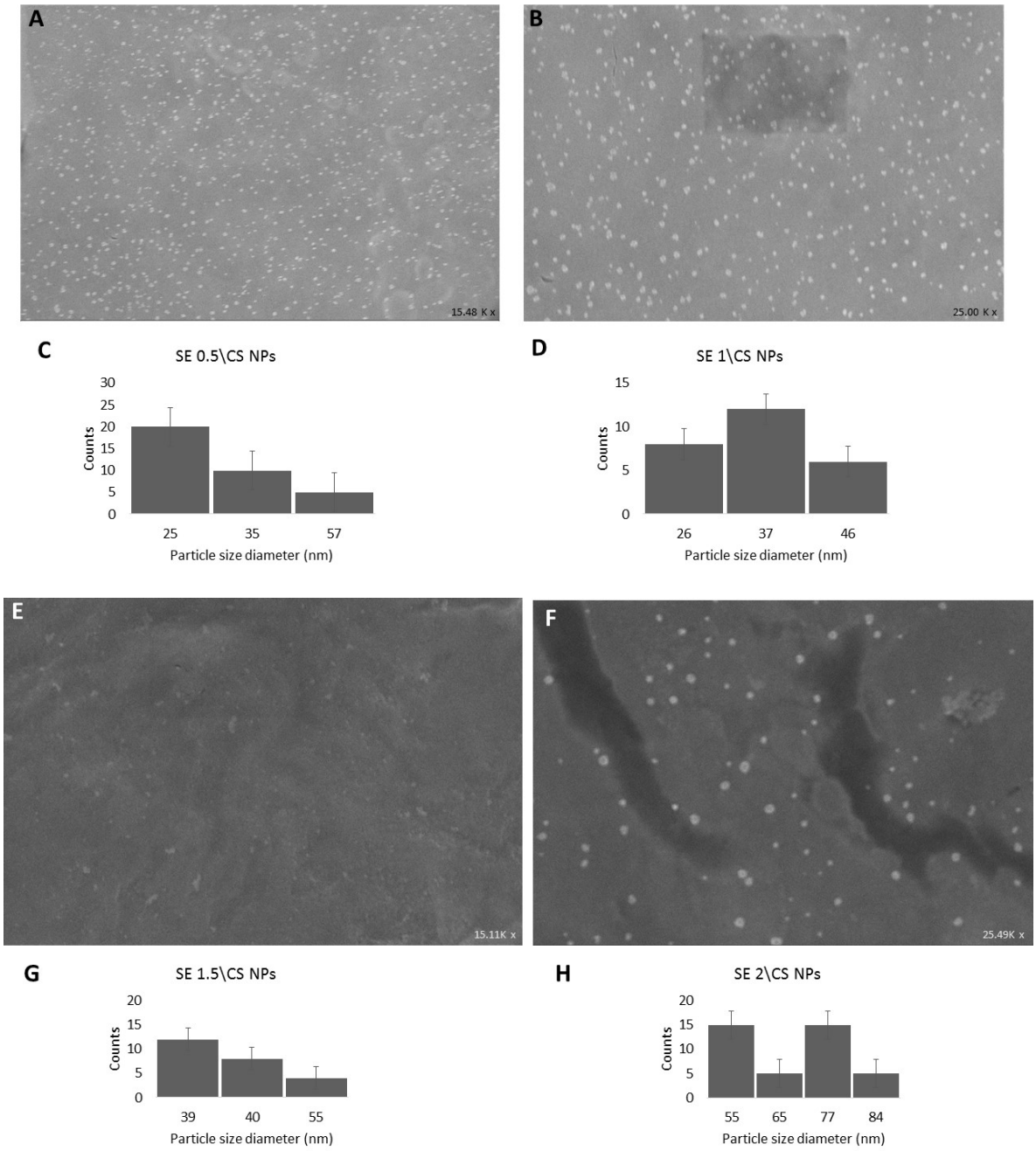

Figure 3.6 SEM pictures and histograms, at the magnification of 15.48 K (A) and (C) SE 0.5\CS NPs while at the magnification of 25 k; (B) and (D) SE 1\CS NPs. At the magnification of 25 k; (E) and (G) SE 1.5\CS NPs , (F) and (H) SE 2\CS NPs.

The SEM results gave more clear observation for the particles size of the four preparations where there was a gradual increase in particles size from 24.72 up to 84.49 nm. Also, it was evident that the encapsulation by SE has influenced the particles size in comparison to the empty CS NPs results 8.59 to 15.43 nm. Mahmoudi *et al.* revealed that the hydrodynamic size measured by the

DLS was much bigger than that of SEM due to the high swelling behavior of CS NPs.[193] Kumar *et al.* studied the encapsulation of flavonoid naringenin in chitosan nanoparticles, and they evident their study by SEM micrographs before and after the encapsulation of naringenin where the particles size of CS NPs had enlarged from 53.2 into 407.47 nm for naringenin\CS NPs. They explained that the CS to TPP mass ratio was 5:1 which was the best formula for the encapsulation.[242] So, the SEM results confirmed the spherical shape and the size distribution of the empty and the encapsulated CS NPs.

3.3.2 Fourier-transform infrared FTIR spectroscopy

As represented in **table 3.6**, The broad band of SE and empty CS NPs shifted from the location at 3388.3 and 3429.1 cm^{-1} respectively to 3434.4 cm^{-1} in the SE 2\CS NPs. Those bands represent the vibrational modes of hydrogen bonded O-H groups. While the bands of the free O-H groups (3822.8 and 3678.1 cm^{-1}) in the blank chitosan NPs were disappeared. Another bands belong to the SE and empty CS NPs which located at 1629.5 and 1629.8 cm^{-1}, represent the alkene groups (C=C) respectively were disappeared. While the positioned band at 1577.9 cm-1 appeared in the SE 2\CS NPs and represent the aromatic groups (C=C). Significantly on the pure extract chart, the band located at 1411.5 cm^{-1} that corresponds to the aromatic functional groups (C=C) appeared again after the encapsulation of the SE in CS NPs. In contrary to the disappeared bands positioned at 2924.9 cm^{-1} that represents (C-H) alkane group, whereas 819, 778.6, and 632.1 cm^{-1} represent (C=O) groups.[243,244]

As shown in **figure 3.7**, specific spectral bands had been changed due to the interaction between the CS and SE. The interaction between CS and phenolic compounds explained by Popa *et al.* who reported that the linear polymeric structure of chitosan with its anhydroglucosmaine compounds act as a linear and active polyelectrolyte. On the other hand, polyphenols act as a complexing agent due to their relative molecular mass (500-4000) and size, the existence of many phenolic groups (range from 12-16) and aromatic rings (range from 5-7) distributed per 1000 relative molecular mass.[245] Pulicharla *et al.* reported the disappearance of peaks between the region of 700-950 cm^{-1} was due to the interaction of NH_2 group of chitosan and C=O groups pf the polyphenols forming hydrogen bonding. Besides, they explained the broadening of the peak at 3200-2000 cm^{-1} indicative for the interaction between polyphenols and CS NPs through O-H-O bonding. [192] So, in addition to the confirmatory results of SEM, FTIR spectroscopy analysis ensured the interaction between SE and CS NPs functional groups through encapsulation mechanism.

Table 3.4 Spectral bands that have been shifted, disappeared, and appeared in SE, empty CS NPs, SE x\CS NPs.

From FTIR chart of	Spectral bands		
	Shifted	Disappeared	Appeared
SE	• (from)3388.3 cm^{-1} (into) 3434.4 cm^{-1} • (from) 1629.5 cm^{-1} (into) 1577.9 cm^{-1} • (from)1077.2 cm^{-1} (into) 1097.2 cm^{-1}	2924.9, 819, 778.6, and 532.1 cm^{-1}	
Empty CS NPs	• (from)3429.1 cm-1 into 3434.4 cm^{-1} • (from) 1629.8 cm-1 into 1577.9 cm^{-1} • (from) 1089.9 cm-1 into 1097.2 cm^{-1}	3822.8 and 3678.1 cm^{-1}	
SE 2\CS NPs			3434.4 cm^{-1} 1577.9 cm^{-1} 1411.5 cm^{-1} 1097.2 cm^{-1}

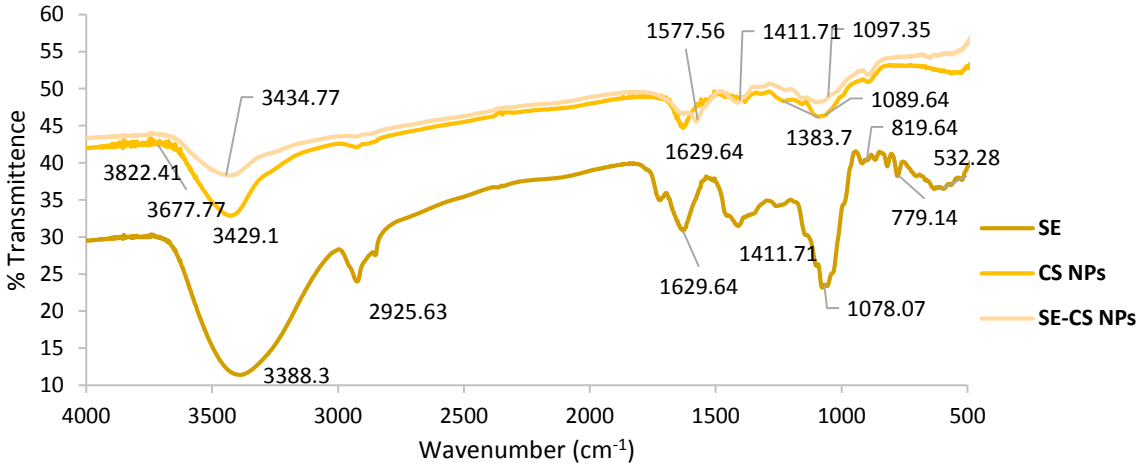

Figure 3.7 FTIR Chart graph for SE, empty CS NPs, and SE 2\CS NPs.

3.3.3 *In vitro* release study

As shown in **figure 3.8**, rapid release of the phenolic content of SE was observed in the first few hours of the encapsulated NPs in both lower and higher pH which was represented as higher release of SE in the pH 7.4 than pH 5.8. 57.8% of the SE was delivered in the system of pH 7.4 after 3 hours while the system of pH 5.8 received 57.8 % of SE after 4 hours. This can be explained as the swelling behaviour of chitosan changes by increasing pH where it allows the penetration of water into its structure and permits the exist of SE in the surrounding system (pH 5.8 or 7.4). [246] Pulicharla *et al.* studied the cumulative release percentage of strawberry polyphenols in similar pH values where the pH 7.4 system showed the highest percentage of the delivered polyphenols. They explained that the diffusion of water into chitosan nanoparticles caused the increase in size of the CS NPs which influenced the higher release of polyphenols.[192] Also, Harris *et al.* investigated polyphenols from yerba mate and the influence of pH 5.7 and 6.5 which corresponds to the pH value of the cosmetic formulations on their release from chitosan hydrochloride nanoparticles, and they confirmed that the release profile of polyphenols in pH 5.7 was much higher than that in pH 6.5 due to the solubility of chitosan hydrochloride in this pH. [247] Both the current study and the previous studies confirm that CS NPs possess specific behaviour in releasing the encapsulated extract. Mohammed *et al.* revealed that CS NPs possess release mechanism that is pH dependent. In addition, they explained the initial burst release of the encapsulated extract is due to the phenomenon of either CS swelling, pores formation in the polymeric structure of CS, or diffusion of the encapsulated extract to the surface of the polymer. [248] SE release behaviour in the tested pH is indicative that SE x\CS NPs can be a promising cosmetic formulation where SE rapid release confirmative for swelling of CS polymer by the imbibition of water. Then, CS polymeric chains formed diffusion barrier that represented in the form of diffusion-controlled release of SE. This study was indicative that SE x\CS NPs could be utilized in topical preparation while sustained releasing of the encapsulated SE takes place.

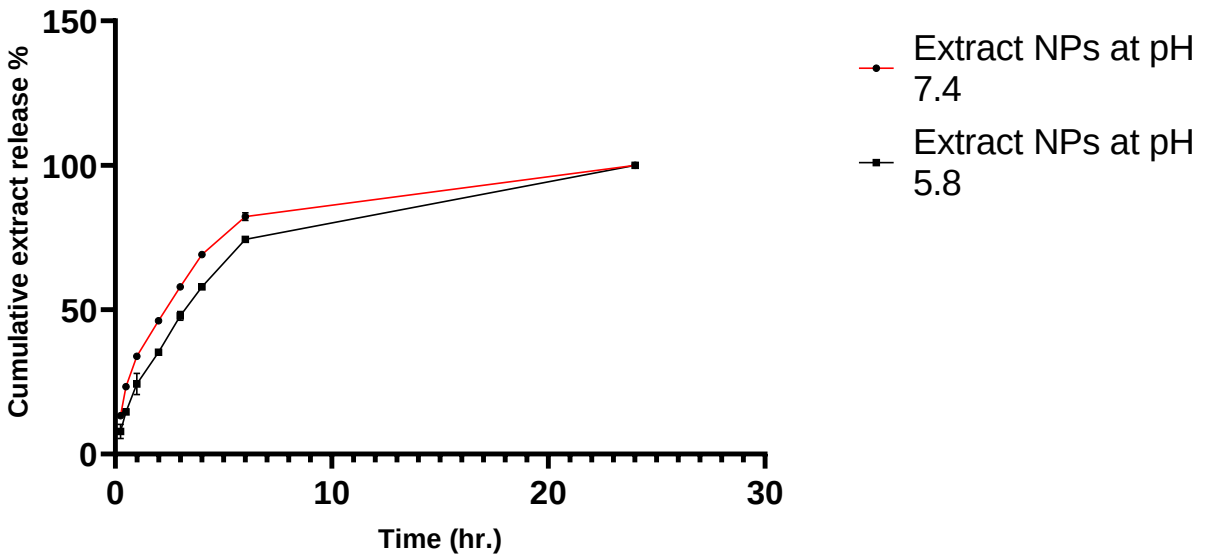

Figure 3.8 Release study patterns of SE 2\CS NPs in pH 7.4 and 5.8.

3.4 Chemical and biological activity of SE x\CS NPs

3.4.1 Antioxidant activity

As shown in **figure 3.9**, The empty CS NPs (SE 0\CS NPs) showed a relatively high scavenging activity (56.3%) which elevated after encapsulating SE in CS NPs from 83.7% up to 95.4% without neglecting the fact that SE alone at increasing concentration had showed increased scavenging activity. The scavenging activity of the corresponding amounts were 31.9 % ± 1.555, 61.1 %± 1.414, 74% ±2.828, and 87.4% ± 1.272 while of the empty CS NPs and the four SE x\CS NPs preparations were 56.3 % ±1.3435, 83.7% ± 1.484, 84.7% ±2.899, 87.4% ±2.689, and 95.4% ±2.121. Ruiz *et al.* reported similar results for the essential oils from thyme encapsulated in CS. Synergistic effect had been observed after combining the CS with increasing amount of essential oils possessing phenolic compounds. The nitrogen free radical of DPPH reacts with the amino (NH_2) groups of chitosan forming stable macromolecule radicals (ammonium groups) after absorbing the hydrogen ion from the sample.[249] Another study conducted by Median *et al.* had proved that phenolic compounds from *Citrus latifolia* waste caused the increase of percentage of inhibition from 58.8% and 9.9% for free extract and CS NPs respectively into 66.6% for encapsulated CS NPs.[243]

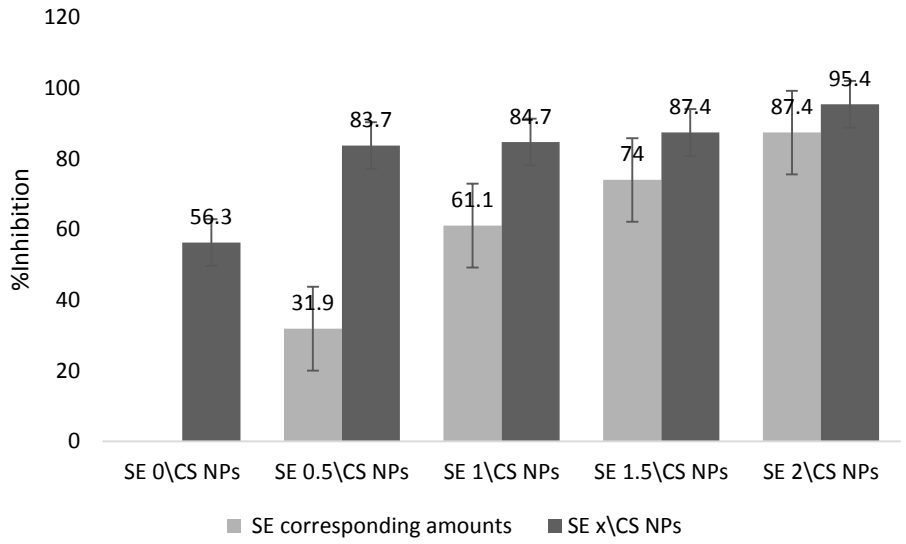

Figure 3.9 DPPH assay (scavenging activity) expressed as the inhibition percentage for free SE, empty and encapsulated CS NPs.

As represented in **figure 3.10**, The corresponding amounts of SE encapsulated in CS NPs showed increasing total phenolic content however surprisingly upon encapsulation the TPC values had decreased dramatically may be due to the very low loading capacity of the four preparations. The TPC values of the corresponding amounts were 16.5 mg GAE\gm sample ±0.989, 20.7 mg GAE\gm sample ±0.848, 25.5 mg GAE\gm sample ±2.757, and 35.7 mg GAE\gm sample ±2.757 while of the SE x\CS NPs preparations were 0.8 mg GAE\gm sample ±0.070, 3.7 mg GAE\gm sample ±0.141, 2.6 mg GAE\gm sample ±0.212, 3.5 mg GAE\gm sample ±0.282, and 3.4 mg GAE\gm sample ±0.212. That was indicative for the amount of encapsulated SE was not enough to be detected by Folin and Ciocalteu reagent. Also, another possible explanation was that the CS system was able to encapsulate the SE efficiently in a way that it slowly releases the SE to be reacted with Folin and Ciocalteu reagent. Ruiz *et al.* reported that a low TPC was obtained for the encapsulated CS NPs and they referred this finding to the reaction of Folin and Ciocalteu reagent with non-phenolic reducing substances.[249] It can concluded that SE encapsulation had elevated its scavenging activity in the presence of CS NPs but the CS prevented the encapsulated SE from exposing their phenolic content to Folin reagent. This indicative that CS NPs entrapped the phenolic content of SE successfully and it may require more time for allowing the interaction between Folin reagent and the encapsulated SE.

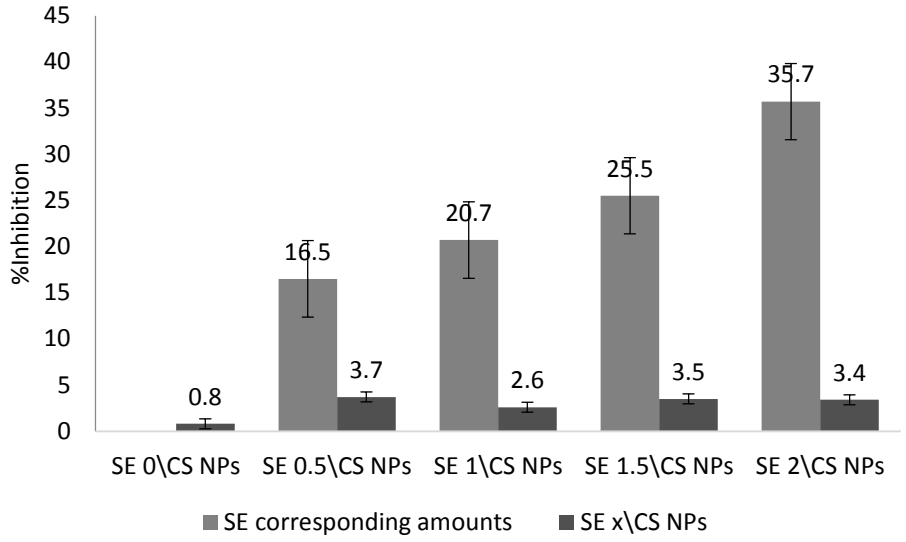

Figure 3.10 TPC values for free SE, empty and encapsulated CS NPs.

3.4.2 Antibacterial activity

The antibacterial activity of SE 0.5\CS NPs, SE 1\CS NPs, SE 1.5\CS NPs, and SE 2\CS NPs showed remarkable efficiency against the gram positive bacteria *S.aureus*. Also, SE at corresponding amounts were able to inhibit them completely. The positive control containing the incubated bacteria showed bacterial growth for both Gram-negative and Gram-positive bacteria while the negative control composed of the LB agar only showed no growth of any bacteria. On the other hand, *E. coli* colonies have been observed in all of the preparations either before or after the extract encapsulation. As shown in **figure 3.11 and 3.12**, the corresponding amounts of SE which were represented from 0.25 to 0.1 mg\mL were able to decrease the *E.coli* colonies count from 412 into 110 colony. This indicated the antibacterial efficiency of SE against gram negative bacteria only upon increasing SE concentration. Surprisingly, in comparison to the colonies count of the empty CS NPs preparation, SE 0.5\CS NPs, SE 1\CS NPs, SE 1.5\CS NPs, and SE 2\CS NPs caused the inhibition of *E.coli* growth as shown in **figure 3.13** and **3.14** where the colonies count decreased from 120 into 7 colony. The percentage of bacterial growth inhibition (%BGI) was calculated in order to clarify the relation between the antibacterial activity of SE x\CS NPs preparations and the bacterial colonies count. As shown in **Table 3.5**, the antibacterial activity of SE alone was relatively low as their % BGI values were ranged from 40.11% to 84.01%, and after encapsulation the %BGI ranged from 70.44% to 98.72%. Moreover, in comparison to %BGI value (92.85%) of the empty CS NPs, SE had an antagonistic effect with CS where SE 0.5\CS NPs, SE 1\CS NPs, and SE 1.5\CS NPs showed decreased % BGI values expect for SE 2\CS NPs. %BGI

of SE 2\CS NPs (98.72%) indicated that after encapsulating certain concentration of SE, SE could show a synergistic antibacterial behavior with CS.

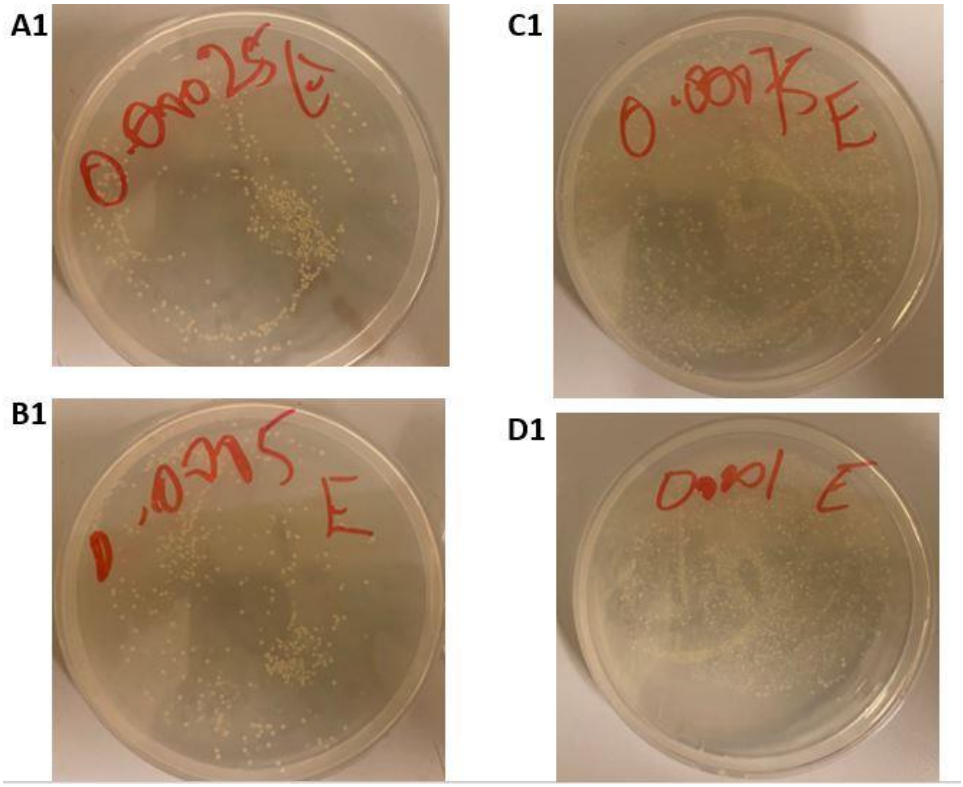

Figure 3.11 Agar plates of *E.coli* colonies for SE corresponding amounts (A1) 0.5 mg\mL. (B1) 1 mg\mL. (C1) 1.5 mg\mL. (D1) 2 mg\mL.

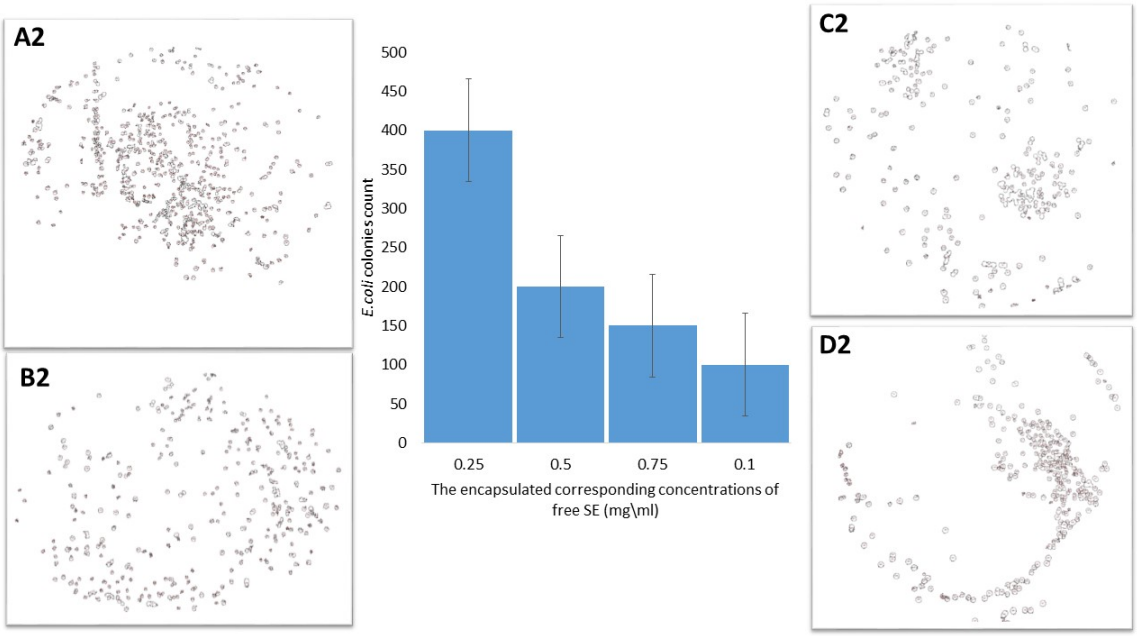

Figure 3.12 *E.coli* colonies counted via imageJ software with their histogram for SE corresponding amounts (A2) 0.5 mg\mL. (B2) 1 mg\mL. (C2) 1.5 mg\mL. (D2) 2 mg\mL.

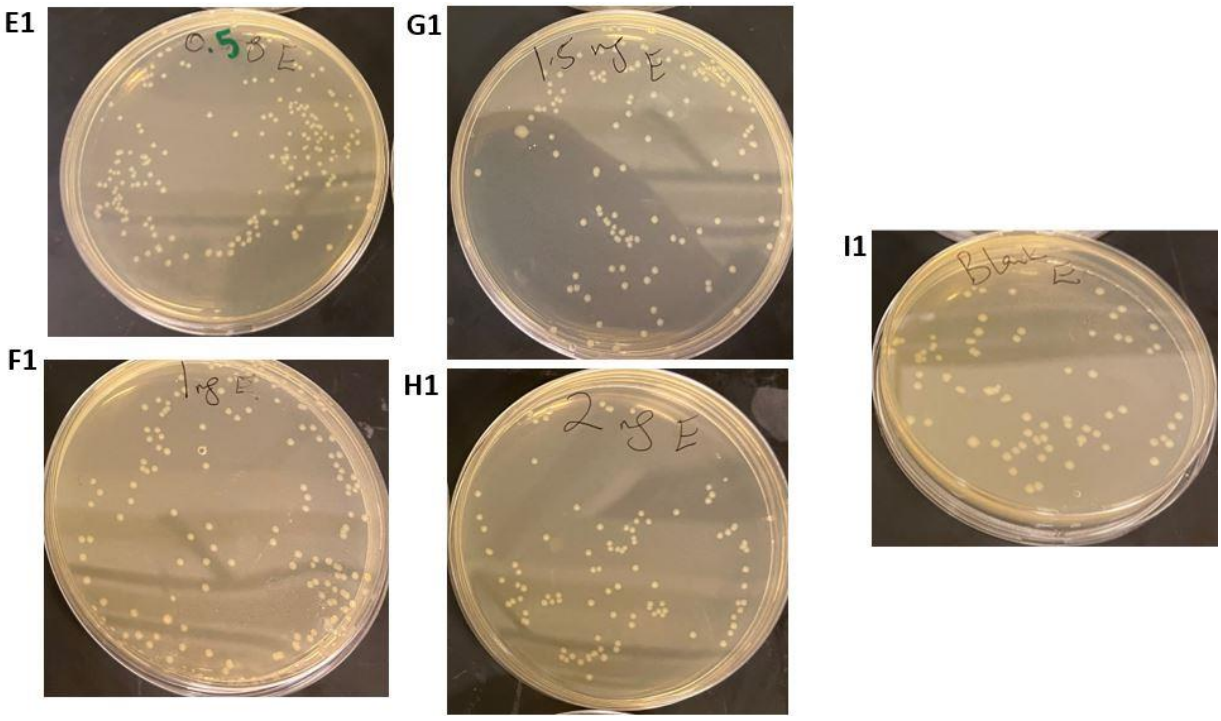

Figure 3.13 Agar plates of *E.coli* colonies for SE x\CS NPs (E1) SE 0.5 \CS NPs. (F1) SE 1 \CS NPs. (G1) SE 1.5 \CS NPs. (H1) SE2 \CS NPs. (I1) Empty CS NPs.

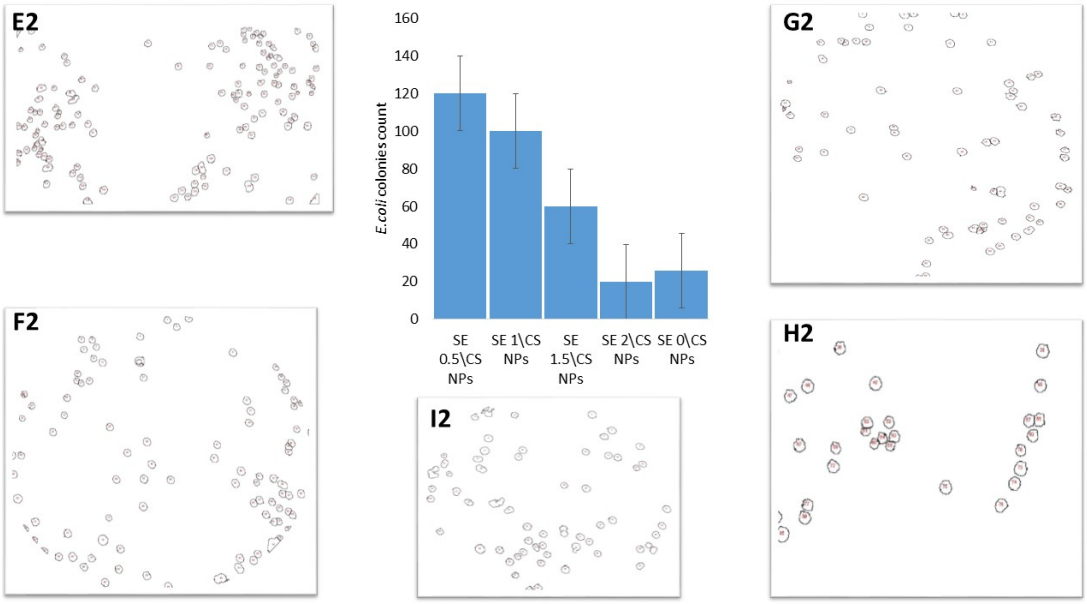

Figure 3.14 *E.coli* colonies counted via imageJ software with their histogram for SE x\CS NPs (E2) SE 0.5 \CS NPs. (F2) SE 1 \CS NPs. (G2) SE 1.5 \CS NPs. (H2) SE2 \CS NPs. (I2) Empty CS NPs.

Table 3.5 Antibacterial activity expressed as % of bacterial growth inhibition for (corresponding concentrations) SE, empty CS NPs, and SE x\CS NPs.

Samples	***E.coli* % bacterial growth inhibition**
Free extracts	
SE (0.25 mg\mL)	40.11 ±1.415
SE (0.5 mg\mL)	59.30 ±2.757
SE(0.75 mg\mL)	73.40 ±2.320
SE (0.1 mg\mL)	84.01 ±2.749
Encapsulated extracts in CS NPs	
SE 0.5\CS NPs	70.44 ±1.414
SE 1\CS NPs	76.10 ±1.418
SE 1.5\CS NPs	82.51 ±2.317
SE 2\CS NPs	98.27 ±2.114
Empty CS NPs	92.85 ±2.640

First of all, the above mentioned results confirmed that SE had antibacterial efficiency against gram positive bacteria rather than the gram negative bacteria. These results already match with Nessa *et al.*, Emmanuel *et al.*, and Morshed *et al.* studies. In each study, methanol extract of corn silk showed bacterial growth inhibition against *S. aureus* higher than that of *E.coli* and in some cases there was no sensitivity at all towards *E.coli*. [161] [250] [251] As mentioned in **table 3.6**, much higher concentration of methanol extract of corn silk were investigated to inhibit the growth of

S.aureus and *E.coli* in comparison with a reference antibacterial agent. Although increasing the concentration of methanol extract of corn silk was an influencing factor to elevate the inhibition growth of *S.aureus*, *E.coli* kept showing higher resistance. Another important factor was the type of bacterial strain utilized in the experiment.

Table 3.6 Various SE concentration antibacterial activity against *S.aureus* and *E.coli.* [161 250 251]

Study	**(Free) SE concentration**	***S.aureus***	**E.coli**
Nessa *et al.*	25 mg\mL	1.4 fold higher sensitive in comparison to gentamycin	Showed no sensitivity
Emmanuel *et al.*	600,300,and 150mg\mL	0.8, 0.64, 0.48 fold higher sensitivity in comparison to ciprofloxacin	lower sensitivity
Morshed *et al.*	10mg\mL	0.7 fold higher sensitivity comparing to streptomycin	Showed no sensitivity

Secondly, the highest bacterial growth inhibition of CS was supported by Sullivan *et al.* study as the native CS NPs of medium molecular weight at pH 5.5 which was prepared at ratio 3:1 CS: TPP, at its lowest amount of 0.5mg\mL killed *S. aureus* and *E.coli*.[252] Shafiei *et al.* reported that medium molecular weight CS at the concentration of 2mg\mL showed bactericidal effect against *S. aureus* higher than that against *E.coli*.[253] Sullivan *et al.* reported that degree of deacetylation is one of the factors that controls the antimicrobial activity of CS NPs which is linked to the number of protonated amino groups. Moreover, it was reported that *S. aureus* were more susceptible to CS due to the disruption of bacterial cell membrane caused by the linkages with lipoteichoic acid on the cell surface of Gram-positive bacteria. Another suggestion mentioned by Shafiei *et al.* is that the medium molecular weight CS had higher antimicrobial efficiency than the low molecular weight as it could form film to surround the bacteria and prevent its nutrients intake causing its death.[252,253] Subsequently, the combination of SE and CS NPs had shifted the values of %BGI almost 2 fold higher in comparison to that of SE alone. However, at certain concentration for SE, SE 2\CS NPs showed 98% of higher %BGI than the empty CS NPs. Our current study confirmed that the CS interaction with very low concentrations of SE influenced their antibacterial efficiency positively by significantly increasing their % BGI specifically against *E.coli*.

Chapter 4

Conclusion and future works

4. Conclusion

The effort behind this work is to tackle three main problems one of which is the bacterial infection, that is occurring worldwide and associating with the antibacterial resistance. Intensive efforts were put into finding novel treatments for preventing the bacterial infections but unfortunately the main obstacle was the antibacterial resistance which resulted from the intensive usage of synthetic antibacterial agents and the bacterial cellular mutation. The other problem is that bacterial invasion and biomolecules deterioration could be facilitated by oxidative stress phenomenon where studies have been proved its contribution in causing many chronic diseases. Last but not least, controlling food wastes is a serious issue requires attention from the governmental sectors especially when we take about the production of fruit and vegetables in huge amounts and not using their byproducts wisely such as the production of corn. Accordingly, novelty is essential to find innovative, eco-friendly, sustainable, and less toxic solutions for these problems.

This research aimed to investigate the corn silk waste potentiality as antioxidant and antibacterial agent, encapsulated in chitosan which is derived from the shellfish wastes. The antioxidant and antibacterial activities of SE after being encapsulated in CS NPs were compared to those biological activities of the bulk (free) SE. From this comparison and by analyzing the morphological features of the samples, it can be concluded that SE encapsulation has an additional benefit that can be utilized in the pharmaceutical sector. The results of the current study showed that the antioxidant activity of SE had been increased after encapsulation in CS NPs based on the free radical scavenging activity DPPH assay values. The % inhibition of the highest concentration of SE encapsulated into CS NPs was found 95.4% which was higher than the empty CS NPs. While, the TPC assay showed lower values after encapsulation of SE. TPC value of the highest concentration of SE encapsulated in CS NPs was 3.4 after being 35.7 mg GAE\gm sample. This interpreted as an excellent entrapping of SE in CS NPs that slowed down the phenolic content of SE from reacting with the Folin reagent. Although the empty CS NPs %BGI was much higher (92.85%) than the free extract, the highest concentration of SE when encapsulated in CS NPs they resulted in higher %BGI (98.7%) than that of the empty CS NPs. This explains that increasing the concentration of the encapsulated extract is essential for increasing the chance of interaction between CS and the extract. Also, the results of the antibacterial tests showed that CS NPs encapsulation of SE had a synergistic effect as it increased the capability of SE to inhibit bacterial growth especially in case of *E.coli*. Furthermore, SEM and FTIR spectroscopy analysis had confirmed the successful interaction and encapsulation of SE in CS NPs. SEM had identified the

SE x\CS NPs and the empty CS NPs in a spherical shape where the particle size diameters of the empty CS NPs were much smaller than that of the encapsulated which confirmed the SE encapsulation. Besides, FTIR spectroscopy had showed the appearance and disappearance of spectral bands representing specific functional groups after the SE encapsulation proving the interaction between the chemical formula of SE and CS. Also, the *in vitro* release study indicated that SE encapsulation would provide a promising topical formula of SE x\CS NPs as they showed a sustained release of SE in the pH 7.4 and 5.8 that mimics the pH of the human blood and skin.

The novelty of the current work was to prove the capability of encapsulation to magnify the biological activity of plant extract, and utilizing the wastes of corn. This approach was accomplished successfully, however more experiments are required such as antibacterial tests are needed against more bacterial strains, and antifungal tests as well. Moreover, animal models can be helpful for testing the antioxidant efficiency of the encapsulated SE.

References

References

(1) Sender, R.; Fuchs, S.; Milo, R. Revised Estimates for the Number of Human and Bacteria Cells in the Body. *PLoS Biol.* **2016**, *14* (8). https://doi.org/10.1371/journal.pbio.1002533.

(2) Microbes Evolved to Colonize Different Parts of the Human Body | Duke GCB https://genome.duke.edu/news/wed-03292017-0853/microbes-evolved-colonize-different-parts-human-body (accessed Apr 13, 2020).

(3) Drexler, M.; Medicine (US), I. of. *How Infection Works*; National Academies Press (US), 2010.

(4) Davis, C. P. Normal Flora. In *Medical Microbiology*; Baron, S., Ed.; University of Texas Medical Branch at Galveston: Galveston (TX), 1996.

(5) Normal Flora. Microbiology Teaching Resource - Microbiology Nuts & Bolts http://www.microbiologynutsandbolts.co.uk/normal-flora.html (accessed Apr 13, 2020).

(6) Molecular Expressions Cell Biology: Bacteria Cell Structure https://micro.magnet.fsu.edu/cells/bacteriacell.html (accessed Apr 13, 2020).

(7) Salton, M. R. J.; Kim, K.-S. Structure. In *Medical Microbiology*; Baron, S., Ed.; University of Texas Medical Branch at Galveston: Galveston (TX), 1996.

(8) Steinert, M.; Hentschel, U.; Hacker, J. Symbiosis and Pathogenesis: Evolution of the Microbe-Host Interaction. *Naturwissenschaften* **2000**, *87* (1), 1–11. https://doi.org/10.1007/s001140050001.

(9) Peterson, J. W. Bacterial Pathogenesis. In *Medical Microbiology*; Baron, S., Ed.; University of Texas Medical Branch at Galveston: Galveston (TX), 1996.

(10) Staphylococcus aureus in Healthcare Settings | HAI | CDC https://www.cdc.gov/hai/organisms/staph.html (accessed Apr 13, 2020).

(11) Tong, S. Y. C.; Davis, J. S.; Eichenberger, E.; Holland, T. L.; Fowler, V. G. Staphylococcus Aureus Infections: Epidemiology, Pathophysiology, Clinical Manifestations, and Management. *Clin. Microbiol. Rev.* **2015**, *28* (3), 603–661. https://doi.org/10.1128/CMR.00134-14.

(12) Henriques-Normark, B.; Tuomanen, E. I. The Pneumococcus: Epidemiology, Microbiology, and Pathogenesis. *Cold Spring Harb. Perspect. Med.* **2013**, *3* (7). https://doi.org/10.1101/cshperspect.a010215.

(13) Pneumococcal Disease (Streptococcus pneumoniae) | Disease Directory | Travelers' Health | CDC https://wwwnc.cdc.gov/travel/diseases/pneumococcal-disease-streptococcus-pneumoniae (accessed Apr 13, 2020).

(14) CDC. Could you have deadly diarrhea (C. diff)? https://www.cdc.gov/cdiff/what-is.html (accessed Apr 13, 2020).

(15) Norén, T. Clostridium Difficile and the Disease It Causes. *Methods Mol. Biol. Clifton NJ* **2010**, *646*, 9–35. https://doi.org/10.1007/978-1-60327-365-7_2.

(16) Clostridium difficile https://www.nhs.uk/conditions/c-difficile/ (accessed Apr 13, 2020).

(17) Klebsiella infection | Genetic and Rare Diseases Information Center (GARD) – an NCATS Program https://rarediseases.info.nih.gov/diseases/10085/klebsiella-infection (accessed Apr 13, 2020).

(18) Klebsiella pneumoniae in Healthcare Settings | HAI | CDC https://www.cdc.gov/hai/organisms/klebsiella/klebsiella.html (accessed Apr 13, 2020).

(19) Vading, M.; Nauclér, P.; Kalin, M.; Giske, C. G. Invasive Infection Caused by Klebsiella Pneumoniae Is a Disease Affecting Patients with High Comorbidity and Associated with High Long-Term Mortality. *PLoS ONE* **2018**, *13* (4). https://doi.org/10.1371/journal.pone.0195258.

(20) Bodey, G. P.; Bolivar, R.; Fainstein, V.; Jadeja, L. Infections Caused by Pseudomonas Aeruginosa. *Rev. Infect. Dis.* **1983**, *5* (2), 279–313. https://doi.org/10.1093/clinids/5.2.279.

(21) Pseudomonas aeruginosa Infection | HAI | CDC https://www.cdc.gov/hai/organisms/pseudomonas.html (accessed Apr 13, 2020).

(22) Allocati, N.; Masulli, M.; Alexeyev, M. F.; Di Ilio, C. Escherichia Coli in Europe: An Overview. *Int. J. Environ. Res. Public. Health* **2013**, *10* (12), 6235–6254. https://doi.org/10.3390/ijerph10126235.

(23) E. coli (Escherichia coli) | E. coli | CDC https://www.cdc.gov/ecoli/index.html (accessed Apr 13, 2020).

(24) Escherichia coli Infections - Infectious Diseases https://www.msdmanuals.com/professional/infectious-diseases/gram-negative-bacilli/escherichia-coli-infections (accessed Apr 13, 2020).

(25) Grant, S. S.; Hung, D. T. Persistent Bacterial Infections, Antibiotic Tolerance, and the Oxidative Stress Response. *Virulence* **2013**, *4* (4), 273–283. https://doi.org/10.4161/viru.23987.

(26) Glover, M.; Moreira, C. G.; Sperandio, V.; Zimmern, P. Recurrent Urinary Tract Infections in Healthy and Nonpregnant Women. *Urol. Sci.* **2014**, *25* (1), 1–8. https://doi.org/10.1016/j.urols.2013.11.007.

(27) Bradley, S. F. *Staphylococcus Aureus* Infections and Antibiotic Resistance in Older Adults. *Clin. Infect. Dis.* **2002**, *34* (2), 211–216. https://doi.org/10.1086/338150.

(28) Hogan, S.; Stevens, N. T.; Humphreys, H.; O'Gara, J. P.; O'Neill, E. Current and Future Approaches to the Prevention and Treatment of Staphylococcal Medical Device-Related Infections. *Curr. Pharm. Des.* **2014**, *21* (1), 100–113. https://doi.org/10.2174/13816128206661409051239OO.

(29) Vasudevan, R. Biofilms: Microbial Cities of Scientific Significance. *J. Microbiol. Exp.* **2014**, *1* (3). https://doi.org/10.15406/jmen.2014.01.00014.

(30) Biofilm bacteria (MPKB) https://mpkb.org/home/pathogenesis/microbiota/biofilm (accessed Apr 14, 2020).

(31) Romanò, C. L.; Romanò, D.; Morelli, I.; Drago, L. The Concept of Biofilm-Related Implant Malfunction and "Low-Grade Infection." In *A Modern Approach to Biofilm-Related Orthopaedic Implant Infections: Advances in Microbiology, Infectious Diseases and Public Health Volume 5*; Drago, L., Ed.; Advances in Experimental Medicine and Biology; Springer International Publishing: Cham, 2017; pp 1–13. https://doi.org/10.1007/5584_2016_158.

(32) Reeves, E. P.; Molloy, K.; Pohl, K.; McElvaney, N. G. Hypertonic Saline in Treatment of Pulmonary Disease in Cystic Fibrosis. *Sci. World J.* **2012**, *2012*, 1–11. https://doi.org/10.1100/2012/465230.

(33) Jamal, M.; Ahmad, W.; Andleeb, S.; Jalil, F.; Imran, M.; Nawaz, M. A.; Hussain, T.; Ali, M.; Rafiq, M.; Kamil, M. A. Bacterial Biofilm and Associated Infections. *J. Chin. Med. Assoc.* **2018**, *81* (1), 7–11. https://doi.org/10.1016/j.jcma.2017.07.012.
(34) Society, M. The history of antibiotics https://microbiologysociety.org/members-outreach-resources/outreach-resources/antibiotics-unearthed/antibiotics-and-antibiotic-resistance/the-history-of-antibiotics.html (accessed Apr 14, 2020).
(35) Ullah, H.; Ali, S. Classification of Anti-Bacterial Agents and Their Functions. *Antibact. Agents* **2017**. https://doi.org/10.5772/intechopen.68695.
(36) Aminov, R. I. A Brief History of the Antibiotic Era: Lessons Learned and Challenges for the Future. *Front. Microbiol.* **2010**, *1*. https://doi.org/10.3389/fmicb.2010.00134.
(37) Gould, K. Antibiotics: From Prehistory to the Present Day. *J. Antimicrob. Chemother.* **2016**, *71* (3), 572–575. https://doi.org/10.1093/jac/dkv484.
(38) WHO | Wide differences in antibiotic use between countries, according to new data from WHO https://www.who.int/medicines/areas/rational_use/oms-amr-amc-report-2016-2018-media-note/en/ (accessed Apr 14, 2020).
(39) Be Antibiotics Aware: Smart Use, Best Care | Patient Safety | CDC https://www.cdc.gov/patientsafety/features/be-antibiotics-aware.html (accessed Apr 14, 2020).
(40) Health matters: antimicrobial resistance - GOV.UK https://www.gov.uk/government/publications/health-matters-antimicrobial-resistance/health-matters-antimicrobial-resistance (accessed Apr 14, 2020).
(41) Plant production | Antimicrobial Resistance | Food and Agriculture Organization of the United Nations http://www.fao.org/antimicrobial-resistance/key-sectors/plant-production/en/ (accessed Apr 14, 2020).
(42) Chakrabarti, S.; Munshi, S.; Banerjee, K.; Thakurta, I. G.; Sinha, M.; Bagh, M. B. Mitochondrial Dysfunction during Brain Aging: Role of Oxidative Stress and Modulation by Antioxidant Supplementation. *Aging Dis.* **2011**, *2* (3), 242–256.
(43) Federico, A.; Cardaioli, E.; Pozzo, P. D.; Formichi, P.; Gallus, G. N.; Radi, E. Mitochondria, Oxidative Stress and Neurodegeneration. *J. Neurol. Sci.* **2012**, *322* (1), 254–262. https://doi.org/10.1016/j.jns.2012.05.030.
(44) Chiurchiù, V.; Orlacchio, A.; Maccarrone, M. Is Modulation of Oxidative Stress an Answer? The State of the Art of Redox Therapeutic Actions in Neurodegenerative Diseases. *Oxid. Med. Cell. Longev.* **2016**, *2016*. https://doi.org/10.1155/2016/7909380.
(45) Aprioku, J. S. Pharmacology of Free Radicals and the Impact of Reactive Oxygen Species on the Testis. *J. Reprod. Infertil.* **2013**, *14* (4), 158–172.
(46) Pizzino, G.; Irrera, N.; Cucinotta, M.; Pallio, G.; Mannino, F.; Arcoraci, V.; Squadrito, F.; Altavilla, D.; Bitto, A. Oxidative Stress: Harms and Benefits for Human Health. *Oxid. Med. Cell. Longev.* **2017**, *2017*. https://doi.org/10.1155/2017/8416763.
(47) Singh, A.; Kukreti, R.; Saso, L.; Kukreti, S. Oxidative Stress: A Key Modulator in Neurodegenerative Diseases. *Molecules* **2019**, *24* (8), 1583. https://doi.org/10.3390/molecules24081583.
(48) Liguori, I.; Russo, G.; Curcio, F.; Bulli, G.; Aran, L.; Della-Morte, D.; Gargiulo, G.; Testa, G.; Cacciatore, F.; Bonaduce, D.; Abete, P. Oxidative Stress, Aging, and Diseases. *Clin. Interv. Aging* **2018**, *13*, 757–772. https://doi.org/10.2147/CIA.S158513.
(49) Kim, G. H.; Kim, J. E.; Rhie, S. J.; Yoon, S. The Role of Oxidative Stress in Neurodegenerative Diseases. *Exp. Neurobiol.* **2015**, *24* (4), 325–340. https://doi.org/10.5607/en.2015.24.4.325.
(50) Krinsky, N. I. Mechanism of Action of Biological Antioxidants. *Exp. Biol. Med.* **1992**, *200* (2), 248–254. https://doi.org/10.3181/00379727-200-43429.
(51) Lobo, V.; Patil, A.; Phatak, A.; Chandra, N. Free Radicals, Antioxidants and Functional Foods: Impact on Human Health. *Pharmacogn. Rev.* **2010**, *4* (8), 118. https://doi.org/10.4103/0973-7847.70902.
(52) Bannister, J. V.; Bannister, W. H.; Rotilio, G. Aspects of the Structure, Function, and Applications of Superoxide Dismutase. *CRC Crit. Rev. Biochem.* **1987**, *22* (2), 111–180. https://doi.org/10.3109/10409238709083738.
(53) Brigelius-Flohé, R. Tissue-Specific Functions of Individual Glutathione Peroxidases. *Free Radic. Biol. Med.* **1999**, *27* (9–10), 951–965. https://doi.org/10.1016/s0891-5849(99)00173-2.
(54) Hayes, J. D.; Flanagan, J. U.; Jowsey, I. R. Glutathione Transferases. *Annu. Rev. Pharmacol. Toxicol.* **2005**, *45*, 51–88. https://doi.org/10.1146/annurev.pharmtox.45.120403.095857.
(55) Tur, J. A.; Sureda, A.; Pons, A. Evaluation of Oxidative Stress in Humans. In *Obesity*; Elsevier, 2018; pp 191–196. https://doi.org/10.1016/B978-0-12-812504-5.00009-X.
(56) Fang, Y.-Z.; Yang, S.; Wu, G. Free Radicals, Antioxidants, and Nutrition. *Nutrition* **2002**, *18* (10), 872–879. https://doi.org/10.1016/S0899-9007(02)00916-4.
(57) Tan, B. L.; Norhaizan, M. E.; Liew, W.-P.-P.; Sulaiman Rahman, H. Antioxidant and Oxidative Stress: A Mutual Interplay in Age-Related Diseases. *Front. Pharmacol.* **2018**, *9*. https://doi.org/10.3389/fphar.2018.01162.
(58) English, A.; Food and Agriculture Organization of the United Nations. *The State of Food and Agriculture. 2019, 2019,*; 2019.
(59) Sagar, N. A.; Pareek, S.; Sharma, S.; Yahia, E. M.; Lobo, M. G. Fruit and Vegetable Waste: Bioactive Compounds, Their Extraction, and Possible Utilization. *Compr. Rev. Food Sci. Food Saf.* **2018**, *17* (3), 512–531. https://doi.org/10.1111/1541-4337.12330.
(60) Corn Production by Country | World Agricultural Production 2019/2020 http://www.worldagriculturalproduction.com/crops/corn.aspx (accessed Apr 15, 2020).
(61) Aukkanit, N.; Kemngoen, T.; Ponharn, N. Utilization of Corn Silk in Low Fat Meatballs and Its Characteristics. *Procedia - Soc. Behav. Sci.* **2015**, *197*, 1403–1410. https://doi.org/10.1016/j.sbspro.2015.07.086.

(62) Tsai, W. T.; Chang, C. Y.; Wang, S. Y.; Chang, C. F.; Chien, S. F.; Sun, H. F. Utilization of Agricultural Waste Corn Cob for the Preparation of Carbon Adsorbent. *J. Environ. Sci. Health B* **2001**, *36* (5), 677–686. https://doi.org/10.1081/PFC-100106194.
(63) [PDF] The Potential of Natural Waste (Corn Husk) for Production of Environmental Friendly Biodegradable Film for Seedling | Semantic Scholar https://www.semanticscholar.org/paper/The-Potential-of-Natural-Waste-(Corn-Husk)-for-of-Norashikin-Ibrahim/6694178cc170d12a0265ac0c15892639b6e21577 (accessed Apr 15, 2020).
(64) Classification | USDA PLANTS https://plants.usda.gov/java/ClassificationServlet?source=display&classid=ZEMA (accessed Apr 19, 2020).
(65) Nawaz, H.; Muzaffar, S.; Aslam, M.; Ahmad, S. Phytochemical Composition: Antioxidant Potential and Biological Activities of Corn. In *Corn - Production and Human Health in Changing Climate*; Amanullah, Fahad, S., Eds.; InTech, 2018. https://doi.org/10.5772/intechopen.79648.
(66) Abdi, A.; Wally, A. Egypt Grain and Feed Annual 2019 Egypt Adds Rice to Its Grain Imports of Wheat and Corn. 13.
(67) World of Corn 2020 http://www.worldofcorn.com/#corn-displaced-by-ddg-cgf-domestic-livestock (accessed Apr 19, 2020).
(68) 10 Ways We Use Corn https://www.mentalfloss.com/article/26030/10-ways-we-use-corn (accessed Apr 19, 2020).
(69) Why CornCob - Green Products Company http://www.greenproducts.com/greentru/why-corncob.aspx (accessed Apr 19, 2020).
(70) Uses Of Corn Husks - Corn Husk Uses & Benefits http://lifestyle.iloveindia.com/lounge/uses-of-corn-husks-8030.html (accessed Apr 19, 2020).
(71) Awosusi, A. A.; Ayeni, A. O.; Adeleke, R.; Daramola, M. O. Biocompositional and Thermodecompositional Analysis of South African Agro-Waste Corncob and Husk towards Production of Biocommodities. *Asia-Pac. J. Chem. Eng.* **2017**, *12* (6), 960–968. https://doi.org/10.1002/apj.2138.
(72) Takada, M.; Niu, R.; Minami, E.; Saka, S. Characterization of Three Tissue Fractions in Corn (Zea Mays) Cob. *Biomass Bioenergy* **2018**, *115*, 130–135. https://doi.org/10.1016/j.biombioe.2018.04.023.
(73) Zheng, A.; Zhao, K.; Li, L.; Zhao, Z.; Jiang, L.; Huang, Z.; Wei, G.; He, F.; Li, H. Quantitative Comparison of Different Chemical Pretreatment Methods on Chemical Structure and Pyrolysis Characteristics of Corncobs. *J. Energy Inst.* **2018**, *91* (5), 676–682. https://doi.org/10.1016/j.joei.2017.06.002.
(74) Foo, K. Y. Value-Added Utilization of Maize Cobs Waste as an Environmental Friendly Solution for the Innovative Treatment of Carbofuran. *Process Saf. Environ. Prot.* **2016**, *100*, 295–304. https://doi.org/10.1016/j.psep.2016.01.020.
(75) Berber-Villamar, N. K.; Netzahuatl-Muñoz, A. R.; Morales-Barrera, L.; Chávez-Camarillo, G. M.; Flores-Ortiz, C. M.; Cristiani-Urbina, E. Corncob as an Effective, Eco-Friendly, and Economic Biosorbent for Removing the Azo Dye Direct Yellow 27 from Aqueous Solutions. *PLOS ONE* **2018**, *13* (4), e0196428. https://doi.org/10.1371/journal.pone.0196428.
(76) Tsai, W. T.; Chang, C. Y.; Lee, S. L. A Low Cost Adsorbent from Agricultural Waste Corn Cob by Zinc Chloride Activation. *Bioresour. Technol.* **1998**, *64* (3), 211–217. https://doi.org/10.1016/S0960-8524(97)00168-5.
(77) Liu, W.; Wu, R.; Wang, B.; Hu, Y.; Hou, Q.; Zhang, P.; Wu, R. Comparative Study on Different Pretreatment on Enzymatic Hydrolysis of Corncob Residues. *Bioresour. Technol.* **2020**, *295*, 122244. https://doi.org/10.1016/j.biortech.2019.122244.
(78) Miranda, M. T.; Sepúlveda, F. J.; Arranz, J. I.; Montero, I.; Rojas, C. V. Analysis of Pelletizing from Corn Cob Waste. *J. Environ. Manage.* **2018**, *228*, 303–311. https://doi.org/10.1016/j.jenvman.2018.08.105.
(79) Ayeni, A. O.; Daramola, M. O. Lignocellulosic Biomass Waste Beneficiation: Evaluation of Oxidative and Non-Oxidative Pretreatment Methodologies of South African Corn Cob. *J. Environ. Chem. Eng.* **2017**, *5* (2), 1771–1779. https://doi.org/10.1016/j.jece.2017.03.019.
(80) Corn cobs – Advanced BioFuels USA https://advancedbiofuelsusa.info/tag/corn-cobs/ (accessed Apr 19, 2020).
(81) Du, C.; Li, H.; Li, B.; Liu, M.; Zhan, H. Characteristics and Properties of Cellulose Nanofibers Prepared by TEMPO Oxidation of Corn Husk. *BioResources* **2016**, *11* (2), 5276–5284.
(82) Yang, X.; Han, F.; Xu, C.; Jiang, S.; Huang, L.; Liu, L.; Xia, Z. Effects of Preparation Methods on the Morphology and Properties of Nanocellulose (NC) Extracted from Corn Husk. *Ind. Crops Prod.* **2017**, *109*, 241–247. https://doi.org/10.1016/j.indcrop.2017.08.032.
(83) Valdebenito, F.; Pereira, M.; Ciudad, G.; Azocar, L.; Briones, R.; Chinga-Carrasco, G. On the Nanofibrillation of Corn Husks and Oat Hulls Fibres. *Ind. Crops Prod.* **2017**, *95*, 528–534. https://doi.org/10.1016/j.indcrop.2016.11.006.
(84) Zuorro, A.; Lavecchia, R.; González-Delgado, Á. D.; García-Martinez, J. B.; L'Abbate, P. Optimization of Enzyme-Assisted Extraction of Flavonoids from Corn Husks. *Processes* **2019**, *7* (11), 804. https://doi.org/10.3390/pr7110804.
(85) Sari, N. H.; Fajrin, J.; Suteja; Fudholi, A. Characterisation of Swellability and Compressive and Impact Strength Properties of Corn Husk Fibre Composites. *Compos. Commun.* **2020**, *18*, 49–54. https://doi.org/10.1016/j.coco.2020.01.009.
(86) Youssef, A. M.; El-Gendy, A.; Kamel, S. Evaluation of Corn Husk Fibers Reinforced Recycled Low Density Polyethylene Composites. *Mater. Chem. Phys.* **2015**, *152*, 26–33. https://doi.org/10.1016/j.matchemphys.2014.12.004.
(87) Kwon, H.-J.; Sunthornvarabhas, J.; Park, J.-W.; Lee, J.-H.; Kim, H.-J.; Piyachomkwan, K.; Sriroth, K.; Cho, D. Tensile Properties of Kenaf Fiber and Corn Husk Flour Reinforced Poly(Lactic Acid) Hybrid Bio-Composites: Role of Aspect Ratio of Natural Fibers. *Compos. Part B Eng.* **2014**, *56*, 232–237. https://doi.org/10.1016/j.compositesb.2013.08.003.
(88) Huda, S.; Yang, Y. Chemically Extracted Cornhusk Fibers as Reinforcement in Light-Weight Poly(Propylene) Composites. *Macromol. Mater. Eng.* **2008**, *293* (3), 235–243. https://doi.org/10.1002/mame.200700317.
(89) Yılmaz, N. D. Effects of Enzymatic Treatments on the Mechanical Properties of Corn Husk Fibers. *J. Text. Inst.* **2013**, *104* (4), 396–406. https://doi.org/10.1080/00405000.2012.736707.
(90) Bioactives From Agri-Food Wastes: Present Insights and Future Challenges. - PubMed - NCBI https://www.ncbi.nlm.nih.gov/pubmed/31991658 (accessed Apr 14, 2020).

(91) Huang, W.-Y.; Cai, Y.-Z.; Zhang, Y. Natural Phenolic Compounds from Medicinal Herbs and Dietary Plants: Potential Use for Cancer Prevention. *Nutr. Cancer* **2010**, *62* (1), 1–20. https://doi.org/10.1080/01635580903191585.
(92) pubmeddev; al, R. J., et. Dietary fiber constituents of selected fruits and vegetables. - PubMed - NCBI https://www.ncbi.nlm.nih.gov/pubmed/2993399 (accessed Apr 15, 2020).
(93) Torres-León, C.; Rojas, R.; Contreras-Esquivel, J. C.; Serna-Cock, L.; Belmares-Cerda, R. E.; Aguilar, C. N. Mango Seed: Functional and Nutritional Properties. *Trends Food Sci. Technol.* **2016**, *55*, 109–117. https://doi.org/10.1016/j.tifs.2016.06.009.
(94) Isolation and Characterization of Cellulose from Different Fruit and Vegetable Pomaces https://www.ncbi.nlm.nih.gov/pmc/articles/PMC6418744/ (accessed Apr 15, 2020).
(95) Socaci, S. A.; Rugină, D. O.; MariaDiaconeasa, Z.; Pop, O. L.; Fărcaş, A. C.; Păucean, A.; Tofană, M.; Pintea, A. Antioxidant Compounds Recovered from Food Wastes. *Funct. Food - Improve Health Adequate Food* **2017**. https://doi.org/10.5772/intechopen.69124.
(96) Fidelis, M.; de Moura, C.; Kabbas Junior, T.; Pap, N.; Mattila, P.; Mäkinen, S.; Putnik, P.; Bursać Kovačević, D.; Tian, Y.; Yang, B.; Granato, D. Fruit Seeds as Sources of Bioactive Compounds: Sustainable Production of High Value-Added Ingredients from By-Products within Circular Economy. *Molecules* **2019**, *24* (21), 3854. https://doi.org/10.3390/molecules24213854.
(97) Harini, K.; Ramya, K.; Sukumar, M. Extraction of Nano Cellulose Fibers from the Banana Peel and Bract for Production of Acetyl and Lauroyl Cellulose. *Carbohydr. Polym.* **2018**, *201*, 329–339. https://doi.org/10.1016/j.carbpol.2018.08.081.
(98) Singh, H. K.; Patil, T.; Vineeth, S. K.; Das, S.; Pramanik, A.; Mhaske, S. T. Isolation of Microcrystalline Cellulose from Corn Stover with Emphasis on Its Constituents: Corn Cover and Corn Cob. *Mater. Today Proc.* **2019**. https://doi.org/10.1016/j.matpr.2019.12.065.
(99) Yang, T.; Hu, J. G.; Yu, Y.; Li, G.; Guo, X.; Li, T.; Liu, R. H. Comparison of Phenolics, Flavonoids, and Cellular Antioxidant Activities in Ear Sections of Sweet Corn (Zea Mays L. Saccharata Sturt). *J. Food Process. Preserv.* **2019**, *43* (1), e13855. https://doi.org/10.1111/jfpp.13855.
(100) de Andrade, M. R.; Nery, T. B. R.; de Santana e Santana, T. I.; Leal, I. L.; Rodrigues, L. A. P.; de Oliveira Reis, J. H.; Druzian, J. I.; Machado, B. A. S. Effect of Cellulose Nanocrystals from Different Lignocellulosic Residues to Chitosan/Glycerol Films. *Polymers* **2019**, *11* (4). https://doi.org/10.3390/polym11040658.
(101) Tsimogiannis, D.; Oreopoulou, V. Chapter 16 - Classification of Phenolic Compounds in Plants. In *Polyphenols in Plants (Second Edition)*; Watson, R. R., Ed.; Academic Press, 2019; pp 263–284. https://doi.org/10.1016/B978-0-12-813768-0.00026-8.
(102) Families of Phenolic Compounds and Means of Classification | SpringerLink https://link.springer.com/chapter/10.1007/978-1-4020-5164-7_1 (accessed Apr 15, 2020).
(103) Tsao, R. Chemistry and Biochemistry of Dietary Polyphenols. *Nutrients* **2010**, *2* (12), 1231–1246. https://doi.org/10.3390/nu2121231.
(104) Utilization of fruit and vegetable wastes as livestock feed and as substrates for generation of other value-added products http://www.fao.org/3/i3273e/i3273e00.htm (accessed Apr 14, 2020).
(105) US EPA, O. Sustainable Management of Food Basics https://www.epa.gov/sustainable-management-food/sustainable-management-food-basics (accessed Apr 14, 2020).
(106) US EPA, O. United States 2030 Food Loss and Waste Reduction Goal https://www.epa.gov/sustainable-management-food/united-states-2030-food-loss-and-waste-reduction-goal (accessed Apr 14, 2020).
(107) Teplova, V. V.; Isakova, E. P.; Klein, O. I.; Dergachova, D. I.; Gessler, N. N.; Deryabina, Y. I. Natural Polyphenols: Biological Activity, Pharmacological Potential, Means of Metabolic Engineering (Review). *Appl. Biochem. Microbiol.* **2018**, *54* (3), 221–237. https://doi.org/10.1134/S0003683818030146.
(108) Rasines-Perea, Z.; Teissedre, P.-L. Grape Polyphenols' Effects in Human Cardiovascular Diseases and Diabetes. *Molecules* **2017**, *22* (1), 68. https://doi.org/10.3390/molecules22010068.
(109) Gormaz, J. G.; Valls, N.; Sotomayor, C.; Turner, T.; Rodrigo, R. Potential Role of Polyphenols in the Prevention of Cardiovascular Diseases: Molecular Bases https://www.ingentaconnect.com/content/ben/cmc/2016/00000023/00000002/art00003 (accessed Apr 16, 2020).
(110) Roleira, F. M. F.; Tavares-da-Silva, E. J.; Varela, C. L.; Costa, S. C.; Silva, T.; Garrido, J.; Borges, F. Plant Derived and Dietary Phenolic Antioxidants: Anticancer Properties. *Food Chem.* **2015**, *183*, 235–258. https://doi.org/10.1016/j.foodchem.2015.03.039.
(111) Baby, B.; Antony, P.; Vijayan, R. Antioxidant and Anticancer Properties of Berries. *Crit. Rev. Food Sci. Nutr.* **2018**, *58* (15), 2491–2507. https://doi.org/10.1080/10408398.2017.1329198.
(112) Zhang, H.; Tsao, R. Dietary Polyphenols, Oxidative Stress and Antioxidant and Anti-Inflammatory Effects. *Curr. Opin. Food Sci.* **2016**, *8*, 33–42. https://doi.org/10.1016/j.cofs.2016.02.002.
(113) Rossi, L.; Mazzitelli, S.; Arciello, M.; Capo, C. R.; Rotilio, G. Benefits from Dietary Polyphenols for Brain Aging and Alzheimer's Disease. *Neurochem. Res.* **2008**, *33* (12), 2390–2400. https://doi.org/10.1007/s11064-008-9696-7.
(114) Li, A.-N.; Li, S.; Zhang, Y.-J.; Xu, X.-R.; Chen, Y.-M.; Li, H.-B. Resources and Biological Activities of Natural Polyphenols. *Nutrients* **2014**, *6* (12), 6020–6047. https://doi.org/10.3390/nu6126020.
(115) Miguel-Chávez, R. S. Phenolic Antioxidant Capacity: A Review of the State of the Art. *Phenolic Compd. - Biol. Act.* **2017**. https://doi.org/10.5772/66897.
(116) Fraga, C. G. Plant Polyphenols: How to Translate Their in Vitro Antioxidant Actions to in Vivo Conditions. *IUBMB Life* **2007**, *59* (4–5), 308–315. https://doi.org/10.1080/15216540701230529.
(117) Papuc, C.; Goran, G. V.; Predescu, C. N.; Nicorescu, V.; Stefan, G. Plant Polyphenols as Antioxidant and Antibacterial Agents for Shelf-Life Extension of Meat and Meat Products: Classification, Structures, Sources, and Action Mechanisms. *Compr. Rev. Food Sci. Food Saf.* **2017**, *16* (6), 1243–1268. https://doi.org/10.1111/1541-4337.12298.

(118) Di Meo, F.; Lemaur, V.; Cornil, J.; Lazzaroni, R.; Duroux, J.-L.; Olivier, Y.; Trouillas, P. Free Radical Scavenging by Natural Polyphenols: Atom versus Electron Transfer. *J. Phys. Chem. A* **2013**, *117* (10), 2082–2092. https://doi.org/10.1021/jp3116319.

(119) Guo, Q.; Zhao, B.; Li, M.; Shen, S.; Xin, W. Studies on Protective Mechanisms of Four Components of Green Tea Polyphenols against Lipid Peroxidation in Synaptosomes. *Biochim. Biophys. Acta* **1996**, *1304* (3), 210–222. https://doi.org/10.1016/s0005-2760(96)00122-1.

(120) Leopoldini, M.; Russo, N.; Toscano, M. The Molecular Basis of Working Mechanism of Natural Polyphenolic Antioxidants. *Food Chem.* **2011**, *125* (2), 288–306. https://doi.org/10.1016/j.foodchem.2010.08.012.

(121) Karakaya, S. Bioavailability of Phenolic Compounds. *Crit. Rev. Food Sci. Nutr.* **2004**, *44* (6), 453–464. https://doi.org/10.1080/10408690490886683.

(122) Gao, S.; Hu, M. Bioavailability Challenges Associated with Development of Anti-Cancer Phenolics. *Mini Rev. Med. Chem.* **2010**, *10* (6), 550–567.

(123) Al-Dabbagh, B.; Elhaty, I. A.; Elhaw, M.; Murali, C.; Al Mansoori, A.; Awad, B.; Amin, A. Antioxidant and Anticancer Activities of Chamomile (Matricaria Recutita L.). *BMC Res. Notes* **2019**, *12* (1), 3. https://doi.org/10.1186/s13104-018-3960-y.

(124) Asekunowo, A. K.; Ashafa, A. O. T.; Okoh, O.; Asekun, O. T.; Familoni, O. B. Polyphenolic Constituents, Antioxidant and Hypoglycaemic Potential of Leaf Extracts of Acalypha Godseffiana from Eastern Nigeria : In Vitro Study: Original Research. *J. Med. Plants Econ. Dev.* **2019**, *3* (1), 1–9. https://doi.org/10.4102/jomped.v3i1.36.

(125) Szymanowska, U.; Baraniak, B.; Bogucka-Kocka, A. Antioxidant, Anti-Inflammatory, and Postulated Cytotoxic Activity of Phenolic and Anthocyanin-Rich Fractions from Polana Raspberry (Rubus Idaeus L.) Fruit and Juice—In Vitro Study. *Molecules* **2018**, *23* (7), 1812. https://doi.org/10.3390/molecules23071812.

(126) Singh, J. P.; Kaur, A.; Singh, N.; Nim, L.; Shevkani, K.; Kaur, H.; Arora, D. S. In Vitro Antioxidant and Antimicrobial Properties of Jambolan (Syzygium Cumini) Fruit Polyphenols. *LWT - Food Sci. Technol.* **2016**, *65*, 1025–1030. https://doi.org/10.1016/j.lwt.2015.09.038.

(127) Tejada, S.; Pinya, S.; del Mar Bibiloni, M.; A. Tur, J.; Pons, A.; Sureda, A. Cardioprotective Effects of the Polyphenol Hydroxytyrosol from Olive Oil https://www.ingentaconnect.com/content/ben/cdt/2017/00000018/00000013/art00004 (accessed Apr 16, 2020). https://doi.org/info:doi/10.2174/1389450117666161005150650.

(128) García-Villalón, A. L.; Amor, S.; Monge, L.; Fernández, N.; Prodanov, M.; Muñoz, M.; Inarejos-García, A. M.; Granado, M. In Vitro Studies of an Aged Black Garlic Extract Enriched in S-Allylcysteine and Polyphenols with Cardioprotective Effects. *J. Funct. Foods* **2016**, *27*, 189–200. https://doi.org/10.1016/j.jff.2016.08.062.

(129) Raybaudi-Massilia, R.; Suárez, A. I.; Arvelo, F.; Zambrano, A.; Sojo, F.; Calderón-Gabaldón, M. I.; Mosqueda-Melgar, J. Cytotoxic, Antioxidant and Antimicrobial Properties of Red Sweet Pepper (Capsicum Annuum L. Var. Llanerón) Extracts: In Vitro Study. *Int. J. Food Stud.* **2017**, *6* (2). https://doi.org/10.7455/ijfs/6.2.2017.a8.

(130) Liu, K.; Xiao, X.; Wang, J.; Chen, C.-Y. O.; Hu, H. Polyphenolic Composition and Antioxidant, Antiproliferative, and Antimicrobial Activities of Mushroom Inonotus Sanghuang. *LWT - Food Sci. Technol.* **2017**, *82*, 154–161. https://doi.org/10.1016/j.lwt.2017.04.041.

(131) Denev, P.; Číž, M.; Kratchanova, M.; Blazheva, D. Black Chokeberry (Aronia Melanocarpa) Polyphenols Reveal Different Antioxidant, Antimicrobial and Neutrophil-Modulating Activities. *Food Chem.* **2019**, *284*, 108–117. https://doi.org/10.1016/j.foodchem.2019.01.108.

(132) Sobeh, M.; Mahmoud, M. F.; Petruk, G.; Rezq, S.; Ashour, M. L.; Youssef, F. S.; El-Shazly, A. M.; Monti, D. M.; Abdel-Naim, A. B.; Wink, M. Syzygium Aqueum: A Polyphenol- Rich Leaf Extract Exhibits Antioxidant, Hepatoprotective, Pain-Killing and Anti-Inflammatory Activities in Animal Models. *Front. Pharmacol.* **2018**, *9*. https://doi.org/10.3389/fphar.2018.00566.

(133) Nowicka, P.; Wojdyło, A. Content of Bioactive Compounds in the Peach Kernels and Their Antioxidant, Anti-Hyperglycemic, Anti-Aging Properties. *Eur. Food Res. Technol.* **2019**, *245* (5), 1123–1136. https://doi.org/10.1007/s00217-018-3214-1.

(134) Pientaweeratch, S.; Panapisal, V.; Tansirikongkol, A. Antioxidant, Anti-Collagenase and Anti-Elastase Activities of Phyllanthus Emblica, Manilkara Zapota and Silymarin: An in Vitro Comparative Study for Anti-Aging Applications. *Pharm. Biol.* **2016**, *54* (9), 1865–1872. https://doi.org/10.3109/13880209.2015.1133658.

(135) George, G. O.; Idu, F. K. Corn Silk Aqueous Extracts and Intraocular Pressure of Systemic and Non-Systemic Hypertensive Subjects: Corn Silk Aqueous Extracts and IOP in Systemic Hypertension. *Clin. Exp. Optom.* **2015**, *98* (2), 138–149. https://doi.org/10.1111/cxo.12240.

(136) Wang, B.; Xiao, T.; Ruan, J.; Liu, W. Beneficial Effects of Corn Silk on Metabolic Syndrome. *Curr. Pharm. Des.* **2018**, *23* (34). https://doi.org/10.2174/1381612823666170926152425.

(137) González-Muñoz, A.; Quesille-Villalobos, A. M.; Fuentealba, C.; Shetty, K.; Gálvez Ranilla, L. Potential of Chilean Native Corn (Zea Mays L.) Accessions as Natural Sources of Phenolic Antioxidants and in Vitro Bioactivity for Hyperglycemia and Hypertension Management. *J. Agric. Food Chem.* **2013**, *61* (46), 10995–11007. https://doi.org/10.1021/jf403237p.

(138) Wang, K.-J.; Zhao, J.-L. Corn Silk (Zea Mays L.), a Source of Natural Antioxidants with α-Amylase, α-Glucosidase, Advanced Glycation and Diabetic Nephropathy Inhibitory Activities. *Biomed. Pharmacother.* **2019**, *110*, 510–517. https://doi.org/10.1016/j.biopha.2018.11.126.

(139) Sabiu, S.; O'Neill, F. H.; Ashafa, A. O. T. Kinetics of α-Amylase and α-Glucosidase Inhibitory Potential of Zea Mays Linnaeus (Poaceae), Stigma Maydis Aqueous Extract: An in Vitro Assessment. *J. Ethnopharmacol.* **2016**, *183*, 1–8. https://doi.org/10.1016/j.jep.2016.02.024.

(140) Sani*, U. M. Anti Diabetic Potential of Methanol Extract of Cooked Corn Silk Stigma Maydis on Alloxan Induced Diabetes in Albino Mice. *J. Pharm. Pharmacol. Sci.* **2016**.

(141) Guo, Q.; Ma, Q.; Xue, Z.; Gao, X.; Chen, H. Studies on the Binding Characteristics of Three Polysaccharides with Different Molecular Weight and Flavonoids from Corn Silk (Maydis Stigma). *Carbohydr. Polym.* **2018**, *198*, 581–588. https://doi.org/10.1016/j.carbpol.2018.06.120.
(142) Tian, J.; Chen, H.; Chen, S.; Xing, L.; Wang, Y.; Wang, J. Comparative Studies on the Constituents, Antioxidant and Anticancer Activities of Extracts from Different Varieties of Corn Silk. *Food Funct.* **2013**, *4* (10), 1526–1534. https://doi.org/10.1039/C3FO60171D.
(143) Kim, J. T.; Son, B. Y.; Lee, J. S.; Baek, S. B.; Woo, K. S.; Jung, G. H.; Kim, M. J.; Jeong, K. H.; Kwon, Y.-U. Effect of Particle Size on Antioxidant Activity and Cytotoxicity in Purple Corn Seed Powder. *KOREAN J. CROP Sci.* **2012**, *57* (4), 353–358. https://doi.org/10.7740/kjcs.2012.57.4.353.
(144) Hasanudin, K.; Hashim, P.; Mustafa, S. Corn Silk (Stigma Maydis) in Healthcare: A Phytochemical and Pharmacological Review. *Molecules* **2012**, *17* (8), 9697–9715. https://doi.org/10.3390/molecules17089697.
(145) Sahib, A. S.; Mohammed, I. H.; Hamdan, S. J. Use of Aqueous Extract of Corn Silk in the Treatment of Urinary Tract Infection. *J. Complement. Med. Res.* **2012**, *1* (2), 93–96.
(146) Amanullah, K.; Fahad, S. *Corn: Production and Human Health in Changing Climate*; BoD – Books on Demand, 2018.
(147) Ren, S. C.; Qiao, Q. Q.; Ding, X. L. Antioxidative Activity of Five Flavones Glycosides from Corn Silk (Stigma Maydis). *Czech J. Food Sci.* **2013**, *31* (No. 2), 148–155. https://doi.org/10.17221/194/2012-CJFS.
(148) Falcone Ferreyra, M. L.; Rodriguez, E.; Casas, M. I.; Labadie, G.; Grotewold, E.; Casati, P. Identification of a Bifunctional Maize C- and O-Glucosyltransferase. *J. Biol. Chem.* **2013**, *288* (44), 31678–31688. https://doi.org/10.1074/jbc.M113.510040.
(149) Limmatvapirat, C.; Nateesathittarn, C.; Dechasathian, K.; Moohummad, T.; Chinajitphan, P.; Limmatvapirat, S. Phytochemical Analysis of Baby Corn Silk Extracts. *J. Ayurveda Integr. Med.* **2020**. https://doi.org/10.1016/j.jaim.2019.10.005.
(150) R., N. A.; I., W. R. W. Evaluation of Polyphenol Content and Antioxidant Activities of Some Selected Organic and Aqueous Extracts of Cornsilk (Zea Mays Hairs). *J. Med. Bioeng.* **2012**, *1* (1), 48–51. https://doi.org/10.12720/jomb.1.1.48-51.
(151) Nurraihana, H.; Wan Rosli, W. I.; Sabreena, S.; Norfarizan-Hanoon, N. A. Optimisation Extraction Procedure and Identification of Phenolic Compounds from Fractional Extract of Corn Silk (Zea Mays Hair) Using LC-TOF/MS System. *J. Food Meas. Charact.* **2018**, *12* (3), 1852–1862. https://doi.org/10.1007/s11694-018-9799-z.
(152) Oyabambi, A. O.; Areola, E. D.; Olatunji, L. A.; Soladoye, A. O. Uric Acid Is a Key Player in Salt-Induced Endothelial Dysfunction: The Therapeutic Role of *Stigma Maydis* (Corn Silk) Extract. *Appl. Physiol. Nutr. Metab.* **2020**, *45* (1), 67–71. https://doi.org/10.1139/apnm-2018-0849.
(153) Qi, X.-L.; Zhang, Y.-Y.; Zhao, P.; Zhou, L.; Wang, X.-B.; Huang, X.-X.; Lin, B.; Song, S.-J. *Ent* -Kaurane Diterpenoids with Neuroprotective Properties from Corn Silk (*Zea Mays*). *J. Nat. Prod.* **2018**, *81* (5), 1225–1234. https://doi.org/10.1021/acs.jnatprod.7b01017.
(154) Zhou, W.-Y.; Lin, B.; Hou, Z.-L.; Shi, S.-C.; Wang, Y.-X.; Huang, X.-X.; Song, S.-J. Isolation of Macrocarpene-Type Sesquiterpenes from Stigma Maydis with Neuroprotective Activities. *Fitoterapia* **2020**, *141*, 104448. https://doi.org/10.1016/j.fitote.2019.104448.
(155) Zhang, Y.; Wu, L.; Ma, Z.; Cheng, J.; Liu, J. Anti-Diabetic, Anti-Oxidant and Anti-Hyperlipidemic Activities of Flavonoids from Corn Silk on STZ-Induced Diabetic Mice. *Molecules* **2015**, *21* (1), 7. https://doi.org/10.3390/molecules21010007.
(156) Chaiittianan, R.; Chayopas, P.; Rattanathongkom, A.; Tippayawat, P.; Sutthanut, K. Anti-Obesity Potential of Corn Silks: Relationships of Phytochemicals and Antioxidation, Anti-Pre-Adipocyte Proliferation, Anti-Adipogenesis, and Lipolysis Induction. *J. Funct. Foods* **2016**, *23*, 497–510. https://doi.org/10.1016/j.jff.2016.03.010.
(157) El-Ghorab, A.; El-Massry, K. F.; Shibamoto, T. Chemical Composition of the Volatile Extract and Antioxidant Activities of the Volatile and Nonvolatile Extracts of Egyptian Corn Silk (*Zea Mays* L.). *J. Agric. Food Chem.* **2007**, *55* (22), 9124–9127. https://doi.org/10.1021/jf071646e.
(158) Ebrahimzadeh, M. A.; Pourmorad, F.; Hafezi, S. Antioxidant Activities of Iranian Corn Silk. 7.
(159) Liu, J.; Wang, C.; Wang, Z.; Zhang, C.; Lu, S.; Liu, J. The Antioxidant and Free-Radical Scavenging Activities of Extract and Fractions from Corn Silk (Zea Mays L.) and Related Flavone Glycosides. *Food Chem.* **2011**, *126* (1), 261–269. https://doi.org/10.1016/j.foodchem.2010.11.014.
(160) Haslina, H.; Eva, M. Extract Corn Silk with Variation of Solvents on Yield, Total Phenolics, Total Flavonoids and Antioxidant Activity. *Indones. Food Nutr. Prog.* **2017**, *14* (1), 21. https://doi.org/10.22146/ifnp.24280.
(161) Nessa, F.; Ismail, Z.; Mohamed, N. Antimicrobial Activities of Extracts and Flavonoid Glycosides of Corn Silk (Zea Mays L). 7.
(162) Carvalho, A.; Cruz, C.; Freitas, C.; Aguiar, J.; Nunes, P.; Lima, V.; Matias, E.; Muniz, D.; Coutinho, H. Chemical Profile, Antibacterial Activity and Antibiotic-Modulating Effect of the Hexanic Zea Mays L. Silk Extract (Poaceae). *Antibiotics* **2019**, *8* (1), 22. https://doi.org/10.3390/antibiotics8010022.
(163) What is Nanotechnology? | Nano https://www.nano.gov/nanotech-101/what/definition (accessed Apr 17, 2020).
(164) The Ethics and politics of nanotechnology - UNESCO Digital Library https://unesdoc.unesco.org/ark:/48223/pf0000145951 (accessed Apr 17, 2020).
(165) 1. What is nanotechnology? https://ec.europa.eu/health/scientific_committees/opinions_layman/en/nanotechnologies/l-3/1-introduction.htm (accessed Apr 17, 2020).
(166) Schwirn, K.; Tietjen, L.; Beer, I. Why Are Nanomaterials Different and How Can They Be Appropriately Regulated under REACH? *Environ. Sci. Eur.* **2014**, *26* (1), 4. https://doi.org/10.1186/2190-4715-26-4.
(167) Bhatia, S. Nanoparticles Types, Classification, Characterization, Fabrication Methods and Drug Delivery Applications. In *Natural Polymer Drug Delivery Systems: Nanoparticles, Plants, and Algae*; Bhatia, S., Ed.; Springer International Publishing: Cham, 2016; pp 33–93. https://doi.org/10.1007/978-3-319-41129-3_2.

(168) Baranwal, A.; Srivastava, A.; Kumar, P.; Bajpai, V. K.; Maurya, P. K.; Chandra, P. Prospects of Nanostructure Materials and Their Composites as Antimicrobial Agents. *Front. Microbiol.* **2018**, *9*. https://doi.org/10.3389/fmicb.2018.00422.
(169) Li, W.; Elzatahry, A.; Aldhayan, D.; Zhao, D. Core–Shell Structured Titanium Dioxide Nanomaterials for Solar Energy Utilization. *Chem. Soc. Rev.* **2018**, *47* (22), 8203–8237. https://doi.org/10.1039/C8CS00443A.
(170) Li, X.; Zhu, J.; Wei, B. Hybrid Nanostructures of Metal/Two-Dimensional Nanomaterials for Plasmon-Enhanced Applications. *Chem. Soc. Rev.* **2016**, *45* (11), 3145–3187. https://doi.org/10.1039/C6CS00195E.
(171) Teradal, N. L.; Jelinek, R. Carbon Nanomaterials in Biological Studies and Biomedicine. *Adv. Healthc. Mater.* **2017**, *6* (17), 1700574. https://doi.org/10.1002/adhm.201700574.
(172) Yang, X.; Yang, M.; Pang, B.; Vara, M.; Xia, Y. Gold Nanomaterials at Work in Biomedicine. *Chem. Rev.* **2015**, *115* (19), 10410–10488. https://doi.org/10.1021/acs.chemrev.5b00193.
(173) He, X.; Hwang, H.-M. Nanotechnology in Food Science: Functionality, Applicability, and Safety Assessment. *J. Food Drug Anal.* **2016**, *24* (4), 671–681. https://doi.org/10.1016/j.jfda.2016.06.001.
(174) Bumbudsanpharoke, N.; Choi, J.; Ko, S. Applications of Nanomaterials in Food Packaging https://www.ingentaconnect.com/content/asp/jnn/2015/00000015/00000009/art00007 (accessed Apr 18, 2020). https://doi.org/info:doi/10.1166/jnn.2015.10847.
(175) Singh, P. K.; Jairath, G.; Ahlawat, S. S. Nanotechnology: A Future Tool to Improve Quality and Safety in Meat Industry. *J. Food Sci. Technol.* **2016**, *53* (4), 1739–1749. https://doi.org/10.1007/s13197-015-2090-y.
(176) Monaco, A. M.; Giugliano, M. Carbon-Based Smart Nanomaterials in Biomedicine and Neuroengineering. *Beilstein J. Nanotechnol.* **2014**, *5* (1), 1849–1863. https://doi.org/10.3762/bjnano.5.196.
(177) Dwivedi, S.; Saquib, Q.; Al-Khedhairy, A. A.; Musarrat, J. Understanding the Role of Nanomaterials in Agriculture. In *Microbial Inoculants in Sustainable Agricultural Productivity: Vol. 2: Functional Applications*; Singh, D. P., Singh, H. B., Prabha, R., Eds.; Springer India: New Delhi, 2016; pp 271–288. https://doi.org/10.1007/978-81-322-2644-4_17.
(178) Yang, Y.; Wang, S.; Wang, Y.; Wang, X.; Wang, Q.; Chen, M. Advances in Self-Assembled Chitosan Nanomaterials for Drug Delivery. *Biotechnol. Adv.* **2014**, *32* (7), 1301–1316. https://doi.org/10.1016/j.biotechadv.2014.07.007.
(179) Srinivasan, M.; Rajabi, M.; Mousa, S. A. Multifunctional Nanomaterials and Their Applications in Drug Delivery and Cancer Therapy. *Nanomaterials* **2015**, *5* (4), 1690–1703. https://doi.org/10.3390/nano5041690.
(180) Nanotechnology in Medical Applications | BCC Research https://www.bccresearch.com/market-research/healthcare/nanotechnology-medical-applications-market.html (accessed Apr 21, 2020).
(181) Pepic, I.; Hafner, A.; Lovric, J.; Perina Lakos, G. Nanotherapeutics in the EU: An Overview on Current State and Future Directions. *Int. J. Nanomedicine* **2014**, 1005. https://doi.org/10.2147/IJN.S55359.
(182) pMD Blog - The Key to Physician Happiness? Patients! https://www.pmd.com/blog/post/the-key-to-physician-happiness-patients (accessed Apr 21, 2020).
(183) Han, J.; Zhao, D.; Li, D.; Wang, X.; Jin, Z.; Zhao, K. Polymer-Based Nanomaterials and Applications for Vaccines and Drugs. *Polymers* **2018**, *10* (1). https://doi.org/10.3390/polym10010031.
(184) Tang, Z.; He, C.; Tian, H.; Ding, J.; Hsiao, B. S.; Chu, B.; Chen, X. Polymeric Nanostructured Materials for Biomedical Applications. *Prog. Polym. Sci.* **2016**, *60*, 86–128. https://doi.org/10.1016/j.progpolymsci.2016.05.005.
(185) Bharadwaz, A.; Jayasuriya, A. C. Recent Trends in the Application of Widely Used Natural and Synthetic Polymer Nanocomposites in Bone Tissue Regeneration. *Mater. Sci. Eng. C* **2020**, *110*, 110698. https://doi.org/10.1016/j.msec.2020.110698.
(186) Patra, J. K.; Das, G.; Fraceto, L. F.; Campos, E. V. R.; Rodriguez-Torres, M. del P.; Acosta-Torres, L. S.; Diaz-Torres, L. A.; Grillo, R.; Swamy, M. K.; Sharma, S.; Habtemariam, S.; Shin, H.-S. Nano Based Drug Delivery Systems: Recent Developments and Future Prospects. *J. Nanobiotechnology* **2018**, *16* (1), 71. https://doi.org/10.1186/s12951-018-0392-8.
(187) Kesarwani, K.; Gupta, R.; Mukerjee, A. Bioavailability Enhancers of Herbal Origin: An Overview. *Asian Pac. J. Trop. Biomed.* **2013**, *3* (4), 253–266. https://doi.org/10.1016/S2221-1691(13)60060-X.
(188) Silva, P.; Bonifácio, B.; Ramos, M.; Negri, K.; Maria Bauab, T.; Chorilli, M. Nanotechnology-Based Drug Delivery Systems and Herbal Medicines: A Review. *Int. J. Nanomedicine* **2013**, 1. https://doi.org/10.2147/IJN.S52634.
(189) Mosaddik, A.; Ravinayagam, V.; Elaanthikkal, S.; Fessi, H.; Badri, W.; Elaissari, A. Development and Use of Polymeric Nanoparticles for the Encapsulation and Administration of Plant Extracts. In *Natural Products as Source of Molecules with Therapeutic Potential*; Cechinel Filho, V., Ed.; Springer International Publishing: Cham, 2018; pp 391–463. https://doi.org/10.1007/978-3-030-00545-0_11.
(190) Ohnishi, T. Enhancement of Hyperthermia on Anti-Tumor Drug Sensitivity. In *Hyperthermic Oncology from Bench to Bedside*; Kokura, S., Yoshikawa, T., Ohnishi, T., Eds.; Springer: Singapore, 2016; pp 109–114. https://doi.org/10.1007/978-981-10-0719-4_10.
(191) Yuan, G.; Jia, Y.; Pan, Y.; Li, W.; Wang, C.; Xu, L.; Wang, C.; Chen, H. Preparation and Characterization of Shrimp Shell Waste Protein-Based Films Modified with Oolong Tea, Corn Silk and Black Soybean Seed Coat Extracts. *Polym. Test.* **2020**, *81*, 106235. https://doi.org/10.1016/j.polymertesting.2019.106235.
(192) Pulicharla, R.; Marques, C.; Das, R. K.; Rouissi, T.; Brar, S. K. Encapsulation and Release Studies of Strawberry Polyphenols in Biodegradable Chitosan Nanoformulation. *Int. J. Biol. Macromol.* **2016**, *88*, 171–178. https://doi.org/10.1016/j.ijbiomac.2016.03.036.
(193) Mahmoudi, R.; Tajali Ardakani, M.; Hajipour Verdom, B.; Bagheri, A.; Mohammad-Beigi, H.; Aliakbari, F.; Salehpour, Z.; Alipour, M.; Afrouz, S.; Bardania, H. Chitosan Nanoparticles Containing Physalis Alkekengi-L Extract: Preparation, Optimization and Their Antioxidant Activity. *Bull. Mater. Sci.* **2019**, *42* (3), 131. https://doi.org/10.1007/s12034-019-1815-3.
(194) Stoica, R.; Ion, R. M. PREPARATION OF CHITOSAN – TRIPOLYPHOSPHATE NANOPARTICLES FOR THE ENCAPSULATION OF POLYPHENOLS EXTRACTED FROM ROSE HIPS. 9.

(195) Talón, E.; Trifkovic, K. T.; Nedovic, V. A.; Bugarski, B. M.; Vargas, M.; Chiralt, A.; González-Martínez, C. Antioxidant Edible Films Based on Chitosan and Starch Containing Polyphenols from Thyme Extracts. *Carbohydr. Polym.* **2017**, *157*, 1153–1161. https://doi.org/10.1016/j.carbpol.2016.10.080.

(196) Cabral, B. R. P.; de Oliveira, P. M.; Gelfuso, G. M.; Quintão, T. de S. C.; Chaker, J. A.; Karnikowski, M. G. de O.; Gris, E. F. Improving Stability of Antioxidant Compounds from Plinia Cauliflora (Jabuticaba) Fruit Peel Extract by Encapsulation in Chitosan Microparticles. *J. Food Eng.* **2018**, *238*, 195–201. https://doi.org/10.1016/j.jfoodeng.2018.06.004.

(197) Muxika, A.; Etxabide, A.; Uranga, J.; Guerrero, P.; de la Caba, K. Chitosan as a Bioactive Polymer: Processing, Properties and Applications. *Int. J. Biol. Macromol.* **2017**, *105*, 1358–1368. https://doi.org/10.1016/j.ijbiomac.2017.07.087.

(198) Younes, I.; Rinaudo, M. Chitin and Chitosan Preparation from Marine Sources. Structure, Properties and Applications. *Mar. Drugs* **2015**, *13* (3), 1133–1174. https://doi.org/10.3390/md13031133.

(199) Yaghoubi, A.; Ghojazadeh, M.; Abolhasani, S.; Alikhah, H.; Khaki-Khatibi, F. Correlation of Serum Levels of Vitronectin, Malondialdehyde and Hs-CRP With Disease Severity in Coronary Artery Disease. *J. Cardiovasc. Thorac. Res.* **2015**, *7* (3), 113–117. https://doi.org/10.15171/jcvtr.2015.24.

(200) Rosch, J. G.; Winter, H.; DuRoss, A. N.; Sahay, G.; Sun, C. Inverse-Micelle Synthesis of Doxorubicin-Loaded Alginate/Chitosan Nanoparticles and in Vitro Assessment of Breast Cancer Cytotoxicity. *Colloid Interface Sci. Commun.* **2019**, *28*, 69–74. https://doi.org/10.1016/j.colcom.2018.12.002.

(201) Emmanuel, S.; Olajide, O.; Abubakar, S.; Akiode, S.; Etuk-Udo, G. Chemical Evaluation, Free Radical Scavenging Activities and Antimicrobial Evaluation of the Methanolic Extracts of Corn Silk (Zea Mays). *J. Adv. Med. Pharm. Sci.* **2016**, *9* (4), 1–8. https://doi.org/10.9734/JAMPS/2016/28530.

(202) Nn, A. A Review on the Extraction Methods Use in Medicinal Plants, Principle, Strength and Limitation https://www.semanticscholar.org/paper/A-Review-on-the-Extraction-Methods-Use-in-Medicinal-Nn/1f57ac7b5510db3fbf1e5066579e35f2dfdb0b11 (accessed Apr 27, 2020).

(203) Zhang, Q.-W.; Lin, L.-G.; Ye, W.-C. Techniques for Extraction and Isolation of Natural Products: A Comprehensive Review. *Chin. Med.* **2018**, *13*. https://doi.org/10.1186/s13020-018-0177-x.

(204) Altemimi, A.; Lakhssassi, N.; Baharlouei, A.; Watson, D. G.; Lightfoot, D. A. Phytochemicals: Extraction, Isolation, and Identification of Bioactive Compounds from Plant Extracts. *Plants* **2017**, *6* (4), 42. https://doi.org/10.3390/plants6040042.

(205) Vijayalaxmi, S.; Jayalakshmi, S. K.; Sreeramulu, K. Polyphenols from Different Agricultural Residues: Extraction, Identification and Their Antioxidant Properties. *J. Food Sci. Technol.* **2015**, *52* (5), 2761–2769. https://doi.org/10.1007/s13197-014-1295-9.

(206) Nawaz, H.; Aslam, M.; Muntaha, S. T. Effect of Solvent Polarity and Extraction Method on Phytochemical Composition and Antioxidant Potential of Corn Silk. *Free Radic. Antioxid.* **2019**, *9* (1), 05–11. https://doi.org/10.5530/fra.2019.1.2.

(207) Bhaigyabati, T. EFFECT OF METHANOLIC EXTRACT OF SWEET CORN SILK ON EXPERIMENTALLY INDUCED HYPERTHYROIDISM IN SWISS ALBINO RATS. **2012**, 5.

(208) Shetta, A.; Kegere, J.; Mamdouh, W. Comparative Study of Encapsulated Peppermint and Green Tea Essential Oils in Chitosan Nanoparticles: Encapsulation, Thermal Stability, in-Vitro Release, Antioxidant and Antibacterial Activities. *Int. J. Biol. Macromol.* **2019**, *126*, 731–742. https://doi.org/10.1016/j.ijbiomac.2018.12.161.

(209) Yousefi, M.; Khorshidian, N.; Mortazavian, A. M.; Khosravi-Darani, K. Preparation Optimization and Characterization of Chitosan-Tripolyphosphate Microcapsules for the Encapsulation of Herbal Galactagogue Extract. *Int. J. Biol. Macromol.* **2019**, *140*, 920–928. https://doi.org/10.1016/j.ijbiomac.2019.08.122.

(210) Othman, N.; Masarudin, M.; Kuen, C.; Dasuan, N.; Abdullah, L.; Md. Jamil, S. Synthesis and Optimization of Chitosan Nanoparticles Loaded with L-Ascorbic Acid and Thymoquinone. *Nanomaterials* **2018**, *8* (11), 920. https://doi.org/10.3390/nano8110920.

(211) Kim, M. K.; Lee, J.-S.; Kim, K. Y.; Lee, H. G. Ascorbyl Palmitate-Loaded Chitosan Nanoparticles: Characteristic and Polyphenol Oxidase Inhibitory Activity. *Colloids Surf. B Biointerfaces* **2013**, *103*, 391–394. https://doi.org/10.1016/j.colsurfb.2012.09.038.

(212) Wei, D.; Sun, W.; Qian, W.; Ye, Y.; Ma, X. The Synthesis of Chitosan-Based Silver Nanoparticles and Their Antibacterial Activity. *Carbohydr. Res.* **2009**, *344* (17), 2375–2382. https://doi.org/10.1016/j.carres.2009.09.001.

(213) Romeo, L.; Lanza Cariccio, V.; Iori, R.; Rollin, P.; Bramanti, P.; Mazzon, E. The α-Cyclodextrin/Moringin Complex: A New Promising Antimicrobial Agent against Staphylococcus Aureus. *Mol. J. Synth. Chem. Nat. Prod. Chem.* **2018**, *23* (9). https://doi.org/10.3390/molecules23092097.

(214) Prior, R. L.; Wu, X.; Schaich, K. Standardized Methods for the Determination of Antioxidant Capacity and Phenolics in Foods and Dietary Supplements. *J. Agric. Food Chem.* **2005**, *53* (10), 4290–4302. https://doi.org/10.1021/jf0502698.

(215) Santos-Sánchez, N. F.; Salas-Coronado, R.; Villanueva-Cañongo, C.; Hernández-Carlos, B. Antioxidant Compounds and Their Antioxidant Mechanism. *Antioxidants* **2019**. https://doi.org/10.5772/intechopen.85270.

(216) Craft, B. D.; Kerrihard, A. L.; Amarowicz, R.; Pegg, R. B. Phenol-Based Antioxidants and the In Vitro Methods Used for Their Assessment. *Compr. Rev. Food Sci. Food Saf.* **2012**, *11* (2), 148–173. https://doi.org/10.1111/j.1541-4337.2011.00173.x.

(217) Debnath, S.; Kumar, R. S.; Babu, M. N. Ionotropic Gelation – A Novel Method to Prepare Chitosan Nanoparticles. **2011**, 5.

(218) Kunjachan, S.; Jose, S. Understanding the Mechanism of Ionic Gelation for Synthesis of Chitosan Nanoparticles Using Qualitative Techniques. *Asian J. Pharm.* **2010**, *4* (2), 148. https://doi.org/10.4103/0973-8398.68467.

(219) Freeze Drying / Lyophilization Information: Basic Principles https://www.spscientific.com/freeze-drying-lyophilization-basics/ (accessed Mar 8, 2020).

(220) Nireesha, G.; Divya, L.; Sowmya, C.; Venkateshan, N.; Babu, M. N.; Lavakumar, V. Lyophilization/Freeze Drying - An Review /paper/Lyophilization%2FFreeze-Drying-An-Review-Nireesha-Divya/d9f4a4b942c8ecaa128daeb1eeb4fde95a80d1e9/figure/1 (accessed Jun 1, 2020).
(221) Stetefeld, J.; McKenna, S. A.; Patel, T. R. Dynamic Light Scattering: A Practical Guide and Applications in Biomedical Sciences. *Biophys. Rev.* **2016**, *8* (4), 409–427. https://doi.org/10.1007/s12551-016-0218-6.
(222) Mahmood Aljamali, N. Zetasizer Technique in Biochemistry. *Biochem. Anal. Biochem.* **2015**, *04* (02). https://doi.org/10.4172/2161-1009.1000168.
(223) Kaszuba, M.; Corbett, J.; Watson, F. M.; Jones, A. High-Concentration Zeta Potential Measurements Using Light-Scattering Techniques. *Philos. Transact. A Math. Phys. Eng. Sci.* **2010**, *368* (1927), 4439–4451. https://doi.org/10.1098/rsta.2010.0175.
(224) Lazaro Garcia, A. A. Nano-Silica Production at Low Temperatures from the Dissolution of Olivine : Synthesis, Tailoring and Modelling. **2014**. https://doi.org/10.6100/IR774494.
(225) Ismail, A. A.; van de Voort, F. R.; Sedman, J. Chapter 4 Fourier Transform Infrared Spectroscopy: Principles and Applications. In *Techniques and Instrumentation in Analytical Chemistry*; Elsevier, 1997; Vol. 18, pp 93–139. https://doi.org/10.1016/S0167-9244(97)80013-3.
(226) Valand, R.; Tanna, S.; Lawson, G.; Bengtström, L. A Review of Fourier Transform Infrared (FTIR) Spectroscopy Used in Food Adulteration and Authenticity Investigations. *Food Addit. Contam. Part A* **2020**, *37* (1), 19–38. https://doi.org/10.1080/19440049.2019.1675909.
(227) Sabbatini, S.; Conti, C.; Orilisi, G.; Giorgini, E. Infrared Spectroscopy as a New Tool for Studying Single Living Cells: Is There a Niche? *Biomed. Spectrosc. Imaging* **2017**, *6* (3–4), 85–99. https://doi.org/10.3233/BSI-170171.
(228) Infrared and FTIR spectroscopy Instrument http://delloyd.50megs.com/MOBILE/infrared_spectroscopy.html (accessed Jun 2, 2020).
(229) Scanning Electron Microscopy. *Nanoscience Instruments*.
(230) Specimen Interaction | Electron Nanoscopy Instrumentation Facility https://ncmn.unl.edu/enif/microscopy/interact.shtml (accessed Jun 2, 2020).
(231) Swapp, S. Scanning Electron Microscopy (SEM). *Scan. Electron Microsc.* 3.
(232) How do electron microscopes work? http://www.explainthatstuff.com/electronmicroscopes.html (accessed May 3, 2020).
(233) Q500_manual_rev_3-12.Pdf.
(234) Karangwa, E. An Overview of Ultrasound-Assisted Food-Grade Nanoemulsions. *Food Eng. Rev.*
(235) Picollo, M.; Aceto, M.; Vitorino, T. UV-Vis Spectroscopy. *Phys. Sci. Rev.* **2019**, *4* (4). https://doi.org/10.1515/psr-2018-0008.
(236) Behera, S.; Ghanty, S.; Ahmad, F.; Santra, S.; Banerjee, S. UV-Visible Spectrophotometric Method Development and Validation of Assay of Paracetamol Tablet Formulation. *J. Anal. Bioanal. Tech.* **2012**, *3* (6), 1–6. https://doi.org/10.4172/2155-9872.1000151.
(237) obpl. Molecular Analysis Using UV/Visible Spectroscopy. *Orbit Biotech*, 2018.
(238) Dong, J.; Cai, L.; Zhu, X.; Huang, X.; Yin, T.; Fang, H.; Ding, Z. Antioxidant Activities and Phenolic Compounds of Cornhusk, Corncob and Stigma Maydis. *J. Braz. Chem. Soc.* **2014**, *25* (11), 1956–1964. https://doi.org/10.5935/0103-5053.20140177.
(239) Solihah, M. A.; Rosli, W. I. W.; Nurhanan, A. R. Phytochemicals screening and total phenolic content of Malaysian Zea mays hair extracts. https://www.semanticscholar.org/paper/Phytochemicals-screening-and-total-phenolic-content-Solihah-Rosli/650ee7dba2d31ee7c8672c8ef0dcaa033fc46f9b (accessed May 2, 2020).
(240) Bai, Y.; Saren, G.; Huo, W. Response Surface Methodology (RSM) in Evaluation of the Vitamin C Concentrations in Microwave Treated Milk. *J. Food Sci. Technol.* **2015**, *52* (7), 4647–4651. https://doi.org/10.1007/s13197-014-1505-5.
(241) Liu, S.; Ho, P. C. Formulation Optimization of Scutellarin-Loaded HP-β-CD/Chitosan Nanoparticles Using Response Surface Methodology with Box–Behnken Design. *Asian J. Pharm. Sci.* **2017**, *12* (4), 378–385. https://doi.org/10.1016/j.ajps.2017.04.003.
(242) Kumar, S. P.; Birundha, K.; Kaveri, K.; Devi, K. T. R. Antioxidant Studies of Chitosan Nanoparticles Containing Naringenin and Their Cytotoxicity Effects in Lung Cancer Cells. *Int. J. Biol. Macromol.* **2015**, *78*, 87–95. https://doi.org/10.1016/j.ijbiomac.2015.03.045.
(243) Medina-Torres, N.; Espinosa-Andrews, H.; Trombotto, S.; Ayora-Talavera, T.; Patrón-Vázquez, J.; González-Flores, T.; Sánchez-Contreras, Á.; Cuevas-Bernardino, J. C.; Pacheco, N. Ultrasound-Assisted Extraction Optimization of Phenolic Compounds from Citrus Latifolia Waste for Chitosan Bioactive Nanoparticles Development. *Mol. Basel Switz.* **2019**, *24* (19). https://doi.org/10.3390/molecules24193541.
(244) IR Spectrum Table & Chart https://www.sigmaaldrich.com/technical-documents/articles/biology/ir-spectrum-table.html (accessed May 8, 2020).
(245) Popa, M.-I.; Aelenei, N.; Popa, V. I.; Andrei, D. Study of the Interactions between Polyphenolic Compounds and Chitosan. *React. Funct. Polym.* **2000**, *45* (1), 35–43. https://doi.org/10.1016/S1381-5148(00)00009-2.
(246) Ajun, W.; Yan, S.; Li, G.; Huili, L. Preparation of Aspirin and Probucol in Combination Loaded Chitosan Nanoparticles and in Vitro Release Study. *Carbohydr. Polym.* **2009**, *75* (4), 566–574. https://doi.org/10.1016/j.carbpol.2008.08.019.
(247) Harris, R.; Lecumberri, E.; Mateos-Aparicio, I.; Mengíbar, M.; Heras, A. Chitosan Nanoparticles and Microspheres for the Encapsulation of Natural Antioxidants Extracted from Ilex Paraguariensis. *Carbohydr. Polym.* **2011**, *84* (2), 803–806. https://doi.org/10.1016/j.carbpol.2010.07.003.
(248) Mohammed, M.; Syeda, J.; Wasan, K.; Wasan, E. An Overview of Chitosan Nanoparticles and Its Application in Non-Parenteral Drug Delivery. *Pharmaceutics* **2017**, *9* (4), 53. https://doi.org/10.3390/pharmaceutics9040053.

(249) Ruiz-Navajas, Y.; Viuda-Martos, M.; Sendra, E.; Perez-Alvarez, J. A.; Fernández-López, J. In Vitro Antibacterial and Antioxidant Properties of Chitosan Edible Films Incorporated with Thymus Moroderi or Thymus Piperella Essential Oils. *Food Control* **2013**, *30* (2), 386–392. https://doi.org/10.1016/j.foodcont.2012.07.052.

(250) Emmanuel, S.; Olajide, O.; Abubakar, S.; Akiode, S.; Etuk-Udo, G. Chemical Evaluation, Free Radical Scavenging Activities and Antimicrobial Evaluation of the Methanolic Extracts of Corn Silk (Zea Mays). *J. Adv. Med. Pharm. Sci.* **2016**, *9* (4), 1–8. https://doi.org/10.9734/JAMPS/2016/28530.

(251) Indian Journals http://www.indianjournals.com/ijor.aspx?target=ijor:skuastjr&volume=17&issue=1&article=002 (accessed Apr 19, 2020).

(252) Sullivan, D. J.; Cruz-Romero, M.; Collins, T.; Cummins, E.; Kerry, J. P.; Morris, M. A. Synthesis of Monodisperse Chitosan Nanoparticles. *Food Hydrocoll.* **2018**, *83*, 355–364. https://doi.org/10.1016/j.foodhyd.2018.05.010.

(253) Shafiei, M.; Jafarizadeh-Malmiri, H.; Rezaei, M. Biological Activities of Chitosan and Prepared Chitosan-Tripolyphosphate Nanoparticles Using Ionic Gelation Method against Various Pathogenic Bacteria and Fungi Strains. *Biologia (Bratisl.)* **2019**, *74* (11), 1561–1568. https://doi.org/10.2478/s11756-019-00299-8.